UNIVERSITAT POLITÈCNICA DE VALÈNCIA

UNIVERSITAT POLITÈCNICA DE VALÈNCIA

Instituto Universitario Mixto de Biología Molecular y Celular de Plantas

Caracterización funcional de los factores de transcripción NGATHA en el desarrollo del carpelo de Oryza sativa.

Trabajo Fin de Máster

Máster Universitario en Biotecnología Molecular y Celular de Plantas

AUTOR/A: Roura Jimenez, Marina

Tutor/a: Bueso Ródenas, Eduardo

Director/a Experimental: DRENI, LUDOVICO

CURSO ACADÉMICO: 2022/2023

Functional characterization of NGATHA transcription factors in *Oryza sativa* carpel development

Master's thesis

Marina Roura Jiménez

Course: 2022-2023

Director: Dr. Ludovico Dreni

UPV director: Dr. Eduardo Bueso Ródenas

Index

Acknowledgements

Huge thanks to Ludovico, my master's thesis director, for teaching me all the things I needed to know to make this master's thesis possible, and for all the guidance you have given me during this period. Also, thanks to Cristina, for giving me the opportunity to do my master's thesis at your lab, and for all the help you have provided. And thanks to all the lab members for your company and your help when I needed it.

I would also like to thank my family for believing in me and encouraging me to achieve my objectives. And my friends, Ana and Ouissal, for their constant support and encouragement.

This master's thesis wouldn't have been possible without all this people, so I thank you all.

Abbreviations

%: Percentage

µg: Microgram

µl: Microliter

AAO2: ALDEHYDE OXIDASE 2

AG: AGAMOUS

AP: APETALA

APO: ABERRANT PANICLE ORGANIZATION

ARF1: AUXIN RESPONSE FACTOR 1

BIF2: BARREN INFLORESCENCE2

BRD: B3 Repression Domain

CKX: Cytokinin dehydrogenases

CLV: CLAVATA

cm: Centimeter

CRC: CRABS CLAW

CRISPR: Clustered Regularly Interspaced Short Palindromic Repeats

CYP: Cytochrome

DEGs: Differentially Expressed Genes

DJ: Dongjin

DL: DROOPING LEAF

DNA: Deoxyribonucleic Acid

EDTA: Ethylenediamine tetraacetic acid

FAA: Formaldehyde, Acetic acid, Ethanol

FC: Fold change

FDM: Floral meristem determinacy

FON: FLORAL ORGAN NUMBER

FPKM: Fragments Per Kilobase Million

GA2OX1: GIBBERELLIN 2-BETA-DIOXYGENASE

HCl: Hydrogen chloride

HEC: HECATE

Hz: Hertz

IAA: Auxin

IBMCP: Instituto de Biología Molecular y Celular de Plantas

IND: INDEHISCENT

KNU: KNUCKLES

LFY: LEAFY

LOG: LONELY GUY

MATE: Multidrug and toxin efflux

MFO1/OsMADS6: MOSAIC FLORAL ORGAN 1

ml: Mililiter

mM: Millimolar

mm: Millimeter

NaCl: Sodium chloride

NGA: NGATHA

NH_4^+: Ammonium

NIR2: NITRITE REDUCTASE 2

NLS: Nuclear Localization Signal

NO_2^-: Nitrite

^oC: Degree Celsius

PCR: Polymerase chain reaction

PDR13: PLEIOTROPIC DRUG RESISTANCE PROTEIN 13

PI: Panicle meristem initiation

PID: PINOID

PTR2: Peptide transporter

RAV: RELATED TO ABI3 AND VP1

REM: REPRODUCTIVE MERISTEM

RIN: RNA Integrity Number

RNA: Ribonucleic Acid

RNA-seq: RNA sequencing

rpm: Revolutions per minute

SDS: Sodium Dodecyl Sulfate

SHI/STY: SHORT INTERNODES/ STYLISH

SPT: SPATULA

SPW1/OsMADS16: SUPERWOMAN1

SUP: SUPERMAN

TPM: Transcripts Per Million

UFO: UNUSUAL FLORAL ORGAN

VIGS: Virus-induced gene silencing

WT: Wild Type

WUS: WUSCHEL

YAB: YABBY

YUC: YUCCA

Abstract

The gynoecium, the female reproductive structure of the flowers, is the most complex plant organ and has a vast morphological diversity among flowering plants. NGATHA (NGA), a small group of transcription factors belonging to the RAV family, are implicated in its formation by specifying style and stigma development in eudicot plants, but little is known about them in other phylogenetically distant plants, such as monocots. Here, we characterize the function of the four *NGA* genes (*NGA1-4*) expressed in rice (*Oryza sativa*) gynoecium by generating different rice *nga* mutants. Our results indicate that, like in *Arabidopsis*, rice *NGA* genes regulate style and stigma development in a redundant and dose-dependent manner, but they are not equally redundant, as some of them (such as *NGA2*) contributes more to their common functions than others. We have also observed that they are essential for plant fertility and fruit development and they also mediate rice vegetative development, but are not involved in pollen fertility. Stigma morphological defects can be one of the factors impairing mutant plant fertility, but our results suggest that other factors are also involved in this outcome. Histological analysis showed that rice *NGA* genes are also involved in ovule enclosure by the carpel primordia during pistil development; and their lack of expression leads to the overgrowth of the ovule and the integument surrounding it, and defects in the embryo sac shape and position. Differentially expressed genes detected by RNA-seq in developing inflorescence primordia suggest that rice *NGA* genes promote style and stigma development by regulating the expression of the transcription factors *REM*, *TCP25*, and a *KNU* homolog (either directly or indirectly). RNA-seq results also suggest that, unlike in *Arabidopsis*, rice *NGA* genes repress auxin biosynthesis and transport, leading to a decrease in auxin response. To sum up, our results suggest that rice *NGA* genes have a conserved function in style and stigma development; however, their molecular mechanism seems to have partially diverged.

Keywords: *Oryza sativa*, rice, *NGATHA*, transcription factors, floral organs, style, stigma, pistil, carpel, fertility, auxin.

1. Introduction

1.1. Rice as a model organism

Arabidopsis thaliana is the most used model species in plant biology due to a set of features that it possesses. Amongst them, the most relevant ones are its small size and short generation time, its prolific seed production accomplished through self-pollination, its wide physiological variation among natural accessions, and the availability of efficient transformation procedures (Koornneef and Meinke, 2010). Nevertheless, there are other widely used plant model organisms, such as *Oryza sativa*, which have been used in the development of this master's thesis.

Oryza sativa (**Figure 1.1**), commonly referred to as rice, is a short-day plant that belongs to the grass family *Poaceae* (*Gramineae*), a large family of monocotyledonous flowering plants in which are included many cultivated species, such as cereals, making them one of the most economically and agriculturally important plant families. Rice is a great food source and serves as a model organism for the study of other monocotyledonous species. (Jain *et al.*, 2019) This plant has been chosen to be the monocot model due to its relatively small genome size and its diploidy (Song *et al.*, 2018), and to the fact that it can be used as a template for other cereal crops with much larger genomes (such as maize and wheat) (Jackson, 2016). There is a considerable genetic synteny between rice and other cereal species; however, there are variations in gene content, repeat structure, and size (Jackson, 2016, Chen *et al.*, 1997). Thus, rice can be used as a base model for cereal crops but it is important to bear in mind that not all the molecular processes may be conserved, for instance, some genes can be missing in rice or in other species (Jackson, 2016). Moreover, like in *Arabidopsis*, a large set of genetic, molecular, and genomic resources have been developed in rice (Rensink and Buell, 2004); and a lot of different rice cultivars have been sequenced to constitute a rice 'pangenome' in the recent years (Song *et al.*, 2018) reaching to more than 3000 rice varieties and species (Jain *et al.*, 2019).

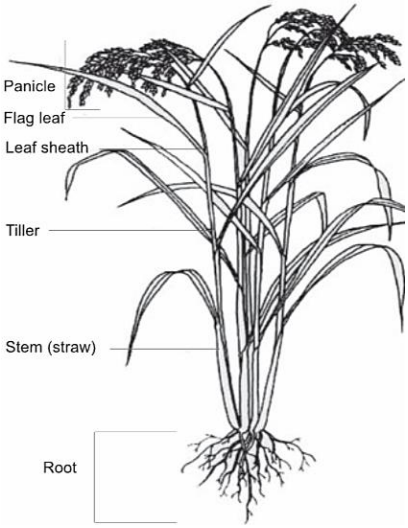

Figure 1.1. Rice plant morphology (Wopereis *et al.,* 2009).

1.2. Rice life cycle

Rice development can be divided into three phases: the vegetative, reproductive, and maturity stage (that happens simultaneous with the development of the new embryo) (**Figure1.2**) (Itoh *et al.*, 2005). Its development begins with the germination of the seed. This establishes the start of the vegetative phase, in which the number of shoots increases, the plant grows taller, and leaves emerge at regular intervals producing a total of 10 or more foliage leaves (the last leaf to emerge, which will be the first below the panicle, is referred as the flag leaf (**Figure 1.1**) (Wopereis *et al.*, 2009; Itoh *et al.*, 2005). The length of this stage diverges between different cultivars and lasts until the panicle meristem initiation (PI), that marks the start of the reproductive phase. As rice is a short-day plant of subtropical origins with no vernalization required, this stage is induced when the plant receives less than 12 hours of light. However, the cultivation of rice expanded much northward (up to North Japan, Europe and USA) and southward (up to Australia and Argentina) along its domestication, and it was the selection of photoperiod-insensitive mutants that allowed its cultivation in such areas, where it must flower at the peak of summer in order that mature grains can be harvested before the cold season (Izawa, 2007). The PI is the moment when the panicle meristem initiates the production of a panicle primordium at the base of each shoot, just above the soil level. At the same time, the shoot internodes subtending the meristem begin to elongate until the plant reaches its full height. After the PI comes the panicle differentiation, that is when its length goes from 1 to 2 mm and the branching of the panicle can be differentiated with the naked eye. Following this, the panicle increases in size and grows up inside the flag leaf sheath in the process called booting, which is followed by the heading, that is when the panicle emerges from the flag leaf sheath after having reached the top of the shoot. Then the anthesis or flowering takes place, a process that lasts from 1 to 2,5 hours (usually between 9 and 11 a.m., even though it largely depends on sunrise time (Wopereis *et al.*, 2009)) in which the pollination happens. It consists of the opening and subsequent closing (within half an hour) of the spikelets that makes pollen exchange possible. This allows the fertilization to take place and leads to the ripening. Until this point, the reproductive phase takes around one month with some variation between cultivars; and from the start of the ripening until the end, another 35-50 days will pass. The ripening is characterized by grain growth via the accumulation of starch and sugars (translocated from the rest of the plant) that cause an increase in its size and weight; following this growth, the grain changes color from green to gold as it matures, and the leaves of the plant begin to senesce (**Figure 1.2**) (Itoh *et al.*, 2005; Hardke *et al.*, 2013;).

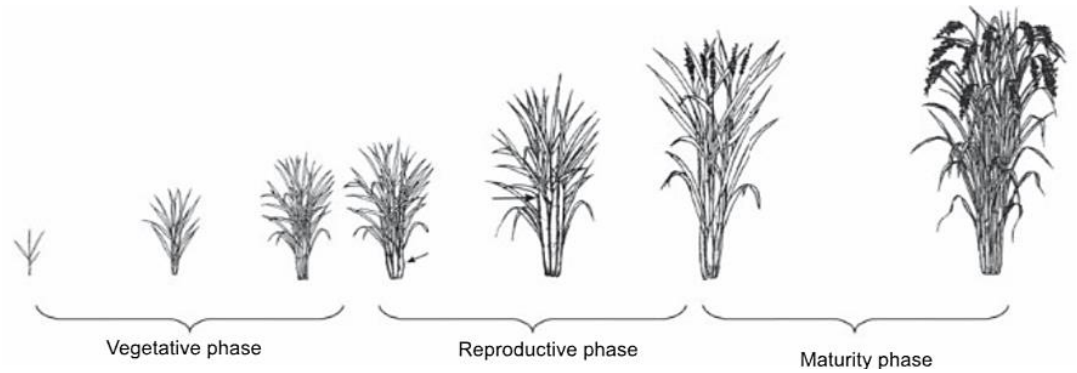

Figure 1.2. Schematic representation of the rice development phases (Wopereis *et al.,* 2009).

1.3. Rice flower structure

This master's thesis is centered around the *NGATHA (NGA)* genes, which are key elements in flower development. In previous studies involving exclusively eudicot model plants (Trigueros *et al.*, 2009; Fourquin and Ferrándiz, 2014), it has been established that these genes have a major effect on carpel development, and their disruption can even lead to floral female sterility (Alvarez *et al.*, 2009; Trigueros *et al.*, 2009). So it is important to know floral and carpel structure and development to fully understand the results shown in this thesis.

The rice inflorescence is called panicle and ends up being located at the top of the plant. It is composed of primary ramifications that, in turn, carry secondary branches where the spikelets are placed (Itoh *et al.*, 2005; Wopereis *et al.*, 2009). The spikelet is the structural unit of the inflorescence of Poaceae and is the combination of the glumes and an extremely variable number of florets. The rice spikelet develops only one terminal fertile floret, enclosed by two large bract- or prophyll-like structures named lemma and palea (**Figure 1.3**) (Yamaguchi and Hirano, 2006), subtended by two tiny glumes (the rudimentary glumes) and two reduced lemmas, called empty glumes or sterile lemmas, which represent the remnants of two lateral repressed florets; indeed, rice is thought to have evolved from an ancestor with three-flowered spikelets (Bommert *et al.*, 2005). The terminal fertile floret has, enclosed by lemma and palea, two lodicules (only formed at the lemma side), six stamens, and one central pistil (**Figure 1.3**) (Yamaguchi and Hirano, 2006). From these organs, the most conserved ones in angiosperms are the stamen and the pistil, even though the rice pistil is very different from the ones in eudicots. The lemma, palea, and lodicules are specific to the grass family, but they are thought to be homologs with other eudicot organs: the lemma and palea would be the bract and prophyll, respectively (Kellogg, 2001), and the lodicule would correspond to the petal. Following this model, first whorl organs homologous to sepals might have been lost in grasses, but it has been also proposed that the palea is a more complex organ derived

from the fusion of a central prophyll and two lateral sepals (Kellogg, 2015; Schrager-Lavelle *et al.*, 2017; Lombardo and Yoshida, 2015).

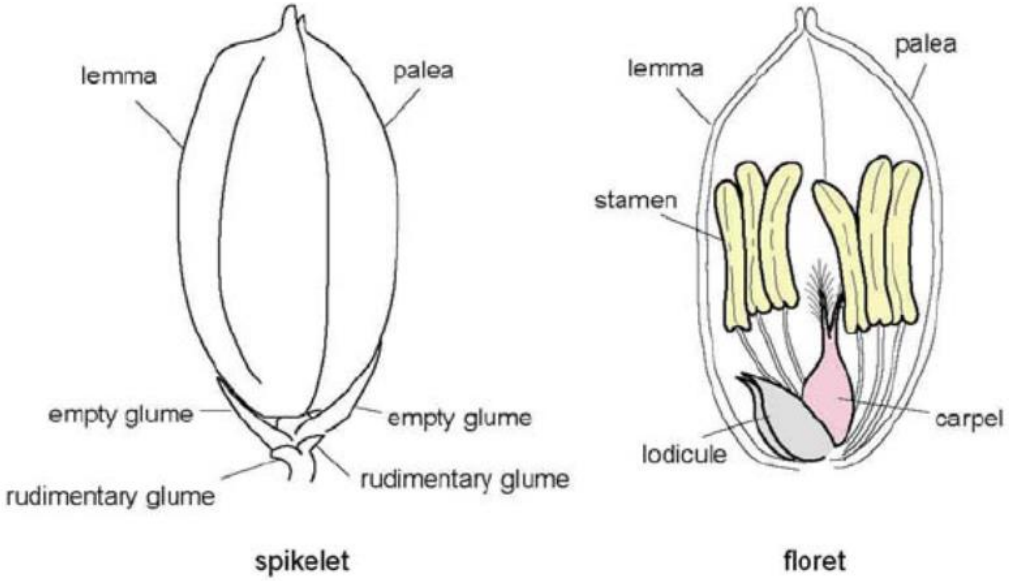

Figure 1.3. Morphology of the rice spikelet and floret. The spikelet is shown from the outside (left) and the floret shows the floral organs found inside the palea and lemma (right) (Yamaguchi and Hirano, 2006).

1.4. Rice pistil importance and structure

The gynoecium is the female reproductive structure of the flowers, making it one of the crucial defining features of angiosperms (Shen *et al.*, 2021). It confers major benefits to flowering plants that lead to an increase in the reproductive efficiency of angiosperms in comparison with gymnosperms (Shen *et al.*, 2021). First of all, the gynoecium is enclosing the ovules and protecting them; it also captures the pollen and guides the pollen tube to ensure the fertilization of the ovules; moreover, after fertilization it turns into the fruit, which will protect the seeds and assist in their dispersal (Trigueros *et al.*, 2009; Ferrandiz *et al.*, 2010; Martínez-Fernández *et al.*, 2014).

The carpel, the basic unit of the gynoecium, has a huge morphological diversity among flowering plants. At the center of a flower there can be a single carpel or multiple carpels, which in turn can be fused into a single pistil (a syncarpic gynoecium) or separated into individual organs that form an apocarpic gynoecium composed of several pistils (**Figure 1.4A**) (Martínez-Fernández *et al.*, 2014; Gomariz-Fernández *et al.*, 2017; Shen *et al.*, 2021). The pistil always follows a basic organization structure composed of three specialized functional modules: the basal ovary, the style, and the apical stigma (**Figure 1.4B**) (Becker, 2020; Shen *et al.*, 2021). The stigma, found at the top of the pistil, is in charge of capturing the pollen grains and promote their hydration and germination

(Ferrandiz *et al.*, 2010; Ballester *et al.*, 2021). Below it there is the style, tasked with directing the pollen tubes to the ovary, which is the basal structure that contains the ovules (Sundberg and Ferrándiz, 2009; Ferrandiz et al., 2010; Martínez-Fernández *et al.*, 2014). Like all grasses, rice flowers have one pistil derived from the early fusion of three carpel primordia (Kellogg, 2001); its structure is composed of the basal ovary, which encloses only one ovule, two partially fused styles, and two feathery stigmas, which are covered with papillae cells to facilitate pollen capture (Shen et al., 2021) (**Figure 1.4B**).

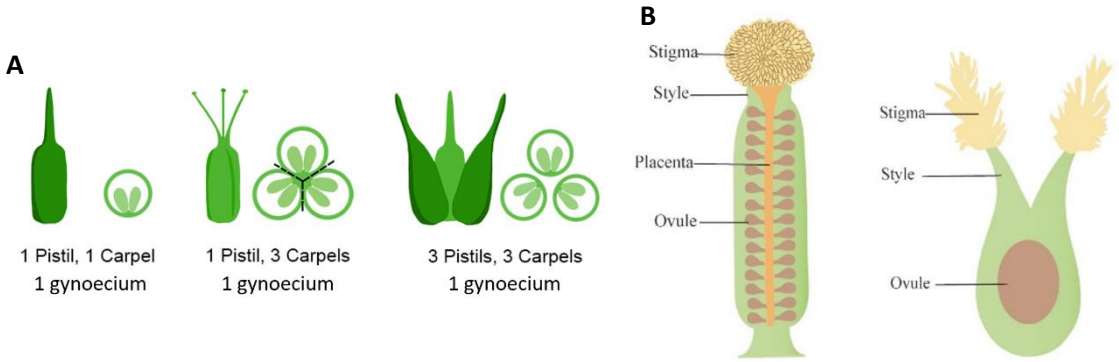

Figure 1.4. (A) Image showing different gynoecium structures to better understand the difference between gynoecium, pistil, and carpel. (B) Representation of the *Arabidopsis* and rice pistils with each of its parts indicated (Shen *et al.*, 2021).

1.5. Flower and carpel development

1.5.1. ABCDE model

In the past decades, the ABCDE model has been established as the central model explaining the genetic mechanism of eudicot flower development (Colombo *et al.*, 1995; Pelaz *et al.*, 2000, 2001; Honma and Goto, 2001; Favaro *et al.*, 2003; Pinyopich *et al.*, 2003); this model has been developed in *Arabidopsis thaliana*, so it is more accurate in this plant. According to this model, *Arabidopsis* flowers are composed of four whorls, each one with a different floral organ identity determined by the combination of genes expressed in each region. (**I**) In the whorl 1 is where the sepals are produced, and it is specified by the expression of A class genes. (**II**) The second whorl corresponds to the petals determined by the A and B class genes. (**III**) The stamens are specified by B and C class genes in the whorl 3. (**IV**) And finally, the carpel (whorl 4) by C class genes alone. There are also E and D class genes: E class genes are necessary for the correct development of all floral organs; and D class genes specify ovule identity, and are closely related phylogenetically to C class genes (Angenent and Colombo, 1996). All these genes encode for conserved MADS-box transcription

factors, with the sole exception of *Arabidopsis APETALA2* (*AP2*) (Riechmann *et al.*, 1996; Theißen, 2001; Paøenicová *et al.*, 2003; Theißen *et al.*, 2016).

This model in rice is not as definite, and it is still unclear if it is conserved in the outer whorls (Litt, 2007; Causier *et al.*, 2010). However, it is known that the C and D MADS-box protein functions in carpel and ovule identity are conserved among angiosperms, and that their protein interaction with E class proteins seems to also be maintained (Dreni and Kater, 2014).

1.5.2. Carpel development in rice

OsMADS3 and *OsMADS58*, the two rice *AGAMOUS (AtAG)* orthologs that belong to the C class genes, are expressed exclusively in the whorl 3 (stamen) and whorl 4 (carpel) (Yamaguchi *et al.*, 2006; Dreni *et al.*, 2011). When mutated, the resulting flowers are devoid of stamens and pistils, which are converted into lodicule- and palea-like structures respectively, except for a residual carpel identity limited to the ovary adaxial (inner) epidermis, indicating that there is another element involved in carpel formation (Dreni *et al.*, 2011). This element is another important AGAMOUS subfamily member, the *OsMADS13*, a D class ovule identity gene (Dreni *et al.*, 2007). When *osmads3 osmads13 osmads58* triple mutants are generated, the residual carpel identity is fully eliminated (Dreni *et al.*, 2011); however, there is still expression of *DROOPING LEAF* (*DL*), a gene required for carpel identity specification, in the palea-like ectopic structures that replace the pistil.

DL is the ortholog of *CRABS CLAW* (*CRC*) in *Arabidopsis*, a gene that encodes a YABBY family transcription factor required to maintain the proper growth of the gynoecium (Alvarez and Smyth, 1999). In rice, *DL* is thought to play an active role in carpel identity determination and in regulating the boundary between whorls 3 and 4, because the gynoecium of *dl* mutants is replaced by ectopic stamens, whereas the opposite happens in *spw1* mutants (which have the class B gene *SUPERWOMAN1 (SPW1)/OsMADS16* mutated) (Nagasawa *et al.*, 2003; Yamaguchi *et al.*, 2004); this suggests that *DL* and B class genes are mutually antagonizing each other. This is markedly different from what happens in *Arabidopsis*, where *CRC* has a more specific function in regulating some aspects of carpel development, is activated directly by *AtAG* (C class genes), and is being inhibited by B class genes but not the other way around (which is done by SUPERMAN (SUP), a C2H2 zinc finger transcription factor) (Schultz *et al.*, 1991; Bowman *et al.*, 1992; Bowman and Smyth, 1999; *Sakai et al.*, 2000).

In short, it is believed that *DL*, *OsMADS3* and *OsMADS58* are all necessary for carpel identity specification and morphogenesis, and *OsMADS13* (the D class

gene) is also playing a role in carpel establishment. This contrasts with *Arabidopsis*, where carpel identity is determined exclusively by C class genes and ovule identity is conferred by C and D class genes (Pinyopich *et al.*, 2003).

In grasses, there are several E class SEP-like genes divided between the LOFSEP clade and the SEP3 clade (Malcomber and Kellogg, 2005; Zahn *et al.*, 2005; Arora *et al.*, 2007). Like in *Arabidopsis*, their absence leads to the reversion of floral organs to leaf-like structures and their encoded proteins can form heterodimers with C and D class proteins, suggesting a conserved role of these genes between these species (Pelaz *et al.*, 2001; Cui *et al.*, 2010; Wu *et al.*, 2017). However, unlike in *Arabidopsis*, LOFSEP clade members seem to act as upstream activators of C class genes (Wu *et al.*, 2017). (**Figure 1.5**).

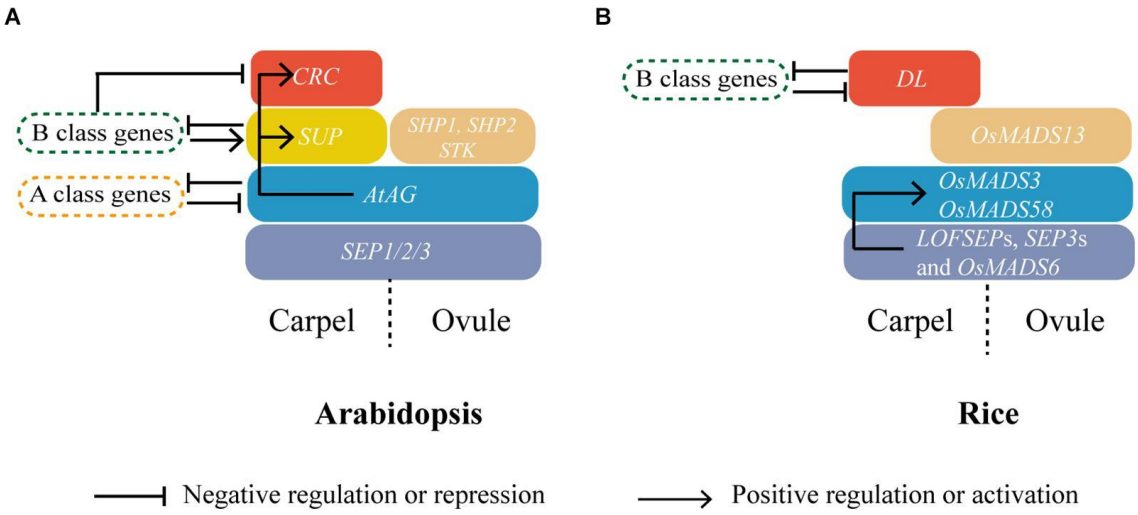

Figure 1.5. Model of the gene regulatory network of carpel and ovule specification in *Arabidopsis* (**A**) and rice (**B**). The different colors are indicating to which group each gene belongs: in blue there are the C class genes, the orange ones are the D class genes, grayish blue is indicating E class genes, *SUP* is in yellow, and *CRC/DL* are marked in red. (Shen *et al.*, 2021).

1.5.3. Floral meristem determinacy in carpel development

The floral meristem is determinate, so all the stem cells will be consumed in the development of the flower. In rice, the carpel primordia encloses the meristem, which remains undifferentiated until ovule development (Itoh *et al.*, 2005). This is different from what happens in *Arabidopsis*, where the floral meristem is consumed in the development of the placenta (Cucinotta *et al.*, 2014).

The CLAVATA (CLV)-WUSCHEL (WUS) pathway and *ABERRANT PANICLE ORGANIZATION* (*APO*)

An important factor controlling floral meristem determinacy (FMD) is the interaction of the CLV-WUS pathway with floral homeotic genes (Brand *et al.*, 2000; Schoof *et al.*, 2000; Ikeda *et al.*, 2009; Pautler *et al.*, 2013). In *Arabidopsis*,

WUS and *CLV1* (stem cell-promoting genes) are able to induce *AtAG* expression, which in turn is inhibiting *WUS* expression after carpel primordia emergence, triggering floral meristem termination (Shang *et al.*, 2019; Clark *et al.*, 1993); and CLV1 and CLV3 form a ligand-receptor system (Willmann, 2000). Rice *FLORAL ORGAN NUMBER1 (FON1)* (ortholog of *CLV1*) and *FON2/FON4* (orthologs of *CLV3*) are also interacting with C class genes in FMD, indicating that this pathway is fairly conserved in these two species (Xu *et al.*, 2017; Yasui *et al.*, 2017). *FON 4* is also believed to repress the expression of *OsMADS13*, the D class ovule identity specification gene, preventing meristem termination in the early stages (Xu *et al.*, 2017).

Other important factors are the *Arabidopsis LEAFY (LFY)* and *UNUSUAL FLORAL ORGAN* (*UFO*), who are regulating the ABC floral organ identity genes (Weigel *et al.*, 1992; Lee *et al.*, 1997; Parcy *et al.*, 1998; Chae *et al.*, 2008). The rice *APO2* and *APO1*, orthologs to *LFY* and *UFO* respectively, act together to regulate inflorescence and flower development (Ikeda et al., 2005; Ikeda-Kawakatsu *et al.*, 2012); besides, *APO1* is positively regulating the C class gene *OsMADS3* but not B class genes (like in *Arabidopsis*) (Lohmann and Weigel, 2002; Ikeda *et al.*, 2005) (**Figure 1.6**).

Floral homeotic genes interaction

Another aspect playing a key role in FMD is the interactions within floral homeotic genes. First of all, C class genes are influencing meristem determination in a dose-dependent manner (Dreni *et al.*, 2011). In *Arabidopsis*, *AtAG* are inducing meristem termination by repressing *WUS*; this repression takes place in part by the activation of the C2H2 zinc finger genes *KNUCKLES* (*KNU*) and *SUP*, and the YABBY gene *CRC* (Alvarez and Smyth, 1999; Payne *et al.*, 2004; Gómez-Mena *et al.*, 2005; Lee *et al.*, 2005; Ó'Maoiléidigh *et al.*, 2013). *CRC* and *SUP* also interact genetically with each other to regulate auxin and cytokinin homeostasis (Yamaguchi *et al.*, 2017; Prunet *et al.*, 2017; Lee *et al.*, 2019). In rice, the *SUP* orthologue has a significantly diverged molecular mechanism in reproductive organ development but still promotes FMD (Xu *et al.*, 2021). And the *DL* gene (ortholog of *CRC*) regulates carpel identity and participates in FMD (Yamaguchi *et al.*, 2004; Sugiyama *et al.*, 2019) by acting synergistically with the C class genes *OsMADS3* and *OsMADS58*, and

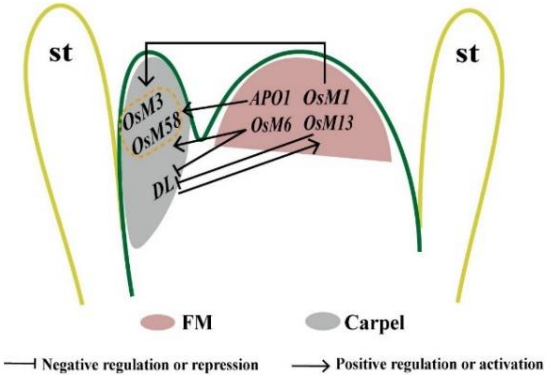

Figure 1.6. Model showing the genetic interactions between rice floral homeotic genes in the whorl 4 during FMD (Shen *et al.,* 2021).

acts in the same pathway as the D class gene *OsMADS13* to specify carpel and ovule identity, and FMD (Li *et al.*, 2011b) (**Figure 1.6**).

The two C class genes (*OsMADS3* and *OsMADS58*) are also interacting with *OsMADS1*, an E class gene, to regulate carpel identity specification; and *OsMADS1* and *OsMADS3* are acting together to repress floral meristem activity (Hu *et al.*, 2015). *MOSAIC FLORAL ORGAN 1* (*MFO1*)/*OsMADS6*, another E class gene, have a key role in early flower development (Li *et al.*, 2011a). On one hand, it is repressing *DL* expression (Li *et al.*, 2011a); and on the other, it is acting redundantly with *OsMADS13* in carpel and ovule identity specification and FMD termination, even though there is no obvious regulation between them at a transcriptional level (Li *et al.*, 2011a). Moreover, it is believed that *OsMADS6* is also promoting the expression of C class genes in early rice flower development (Li *et al.*, 2011a) (**Figure 1.6**).

1.5.4. Plant hormone's role in carpel development

Hormones also play a key role in carpel development, specifically auxin and cytokinin. First of all, an auxin concentration threshold controls plant organ initiation, making it essential for almost all developmental processes, including carpel development (Reinhardt *et al.*, 2003). In *Arabidopsis* and maize, disruption of *PINOID* (*PID*) (or *BARREN INFLORESCENCE2* (*BIF2*), the maize ortholog), a gene involved in polar auxin transport, causes severe defects in flower initiation resulting in pin-like inflorescences (Bennett *et al.*, 1995; McSteen *et al.*, 2007). However, rice *ospid* mutants do not develop these pin-like inflorescences; instead, the stigma is eliminated, and normal ovules fail to develop (He *et al.*, 2019; Xu *et al.*, 2019), they also have most auxin response factors downregulated and *FON4* upregulated in the pistil primordium, suggesting that *OsPID* may regulate stigma and ovule initiation by maintaining stem cell identity through auxin signaling (Xu *et al.*, 2019). The auxin-responsive gene *OsMGH3* (a GH3 domain-encoding gene) is a downstream target of the E class transcription factors OsMADS1 and OsMADS6 (Prasad *et al.*, 2005; Zhang *et al.*, 2010). The GH3 domain-containing proteins are responsible of inactivating auxin excess to maintain its homeostasis (Woodward and Bartel, 2005). *OsMGH3* knockdown plants and other auxin response factors mutants have their carpels affected, suggesting that the regulation of auxin-responsive genes plays a key role in carpel development (Sessions *et al.*, 1997; Okushima *et al.*, 2005).

Cytokinin controls cell division and differentiation making it a key regulator of meristem size and activity. The rice gene *LONELY GUY* (*LOG*) encodes a cytokinin-activating enzyme, it acts in the final step of cytokinin biosynthesis and

is required to maintain meristem activity. It is also necessary for a correct ovule formation by maintaining a sufficient volume of cells in the floral meristem (Yamaki *et al.*, 2011).

1.6. *NGATHA* (*NGA*) genes

The *NGA* genes form a small subfamily belonging to the RAV family, which is part of the B3 transcription factor superfamily (Alvarez *et al.*, 2009; Trigueros *et al.*, 2009). The RAV (RELATED TO ABI3 AND VP1) family members are plant-specific and have two different DNA binding domains: a C-terminal B3 domain, which recognizes the consensus sequence CACCTG; and an N-terminal AP2 domain that recognizes the consensus sequence CAACA (Kagaya *et al.*, 1999). They also possess a Nuclear Localization Signal (NLS), suggesting that they are present in the cell nucleus; and a B3 Repression Domain (BRD), indicating their repressive activity (**Figure 1.7**) (Karami *et al.*, 2021; (Matías-Hernández *et al.*, 2014). The RAV subfamily is subdivided into two categories depending on whether or not they have lost the AP2 domain: Class-I, with a B3 and an AP2 domain; and Class-II, with only a B3 domain (Romanel *et al.*, 2009; Salava *et al.*, 2022). The *NGA* genes belong to the Class-II category, having a B3 domain and two NGA domains (NGA-I and NGA-II) flanking the repressor BRD (**Figure 1.7**) (Salava *et al.*, 2022).

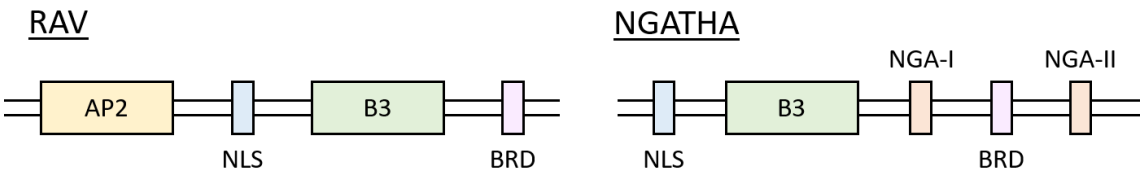

Figure 1.7. Schematic representation of the gene structure of the RAV gene family and the *NGA* genes. NLS: Nuclear Localization Signal. BDR: B3 Repression Domain.

The *NGA* genes were first characterized in *Arabidopsis thaliana*, and the molecular mechanism by which they act has been mainly studied in this species. They have been found to be expressed in many plant organs such as leaves, shoot meristems, flowers, seeds, and roots (Swaminathan *et al.*, 2008). This includes the carpel, where they act in a dose-dependent manner as key elements for its correct development (Alvarez *et al.*, 2009; Trigueros *et al.*, 2009). *Arabidopsis* has a total of four *NGA* genes (*NGA1* to *NGA4*) (Alvarez *et al.*, 2006). Single *nga* mutants present very little or no defects in carpel morphology (only an occasional misshapen style and reduced stigmatic papillae); but when the number of mutated genes increases, the carpel defects are also greater, reaching the peak in the quadruple mutant, where the style and stigma tissues are

completely replaced by projections with valve morphology (Alvarez *et al.*, 2009; Trigueros *et al.*, 2009) (**Figure 1.8A**). However, the specific molecular mechanism by which this gene family is acting is still unclear. Even so, they seem to be directing pistil development together with the SHORT INTERNODES/ STYLISH (SHI/STY) gene family, a group of zinc-finger transcription factors that share an almost identical expression pattern as *NGA*, and multiple combinations of mutations of these genes cause similar phenotypes as the observed in *NGA* mutants.

There are different hypotheses that try to answer this issue: (**I**) Alvarez *et al.*, 2009 suggest that *STY1* and other members of the SHI/STY gene family are involved in the positive regulation of the *NGA* genes at a transcriptional level in a context-dependent way, due to the presence of the STY1 much earlier than the appearance of NGA. It has been reported that STY1 is an activator of *YUCCA4* (*YUC4* – an auxin biosynthesis enzyme (Cheng *et al*., 2006; Sohlberg *et al.*, 2006)), so it is proposed that STY1 promotes auxin synthesis through YUC4, and once auxin levels reach a certain threshold *NGA* expression is stimulated. Once *NGA* genes are activated, they generate a positive feedback between them and *SHI/STY* family members to promote and maintain their expression and to activate additional genes, such as MADS-box genes of the *AGAMOUS* clade. During this process, early ovary factors such as the *YABBY1* (*YAB1*) genes are suppressing *NGA* gene activity directly, or indirectly by maintaining a cellular environment that hinders *NGA* sensitivity to the STY signal. But upon *NGA* activation, they suppress YAB1 and other early ovary factors activity (**Figure 1.8B**). (**II**) Alternatively, Trigueros *et al.*, 2009 propose a model in which *NGA* and *STY* do not regulate each other at a transcriptional level (even though they may be coregulated) but act together to direct style formation by regulating common targets, one of which is the promotion of auxin synthesis in the apical gynoecium by the upregulation of *YUC* gene expression. Later, Ballester *et al.*, 2021 suggested that NGA and HECATE (HEC) require each other to direct stigma development. They proposed a model in which NGA and HEC form a heterodimer in the apical gynoecium before stigma differentiation. This heterodimer would reinforce each other's expression and activate *INDEHISCENT* (*IND)* expression; the resulting protein, would form a complex with NGA and probably HEC to activate *SPATULA (SPT)*. Then, SPT would be incorporated into the complex to regulate other downstream targets such as *PID* or *WAG2*, two genes related to auxin transport, ultimately leading to stigma formation (**Figure 1.8C**).

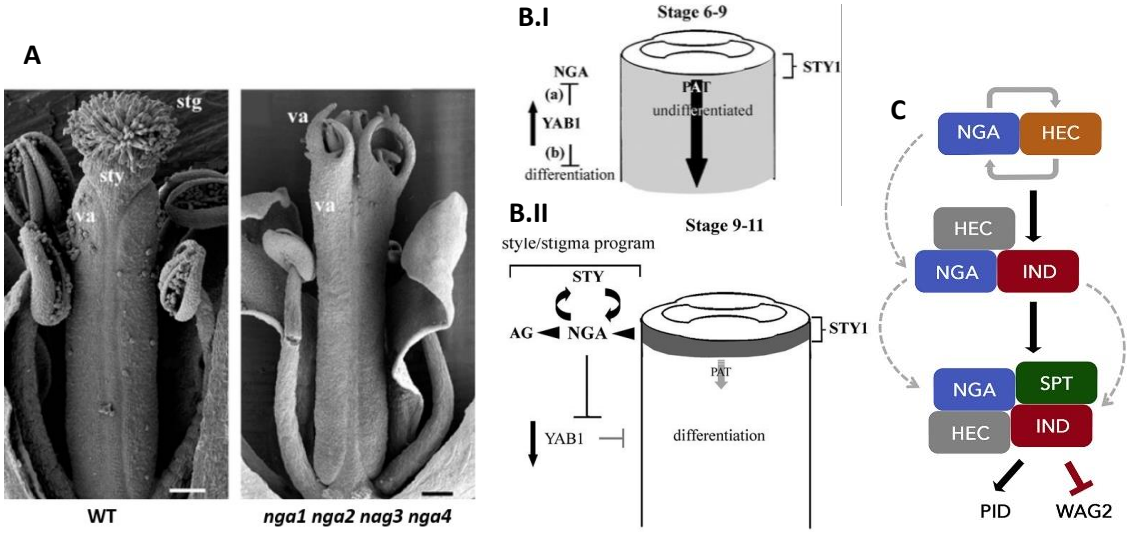

Figure 1.8. (A) Images showing *Arabidopsis*'s gynoecium from WT (Wild Type) and *NGA* quadruple homozygous mutant plants. (va: valve, sty: stigmatic papillae, stg: stigmatic papillae) (Alvarez *et al.*, 2009) (B) The genetic model proposed by Alvarez *et al.*, 2009 of the regulation pathway of *NGA* in promoting style formation at the 6-9 stages (when *NGA* is not expressed – B.I), and at the 9-11 stages (when *NGA* is expressed – B.II). (C) Sequential activation of transcription factors and heterodimer formation required to direct stigma development proposed by Ballester *et al.*, 2021 The solid gray lines indicate that the NGA-HEC heterodimer is likely reinforcing each other's expression. HEC being in a gray square means that its incorporation into this complex is not fully validated. Solid black lines indicate gene activation. Gray dashed lines represent the incorporation of the transcription factors into the protein complex.

The *NGA* genes are not as studied in other species as in *Arabidopsis*. Nonetheless, their role in carpel development seems to be conserved in other flowering pants. Virus-induced gene silencing (VIGS) mediated inactivation of *NGA* genes in the basal eudicot *Eschscholzia californica* and in the core eudicot asterid *Nicotiana benthamiana* provoked the loss of style and stigma development; however, their molecular mechanism in these plants has not been studied yet (Fourquin and Ferrándiz, 2014) (**Figure 1.9**).

Figure 1.9. *Eschscholzia californica* (A) and *Nicotiana benthamiana* (B) carpels from WT plants and from plants with the *NGA* genes silenced by VIGS. (Fourquin and Ferrándiz, 2014).

In this master's thesis I have studied the function of *NGA* genes in rice to see if their role is also conserved in phylogenetically distant plants such as monocots. Rice has a total of 7 NGA genes (Pfannebecker *et al.*, 2017), but previous studies in our lab clarified that only 4 of them are expressed in the flower carpel (Dreni *et al.*, unpublished), suggesting that the other 3 are not involved in its development. For this reason, only these 4 genes have been considered in this master's thesis.

2. Objectives

The main objective of this master's thesis is to characterize the function of the four rice *NGA* genes (*NGA1*, *NGA2*, *NGA3,* and *NGA4*) that are expressed in the gynoecium. To achieve this objective, a series of sub-objectives were proposed:

1. Obtain, propagate, and grow WT and *nga* mutant rice plants.
2. Analyse the fertility and fruit development capacity of the mutant plants.
3. Characterize the mutant plants' pistil and developing fruits phenotypes.
4. Determine if the mutants have their vegetative development altered.
5. Check if these *NGA* are also involved in pollen development and viability.
6. Do a histological analysis of mutant inflorescence primordia to determine the effect of the lack of *NGA* expression to style, stigma, and ovule from early to mature stages of development.
7. Perform an RNA-seq analysis to compare gene expression in inflorescence meristems from WT and *nga* quadruple homozygous mutant plants.

3. Materials and methods

3.1. Plant material and growth conditions

3.1.1. Mutations

Oryza sativa plants, specifically from the Dongjin cultivar, were used in the development of this master's thesis. The plants used had different combinations of mutations in the *NGA* genes, but the most extensively studied in this thesis is the quadruple homozygous mutant, with all four *NGA* genes mutated. These mutations had been generated before the start of this project. They consist of two mutations done by CRISPR/Cas9 in *NGA1* (LOC_Os02g45850) and *NGA2*

(LOC_Os03g02900) that cause these genes to not be functional. These mutations consist of a single nucleotide deletion in *NGA1* disrupting the reading frame from inside the B3 DNA binding domain; and a deletion of 17 nucleotides, followed by a single nucleotide deletion which restores the correct reading frame 41 nucleotides downstream in *NGA2*, resulting in a putative translated NGA2 protein where the only the B3 DNA binding domain is disrupted. The *NGA3* (LOC_Os04g49230) and *NGA4* (LOC_Os10g39190) have a T-DNA insertion in the gene promoter that leads to the decrease of their expression, which means that they are not null mutants. Two different T-DNA mutant alleles for each gene have been discovered and characterized in the host lab before this master thesis (all of them are ~10 kb T-DNA insertions in the promoter but in different positions): the *nga3-1* and *nga3-2*, and the *nga4-1* and *nga4-2* (**Figure 3.1**).

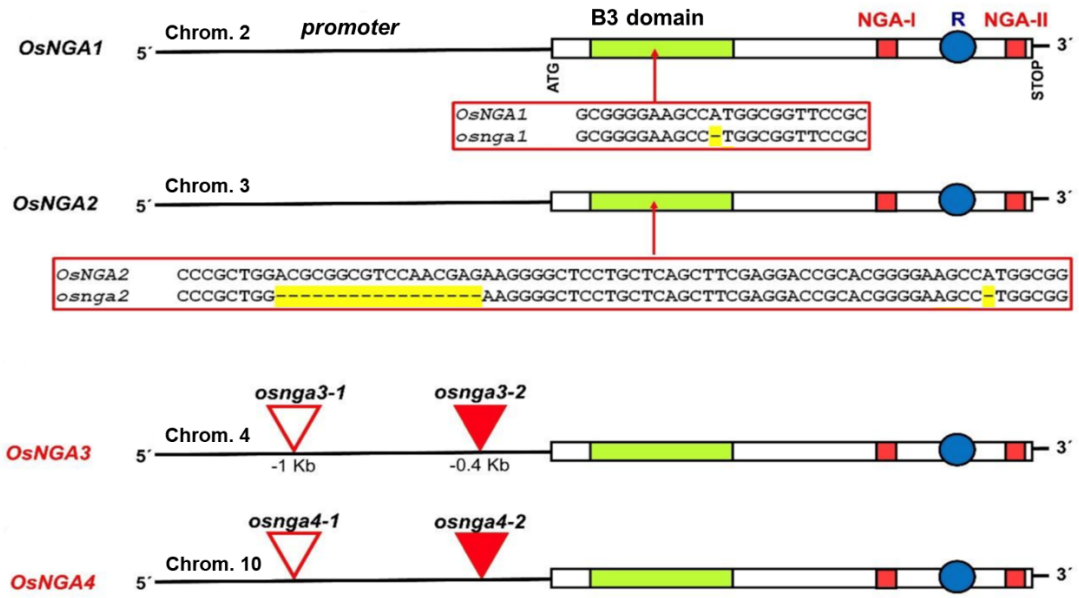

Figure 3.1. Schematic representation of the 4 *NGA* genes of rice that were studied and of their mutant alleles. The deleted nucleotides in *NGA1* and *NGA2* open reading frames are indicated in the insets. The red triangles are showing the T-DNA insertions found in *NGA3* and *NGA4*.

3.1.2. Plant propagation and growth

There are two ways to propagate the plants, it can be done via seeds (sexual reproduction) or in a vegetative way (clonal reproduction). To propagate them using seeds, the following method is used. The rice panicles are harvested a month or more after fertilization, put into paper bags, and left to dry for a minimum of three days. After that, the lemma and palea are discarded (optional) and the rice grains are submerged in water with some drops of Fe3+ solution, for another two or three days at 28oC. After the time has passed, the shoot should have begun to emerge, and the seed is ready to be planted. Plastic pots 20 cm in diameter and 25 cm in height, filled whit a mixture of peat:perlite:vermiculite

(1:1:1), were used to grow the plants. Before planting the germinated seeds, the pots are filled with the soil mixture and soaked with hydroponic solution until all the substrate is wet. Then, the pregerminated seeds are buried in the soil leaving the small shoot on the surface. After that, the pots are carefully watered with a mix of the hydroponic solution supplemented with Fe3+, covered with plastic bags with a small hole to maintain humidity, and placed in the phytotron at long day conditions (16 h of light (28 ºC) and 8 h of darkness (22 ºC)).

Rice plants can also be propagated vegetatively after fruit development and maturation. This process consists of cutting the aerial part of old multistemmed plants after their reproductive cycle, in a way that its total height is about 10 cm, and then removing the old roots and dead tissues. Then, the different shoots of a plant can be separated to generate more new clone plants. Finally, all the shoots are planted in new pots with wet soil and placed in the phytotron at long-day conditions (16 h of light (28 ºC) and 8 h of darkness (22 ºC)).

After the plants have grown enough, they are ready to be moved to short-day conditions (10 h of light (28 ºC) and 14 h of darkness (22 ºC)) to induce flowering. After about a month the flowers will be fully developed, and the pollination will take place; after another 30-40 days, the panicles will be ready to be harvested.

3.2. Genotyping

3.2.1. Genomic DNA extraction

The genomic DNA was extracted using the “Quick & Dirty” method. The samples used for this process were portions of 2 cm of young leaves. The samples were introduced in 2 ml Eppendorf tubes together with a steel bead, some grains of sea sand, and 380 µl of extraction buffer (Tris-HCl 200 mM pH 7,5; NaCl 250 mM; EDTA 25 mM pH 7,5). Then, the samples were ground using a Retsch Mixer Mill 400 at 30 Hz for 1 minute (or until the sample is smashed). Add 20 µl of SDS 20% reaching a final volume of 400 µl in each tube. Mix the contents of the tubes using a vortex; and centrifugate them at 13.000 rpm for 2 minutes. Select the supernatant by transferring 300 µl of it into a new 1,5 ml Eppendorf tube, and add 270 µl of isopropanol; then invert the tubes several times to make sure everything is mixed. To precipitate the genomic DNA, centrifugate the mix at 13.000 rpm for 15 minutes and discard the supernatant. Then, wash the pellet with 1 ml of ethanol 70%, mix by inverting the tubes gently, and discard the ethanol (to eliminate the final residue make a centrifuge pulse and use a pipette to extract as much liquid as possible without disturbing the pellet). Leave the tubes open inside the extraction hood for 30 minutes to dry the pellet and resuspend it with 30 µl of an RNase-A solution (at a concentration of 10 µg/ml distilled water).

Finally, incubate the mix in a thermoblock for 30 minutes at 27ºC while shaking at 1200 rpm. The purified genomic DNA can be stored at 4ºC or -20ºC until the time to use it.

3.2.2. Sequencing

To be able to sequence a DNA section it has to be amplified by a Polymerase Chain Reaction (PCR) first; and then, this PCR product has to be prepared accordingly. To carry out this process we start by taking 10 µl of the PCR product and transferring it into a new 1,5 ml Eppendorf tube. Add 9 µl (90% of the PCR product volume used) of isopropanol and mix by inverting the tube. Centrifugate for 15 minutes at maximum rpm and discard the supernatant with a pipette. Wash the pellet with 200 µl of ethanol 70% previously cooled in ice, and dry the pellet leaving the tube open inside the extraction hood turned on for 15 minutes. Next, resuspend the pellet with 10 µl of milli-Q water and measure the DNA concentration with the nanodrop to determine the dilution needed to reach 10 ng/µl, which is the concentration required for the Sanger sequencing service.

3.2.3. Genotyping

The purified genomic DNA is ready to be used for genotyping by PCR or by sequencing (after performing PCR). In **Table 3.1** are indicated the different primers used for each PCR reaction done during the genotyping process. The mutations in the *NGA3* and *NGA4* genes can easily be detected by doing a PCR followed by an electrophoresis in a 1,5% agarose gel, due to their nature as T-DNA insertions. Their identification consists of doing a pair of PCR reactions with different primers: (I) one reaction to detect the presence of the T-DNA; it uses one primer corresponding to a known genomic sequence near the T-DNA insertion, and the other primer belonging to the T-DNA left or right border sequence. (II) And the other reaction to detect the absence of the T-DNA, in which the two primers correspond to a known genomic sequence, each one flanking the insertion site of the T-DNA so that the amplification is only possible from the wild type (WT) allele lacking the large insertion. Analyzing the PCR results with an electrophoresis allows to identify if the plants are WT, mutants homozygous, or mutant heterozygous for each gene.

Sequencing is indispensable to detect *NGA1* mutation because it consists of a single nucleotide deletion. To characterize this mutation, the first step is to do a PCR reaction to amplify the gene, then run a 1,5% agarose gel to make sure the PCR worked properly. Then, prepare the DNA for sequencing and sequence it using the IBMCP Sanger sequencing service. Finally, analyze the sequence obtained to see if the deletion is present in homozygosis, heterozygosis, or not at

all, using the http://crispid.gbiomed.kuleuven.be/ website, which allows to differentiate overlapping sequences from a sample that have a deletion generated by CRISPR/Cas9 in one allele.

The mutation in *NGA2* has a considerable deletion, so it is possible to identify it by running a high concentration agarose gel (around 3,5-4%) after performing a PCR reaction in which a small DNA segment encompassing the mutation has been amplified. The difference in size between the WT gene and the mutant one is enough to be appreciated as two different bands in this agarose gel. However, it is also recommended to sequence the gene to validate the electrophoresis results.

Table 3.1. Primers used to genotype the NGA genes in the rice plants.

Primer	Sequence	Affected gene
LD321 LD232	5´-GTCGTCTCCTGCTCATCACG-3´ 5´-AAGTCGAGGCCTTGCCTGAG-3´	*NGA1* (WT and mutant)
LD341 LD234	5'-AGCACGCGGAGAAGTACTTC-3' 5´-GCCAGTCGATGAAGAGCCTC-3´	*NGA2* – to genotype by electrophoresis
LD233 LD234	5´-GCCAGTCGATGAAGAGCCTC-3´ 5´-GCCAGTCGATGAAGAGCCTC-3´	*NGA2* – to sequence
LD131 LD132	5´-AGCTTTGCATCACGTACTGG-3´ 5´-AATGGGAATTGATGGTGCTG-3´	*NGA3* WT to genotype *nga3-1*
LD131 Osp95	5´-AGCTTTGCATCACGTACTGG-3´ 5´-GTCCGCAATGTGTTATTAAGTTGTC-3´	*nga3-1: NGA3* with T-DNA insertion
LD133 LD134	5´-CTCGCAGCAAGATCCAAACG-3´ 5´-AAGCCGTGGTATGGTACGAG-3´	*NGA3* WT to genotype *nga3-2*
LD133 Osp79	5´-CTCGCAGCAAGATCCAAACG-3´ 5´-GGACGTAACATAAGGGACTGAC-3´	*nga3-2: NGA3* with T-DNA insertion
LD125 LD126	5´-TGCTTCCAGTACTGCTCATG-3' 5´-GATTCTGATTGGCTCTAGCAC-3´	*NGA4* WT to genotype *nga4-1*
LD126 Osp79	5´-GATTCTGATTGGCTCTAGCAC-3´ 5´-GGACGTAACATAAGGGACTGAC-3´	*nga4-1: NGA4* with T-DNA insertion
LD127 LD128	5´-GGCTATATACCTACTTGTGC-3´ 5´-AATTCCGGGAGCTAAGTTGG-3´	*NGA4* WT to genotype *nga4-2*
LD127 Osp79	5´-GGCTATATACCTACTTGTGC-3´ 5´-GGACGTAACATAAGGGACTGAC-3´	*nga4-2: NGA4* with T-DNA insertion

3.3. Phenotyping

3.3.1. Fertility and fruit development

During the mutant phenotyping, panicles from the different plants were collected at the end of reproductive phase and left to dry at room temperature. To calculate plant female fertility, the percentage of mature fruits was estimated (the rice fruit contains only one seed); and to find statistical differences, an ANOVA test followed by a post hoc test was performed using the JASP software. Then, to

determine the fruit development capacity of each genotype, the fruits were divided into four groups depending on their phenotype (mature fruits, late abortions, early abortions, and not pollinated (**Figure 4.3C**)), and the number of fruits in each category was counted to calculate the percentage of fruits from each phenotype.

- Mature fruits: Viable mature fruits properly developed.
- Late abortions: Fruits that abort after filling almost all the floret.
- Early abortions: Fruits that begin their development but abort shortly after.
- Not pollinated: Ovaries that have not been fertilized, and so there is no fruit development.

For these analysis, the fruits from three panicles for each genotype were sorted into the different categories (except in two genotypes in which only two panicles were available). In total, the number of fruits counted range between 100 – 200.

3.3.2. Pistil and developing fruit shape analysis

For pistil shape analysis, developed florets that did not have performed anthesis yet were stored in 2 ml Eppendorf tubes with a piece of damp paper at the bottom. The tubes were put in ice and taken to the laboratory for analysis. With the help of a tweezer, needles and a pointy stick, the lemma, palea, lodicules, and stamens were removed from each floret leaving only the pistil. Finally, images of each pistil were taken using a Leica macroscope and the Leica LAS X software. The same steps were followed for developing fruit shape analysis, but the florets were taken 2-7 days after anthesis, when the fruit had already begun its development.

3.3.3. Flag leaf analysis

The middle section of the flag leaf of the desired plants was collected some days after anthesis. It was placed in small glass bottles filled with ethanol 70% to conserve them and to remove the chlorophyll for better visualization. The ethanol 70% solution was replaced regularly until the leaves were completely white. Then, a 3 cm wide band from each leaf was cut and mounted between two glass microscope slides with a little bit of ethanol 70% to avoid dehydration. A picture of each band was taken using a Leica macroscope and the Leica LAS X software. From these pictures, the leaf width and the vein number were analyzed using ImageJ.

3.4. Rice plants crossing

To make a cross between two specific plants, it is important to choose parents that are flowering more or less at the same time. The cross has to be done in the morning just before the anthesis. It consists of the emasculation of the mother plant inflorescence by removing the anthers when they have grown enough to reach the top of the spikelet. To remove the anthers, the tip of the spikelet is carefully cut so all the anthers can be removed by using histological tweezers but the pistil is still intact. Then, the parental panicles are covered together by a paper box and the plant is shaken 2-3 times a day for 3 days, until anthesis has passed. Then the paper box is left covering the panicles for some more days to prevent pollen contamination from surrounding plants and to protect the young naked fruits.

3.5. Histology

3.5.1. Inflorescence primordia, flower, and fruit sampling and fixation

Rice inflorescence begin to develop from the apical meristem at the base of the shoot protected by several wrapped leaf primordia, so to extract them the shoot has to be cut and the leaf sheaths have to be removed until reaching the center, where the inflorescence is developing. This process is done very carefully, with the help of tweezers so the inflorescence primordia is not damaged, since the amount of material from plants grown in chambers is very limited, in particular from sterile quadruple mutants. Inflorescence primordium is initiated around 13-15 days after floral induction (done by putting the plants in short-day conditions), so starting after the 13^{th} day, each day a shoot is cut to check the stage of inflorescence development until it is at the desired stage; at that moment, all the required primordia are collected. Flower and fruit collection are easier, as they can be picked up from the panicle when they are in the desired stage.

The collected samples are put in falcon tubes with FAA 4% fixation buffer (containing formaldehyde 4%, acetic acid 5%, ethanol 50%, and the remaining volume filled with milli-Q water) and maintained in ice. Once the samples are collected, apply vacuum for 15 minutes under the fume hood and leave them overnight. The next day, wash the samples three times with ethanol 70%, leaving 5 minutes between washes, and store them at $4^{o}C$ in ethanol 70% until the time of use.

3.5.2. Tissue embedding in Technovit 7100

The collected samples are fixed in FAA buffer as described above, and then they are embedded. First, they have to be dehydrated by increasing the ethanol concentration in which they are submerged, beginning with 80%, then 90%, and

95%, leaving one hour between each change. To finish the dehydration process, use ethanol 100% two times, changing it after 30 minutes. After another 30 minutes begins the infiltration, that consists of placing the samples in solution A:ethanol 100% at a 1:1 ratio. Solution A is composed of 100 ml of Technovit 7100 and one bag of hardener I provided with the Technovit 7100 kit. After leaving the samples 2 hours at 4ºC put them in solution A 100%, apply vacuum for 10 minutes, and leave them overnight at 4ºC. The following day it's time to do the polymerization. To do it, first preheat the histoform mold at 37ºC and fill it with solution B (composed of solution A and hardener II in an 11:1 ratio, mixed at the moment of use). Then, put the samples inside the mold making sure it is placed in the desired position, because when the polymerization and hardening of the resin starts, the sample can not be moved anymore. Incubate at 37ºC for 1 hour and leave it at 4ºC overnight. The next day, to attach the plastic histoblocs to the solid histoform, apply the 3400 resin and leave it harden for at least a few hours under the fume hood. Then, extract the histoforms from the mold and use a microtome with specific holder and blades for this kind of hard resins, to cut them into 6 nm sections.

Each section has to be cut independently, picked with the tweezers making sure it does not fold (and if it does, unfold it with a small painter brush), and let it fall into a microscope slide with milli-Q water on top so it floats and stretches properly. When the slide is full of sections (usually six), remove the excess of water and let the slide dry by putting it on top of a heater at 45ºC. When it is completely dry, store it to protect it from dust.

3.5.3. Toluidine blue staining and histological analysis

For staining, preheat the slides at 65ºC for 15 minutes, dip them in Toluidine Blue solution 0,1% for two minutes, and rinse them twice with milli-Q water. Let them dry and store them until mounting with milli-Q water and a coverslip, and observation at the microscope equipped with a digital camera.

3.6. RNA sequencing of rice inflorescence primordia

3.6.1. Tissue collection and RNA extraction

The primordia were obtained in the same way as described above (3.5.1), staged with a ruler, frozen in Eppendorf tubes in liquid nitrogen, and stored at -80°C. For RNA extraction, the RNeasy Plant Mini Kit Qiagen was used. Grind the samples inside the tubes using frozen small plastic sticks, or into frozen mortars, and place them into a 2 ml microcentrifuge tube (being careful not to let the tissue thaw). Add 450 µl of Buffer RLT (provided by the Kit), mix with a vortex, and incubate at 56ºC for 1-3 minutes. Transfer the lysate to a QIAshredder spin column provided

by the kit, centrifugate for 2 minutes at full speed, and transfer the supernatant of the flow-through to a new 1,5 ml tube. Add ½ volume of ethanol 96-100%, mix, and transfer everything to an RNeasy spin column provided by the Kit. Centrifugate at more than 10.000 rpm for 15 seconds and discard the flow-through. Add 350 µl of Buffer RW1 (provided by the Kit) to the column, centrifugate at more than 10.000 rpm for 15 seconds, and discard the flow-through. Purification from genomic DNA contaminations: mix 10 µl of DNase I and 70 µl of Buffer RDD (both provided by the Kit), transfer it to the column, and incubate at room temperature for 15 minutes. After the time has passed, add 350 µl of Buffer RW1, centrifugate at more than 10.000 rpm for 15 seconds, and discard the flow-through. Add 500 µl of Buffer RPE, centrifugate at more than 10.000 rpm for 15 seconds, and discard the flow-through to clean the column. Repeat this step again but centrifuging for 2 minutes. Place the RNeasy spin column in a new 1,5 ml collection tube, place 30-50 µl of RNAse-free water to elute the RNA, centrifugate at more than 10.000 rpm for 1 minute and keep the flow-through, which will be sent to sequence. Meanwhile, samples are handled wearing clean gloves and with special care to avoid RNAse contamination, and stored at -80°C.

3.6.2. RNA sequencing and analysis

The purified RNA was sent to BGI Hong Kong genomics for sequencing. This company takes care of sample quality checks, preparation, library construction, sequencing, processing the raw data output, and doing the bioinformatics analysis. The RIN (RNA Integrity Number) value of our samples was 10 (intact RNA). Paired end reads of 100 bp were sequenced using the DNBSEQ sequencing platform to generate at least 70 million reads per sample. Then the raw data (containing low quality reads, reads with adaptor sequences, and reads with high levels of N base) were filtered before data analysis. In our analysis, this resulted in ~ 94% of clean reads for most of the samples. HISAT was used to align the clean reads to the reference genome, with a total mapping ratio of ~ 97, and Bowtie2 to align them to the reference genes, with a total mapping ratio of ~ 84. We requested to use the most recent MSU Rice Genome Annotation Release 7. For each sample, the read count, the FPKM (Fragments Per Kilobase Million), and the TPM (Transcripts Per Million) were calculated, and with this information the Differentially Expressed Genes (DEGs) were determined.

4. Results

4.1. Genotyping and phenotyping the *NGA* mutants

4.1.1. Mutant plant obtention

Previous analyses of several CRISPR alleles done in the host lab identified *nga1-1* and *nga2-1* mutants as likely null alleles that were therefore selected for this thesis, and I will simply refer to them as *nga1* and *nga2* hereafter. During the development of my master's thesis, I analyzed two segregating generations of *NGA* quadruple mutants and an independent group of triple *NGA* mutants (*NGA1 nga2 nga3-1 nga4-1*). The first generation was the result of a screening of the quadruple mutant heterozygous (*nga1/+ nga2/+ nga3-2/+ nga4-2/+*) descendants (F2, more than 300 plants); which had the aim of finding quadruple homozygous mutant (*nga1 nga2 nga3-2 nga4-2*) and other interesting combinations of mutant genotypes. This screening was done before the start of this thesis, and I started with 19 preselected plants that had different combinations of the *nga1, nga2, nga3-2* and *nga4-2* mutations, including only one quadruple homozygous mutant for the four *NGA* genes studied. I genotyped these plants again to make sure that the genotype previously assigned to each one was correct (**Table 4.1**) (**Annex 1**). With this first generation I also analyzed the plants from the independent group carrying different T-DNA alleles in *NGA3* and *NGA4*, in which all of them had the same genotype: *NGA1 nga2 nga3-1 nga4-1* (**Table 4.2**) (**Annex 1**).

Table 4.1. Members of the first generation of plants and their genotypes. The colors are indicating the state of the genes: Blue for WT genes, black for mutations in heterozygosis, and red for mutations in homozygosis.

	F2 progeny of the quadruple heterozygote:			
Plant code	***OsNGA1***	***OsNGA2***	***OsNGA3***	***OsNGA4***
8	*nga1*	*nga2*	*nga3-2*	*nga4-2*
11	*nga1/+*	*nga2*	*nga3-2*	*nga4-2/+*
12	*nga1*	*nga2/+*	*nga3-2*	*nga4-2/+*
14	*nga1*	*nga2/+*	*nga3-2*	*nga4-2*
1C6	*nga1*	*nga2*	*nga3-2*	*NGA4*
1C7	*nga1*	*nga2/+*	*nga3-2*	*nga4-2*
1C12	*NGA1*	*nga2/+*	*nga3-2*	*nga4-2*
1F6	*nga1*	*nga2/+*	*nga3-2*	*nga4-2/+*
2C12	*nga1/+*	*nga2*	*nga3-2*	*nga4-2/+*
2D7	*nga1*	*nga2/+*	*nga3-2*	*nga4-2/+*
2G4	*nga1*	*nga2/+*	*nga3-2*	*nga4-2*
2H12	*nga1/+*	*nga2*	*nga3-2*	*nga4-2/+*
3A11	*nga1*	*nga2/+*	*nga3-2*	*nga4-2/+*
3A12	*nga1*	*nga2*	*NGA3*	*nga4-2/+*

3D8	*NGA1*	*nga2/+*	*nga3-2*	*nga4-2/+*
3D9	*nga1*	*nga2/+*	*nga3-2*	*nga4-2/+*
3F6	*nga1*	*nga2*	*nga3-2*	*nga4-2/+*
4A11	*nga1/+*	*nga2*	*nga3-2*	*nga4-2/+*
4B12	*nga1/+*	*nga2*	*nga3-2*	*nga4-2*

Table 4.2. Members of the independent group of triple mutant plants (*NGA1 nga2 nga3-1 nga4-1*). The colors follow the same code as in the previous table.

Triple homozygotes *nga2 nga3-1 nga4-1*:

Plant code	***OsNGA1***	***OsNGA2***	***OsNGA3***	***OsNGA4***
7	*NGA1*	*nga2*	*nga3-1*	*nga4-1*
8	*NGA1*	*nga2*	*nga3-1*	*nga4-1*
9	*NGA1*	*nga2*	*nga3-1*	*nga4-1*
F2 8-1	*NGA1*	*nga2*	*nga3-1*	*nga4-1*
F2 8-2	*NGA1*	*nga2*	*nga3-1*	*nga4-1*
F2 8-3	*NGA1*	*nga2*	*nga3-1*	*nga4-1*
F2 8-4	*NGA1*	*nga2*	*nga3-1*	*nga4-1*
F2 8-5	*NGA1*	*nga2*	*nga3-1*	*nga4-1*

The quadruple homozygous mutant plants are infertile, as they do not develop viable fruits. To obtain more quadruple homozygous mutant plants, the second generation of *NGA* mutants was developed. It consists of the descendants of 3 plants from the first generation that had the *nga1 nga2/+ nga3-2 nga4-2* mutations. This genotype was chosen because it was the one that had the maximum number of *NGA* genes mutated in homozygosis while also having enough viable fruits (see paragraph 4.1.2), suggesting that the four genes are not equally redundant and that *NGA2* contributes more to their common functions in floral development. Since only one *NGA* gene is heterozygous in these plants (*NGA2*), ¼ of the descendants should be quadruple homozygous mutants. Indeed, from a total of 36 seeds, I obtained 9 quadruple homozygous mutants (*nga1 nga2/+ nga3-2 nga4-2*), 18 that maintained the parental's phenotype (*nga1 nga2/+ nga3-2 nga4-2*), and 9 triple mutants with *NGA2* WT (*nga1 NGA2 nga3-2 nga4-2*) (**Annex 2**). From these plants I selected 9 from each genotype and transplanted them into several pots (three plants per pot) (**Table 4.3**).

Table 4.3. Members of the second generation of plants and their genotypes. The colors follow the same code as in the previous tables.

Progeny of *nga1 nga2/+ nga3-2 nga4-2*:

Plant code	*OsNGA1*	*OsNGA2*	*OsNGA3*	*OsNGA4*
1	*nga1*	*NGA2*	*nga3-2*	*nga4-2*
2	*nga1*	*nga2*	*nga3-2*	*nga4-2*
4	*nga1*	*nga2*	*nga3-2*	*nga4-2*
5	*nga1*	*nga2*	*nga3-2*	*nga4-2*
6	*nga1*	*NGA2*	*nga3-2*	*nga4-2*
7	*nga1*	*nga2*	*nga3-2*	*nga4-2*
9	*nga1*	*nga2*	*nga3-2*	*nga4-2*
10	*nga1*	*nga2/+*	*nga3-2*	*nga4-2*
11	*nga1*	*nga2/+*	*nga3-2*	*nga4-2*
12	*nga1*	*NGA2*	*nga3-2*	*nga4-2*
13	*nga1*	*nga2/+*	*nga3-2*	*nga4-2*
14	*nga1*	*nga2/+*	*nga3-2*	*nga4-2*
15	*nga1*	*NGA2*	*nga3-2*	*nga4-2*
16	*nga1*	*NGA2*	*nga3-2*	*nga4-2*
17	*nga1*	*NGA2*	*nga3-2*	*nga4-2*
18	*nga1*	*NGA2*	*nga3-2*	*nga4-2*
21	*nga1*	*NGA2*	*nga3-2*	*nga4-2*
24	*nga1*	*nga2*	*nga3-2*	*nga4-2*
25	*nga1*	*nga2*	*nga3-2*	*nga4-2*
27	*nga1*	*nga2*	*nga3-2*	*nga4-2*
29	*nga1*	*nga2/+*	*nga3-2*	*nga4-2*
30	*nga1*	*NGA2*	*nga3-2*	*nga4-2*
31	*nga1*	*nga2/+*	*nga3-2*	*nga4-2*
33	*nga1*	*nga2*	*nga3-2*	*nga4-2*
34	*nga1*	*nga2/+*	*nga3-2*	*nga4-2*
35	*nga1*	*nga2/+*	*nga3-2*	*nga4-2*
36	*nga1*	*nga2/+*	*nga3-2*	*nga4-2*

In summary, from both generations I obtained quadruple homozygous mutant plants. From the first one I only had one plant, which was later propagated vegetatively to generate several clones (**Figure 4.1A**). From the second generation I obtained 9 plants that were ready to be analyzed after summer 2022 (**Figure 4.1B**). When comparing the DJ (WT) and the quadruple homozygous mutant (*nga1 nga2 nga3-2 nga4-2*) obtained, it was apparent that the mutant plants were shorter, more compact, and with wider leaves than the WT (**Figure 4.1**).

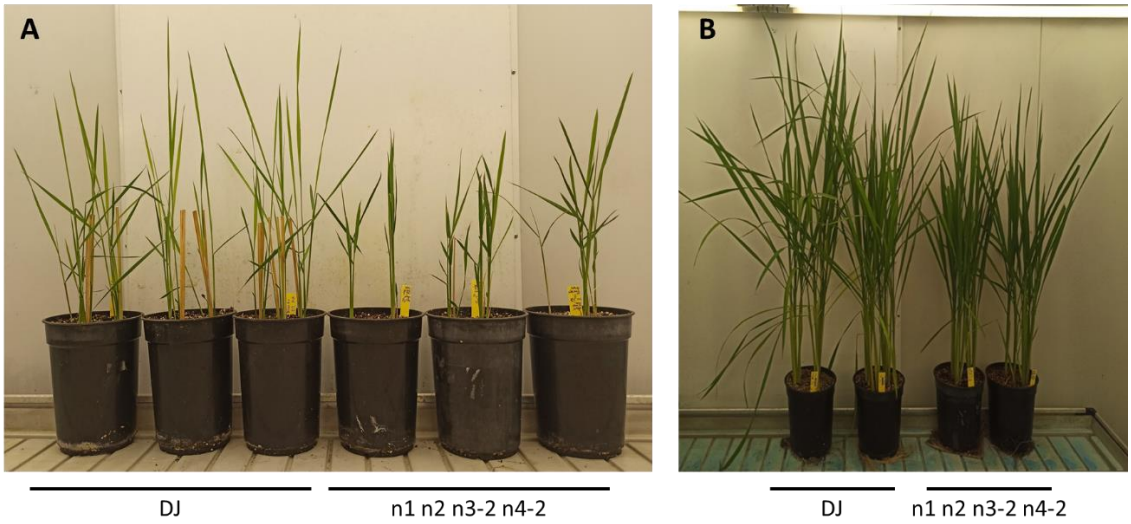

Figure 4.1. Photographies of WT controls and quadruple mutant homozygotes (*nga1 nga2 nga3-2 nga4-2*) obtained by vegetative propagation (A) and from seeds (B).

4.1.2. Analysis of the mutant's fertility and fruit development capacity

From the first generation of plants, I selected the ones with the most interesting genotypes and analyzed their phenotype by measuring their ability to develop fruits, and their fertility (by counting the number of mature fruits they were able to develop) (**Figures 4.2A and 4.3A**) (**Annex 3-8**). At the same time, I also analyzed these parameters in the independent group of triple mutant plants (*NGA1 nga2 nga3-1 nga4-1*) which grew and flowered together (**Figures 4.2A and 4.3A**); and later, in the second generation of plants (**Figures 4.2B and 4.3B**).

The fertility level of the different mutants indicates that the *NGA* genes act in a dose-dependent manner because the accumulation of mutated genes leads to a progressive decrease in fertility (**Figure 4.2**). As can be seen in the results from the first generation of mutant plants (**Figure 4.2A**), the DJ (WT) are the most fertile ones (with a fertility of the 95,8%), followed by the quadruple mutant heterozygous (*nga1/+ nga2/+ nga3-2/+ nga4-2/+*) (that has a 91,9% of fertility), however, there are no statistically significant differences between these two groups (p-value > 0,05). The next genotype with higher levels of fertility is the *nga1 nga2/+ nga3-2 nga4-2/+*, that has two mutant genes in homozygosis and the other two in heterozygosis; at this point plant fertility has been halved (45,2%). Next, comes another combination of two mutant genes in homozygosis and the other two in heterozygosis, *nga1/+ nga2 nga3-2 nga4-2/+*, which has its level of fertility (30,2%) reduced with statistical significance in comparison with the previous one. Then there are the mutants with all the genes in homozygosis except one that is in heterozygosis (*nga1 nga2/+ nga3-2 nga4-2*, *nga1/+ nga2 nga3-2 nga4-2* and *nga1 nga2 nga3-2 nga4-2/+*), with fertility levels of 9,9%, 0,7%, and 0%, respectively. These three genotypes, together with the quadruple

homozygous mutant (*nga1 nga2 nga3-2 nga4-2* – 0% fertility) and the independent group of triple mutants (*NGA1 nga2 nga3-1 nga4-1* – 1,6% fertility), do not show statistically significant differences. However, the most fertile one of these five genotypes (*nga1 nga2/+ nga3-2 nga4-2*) was the perfect candidate to produce new quadruple homozygous mutant plants, because it developed enough mature fruits to have a decent number of descendants, and at the same time only has one gene in heterozygosis, making genotyping almost effortless.

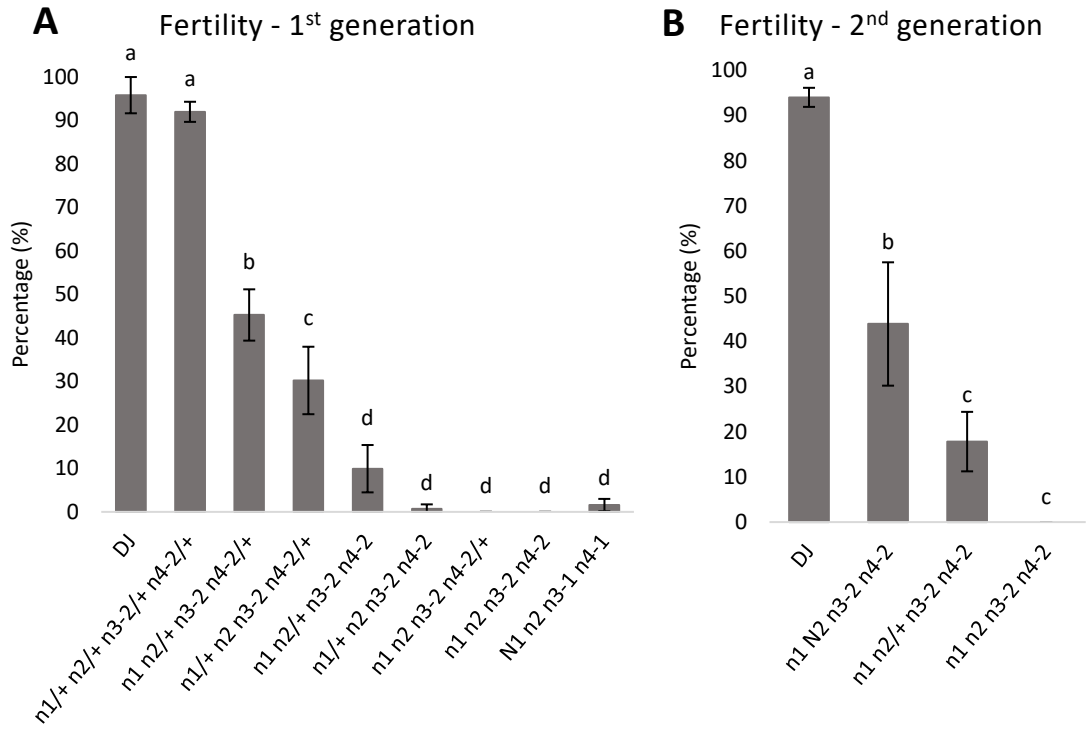

Figure 4.2. Graphs displaying the percentage of fertility from DJ (WT) plants and from plants with different combinations of *NGA* mutations from the first generation (A) and from the second generation (B). The different letters indicate statistically significant differences determined by a p-value < 0,05 (Statistic test: ANOVA followed by a post hoc test) (*n* = *nga; N* = *NGA*).

The tendency observed in the fertility of the first generation of plants was conserved in the second generation: where the DJ was still the most fertile one (94%); the *nga1 nga2/+ nga3-2 nga4-2* genotype had a similar level of fertility as seen in the previous generation (17,8%); and the quadruple homozygous mutant (*nga1 nga2 nga3-2 nga4-2*) was still infertile. The new phenotype characterized in this generation, the triple mutant *nga1 NGA2 nga3-2 nga4-2*, had around half the fertility of the DJ (43,9%), which, as expected, situates its fertility level between the DJ and the *nga1 nga2/+ nga3-2 nga4-2*. Between the two least fertile genotypes there was no statistically significant difference, but there were significant differences in fertility between the others genotypes from this generation (**Figure 4.2.B**).

Then, I also analyzed the fruits developed by the different mutants (**Figure 4.3**). I divided the fruits found into 4 categories according to their phenotype (**Figure 4.3C**): (**I**) Mature fruits are the ones that have developed correctly and are viable. (**II**) Late abortions happen when the fruit grows until almost filling the inside of the floret and then stops. (**III**) Early abortions are found in fruits that began to develop but abort shortly after, so they are very small. (**IV**) Not fertilized typically happens when the embryo sac is not fertilized and there is no fruit development. Fruits in categories II and III were typically filled by clear liquid, rather than starch and embryo as expected, before abortion and desiccation began. It is important to point out that such abortions could either develop from truly fertilized ovaries or as the result of some unexpected parthenocarpic effect, which is never seen in WT. Subsequent detailed histology will be required to clarify this phenotype.

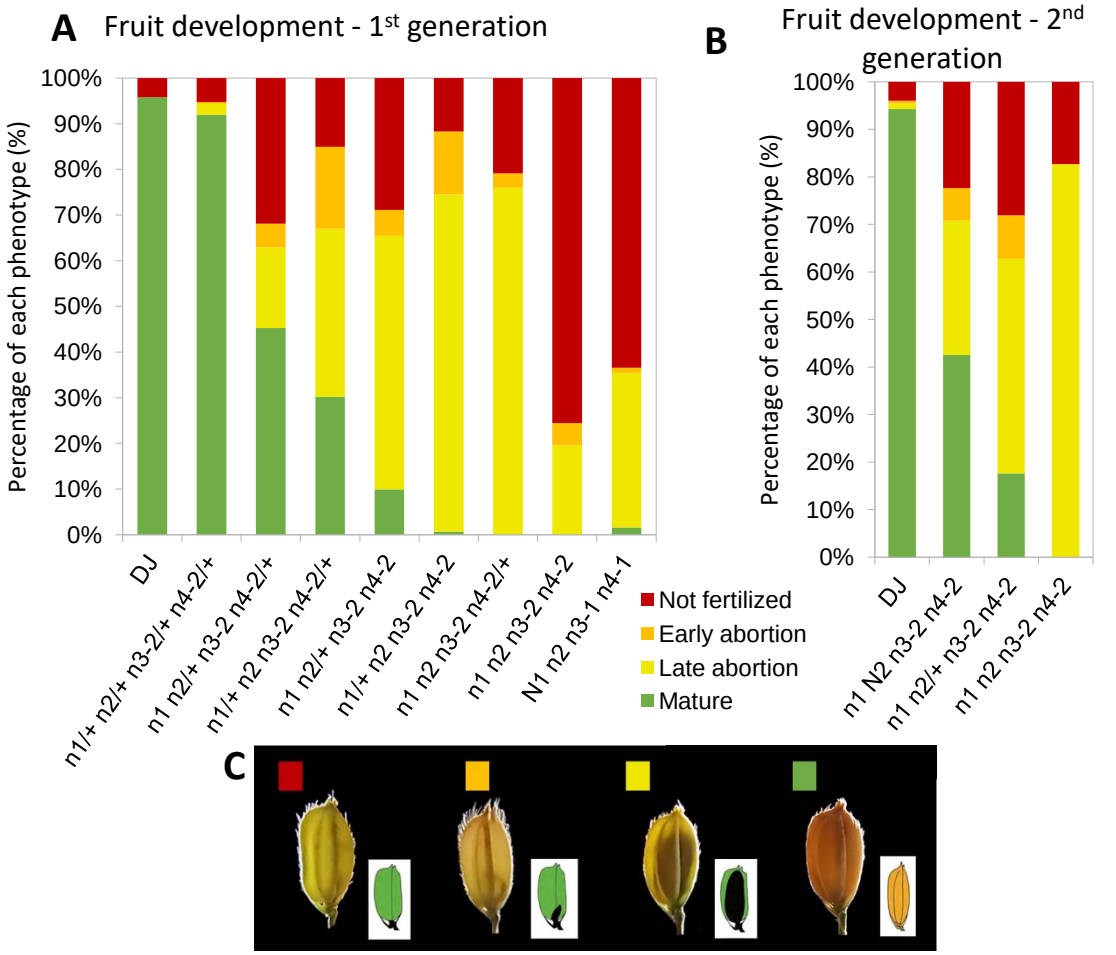

Figure 4.3. Image showing the four fruit phenotypes found in the studied plants (C), and graphs indicating the percentage of these phenotypes present in the same genotypes from Figure 4.2 (*n = nga; N = NGA*). (A) Representation of the results from the first generation of plants. (B) Representation of the results from the second generation of plants. The fruit phenotype percentage is indicated by colors: red displays not fertilized flowers; orange means ovaries that began their development but aborted very soon; yellow is indicating fruits that aborted their development later than the previous ones; and green is representing the fully developed mature fruits. (Drawings of the phenotypes adapted from Hardke *et al.*, 2013).

In the first generation of plants (**Figure 4.3A**), the results show that as the number of mutations in homozygosis grows, the percentage of mature fruits decreases; this is to be expected because the percentage of mature fruits corresponds to the plant fertility percentage. However, the percentage of not pollinated and early abortions stays more or less constant, whereas late abortions become more common. This happens until reaching the quadruple homozygous mutant (*nga1 nga2 nga3-2 nga4-2*), where the not fertilized is the predominant category found. However, the triple mutant plants from the independent group (*NGA1 nga2 nga3-1 nga4-1*) show a similar behavior as the quadruple homozygous mutant, with a majority of not fertilized pistils, despite their reduction in style and stigma development is relatively mild (see next paragraph and **Figure 4.4**).

In the second generation this tendency is maintained (**Figure 4.3B**). With the percentage of mature fruits decreasing as the number of mutations increases; and the percentage of late abortions increasing, while the early abortions and the not fertilized flower percentages remain more or less the same. Nevertheless, in this generation, this tendency is also conserved in the quadruple homozygous mutant, unlike in the first generation.

4.1.3. Analysis of the mutant's pistil development

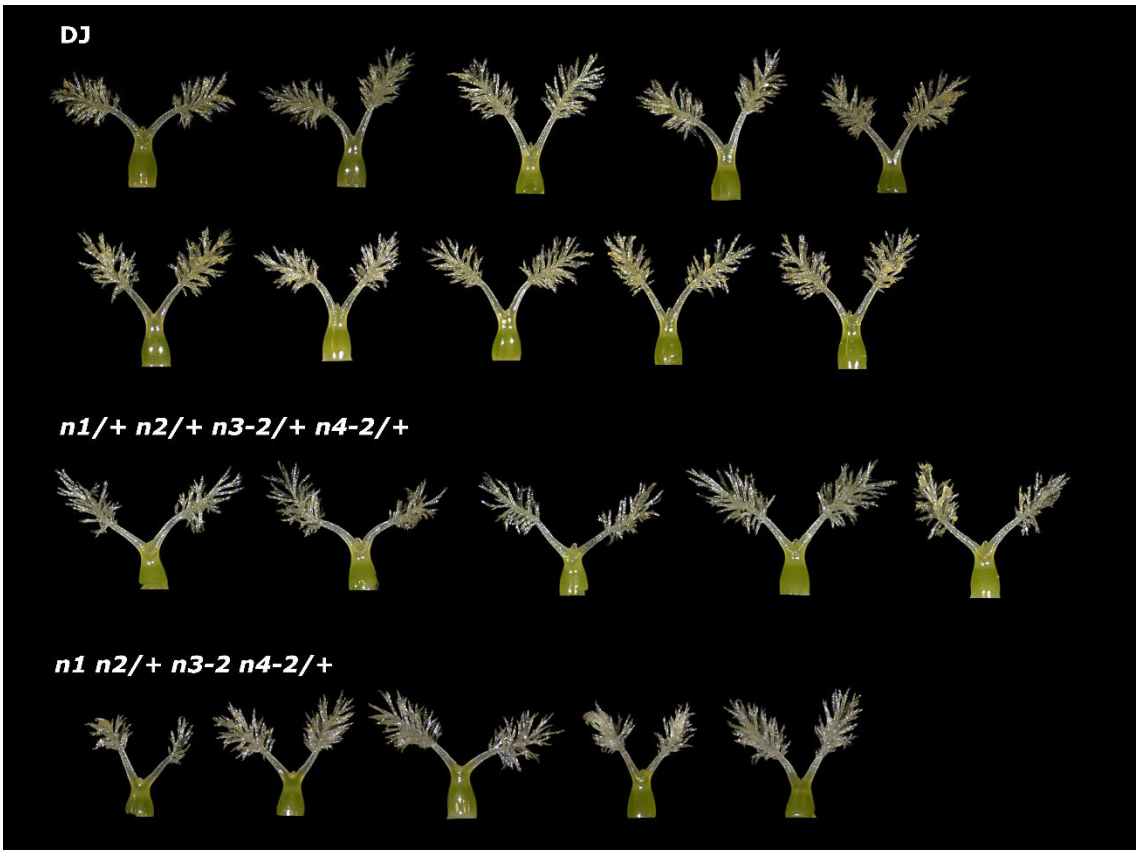

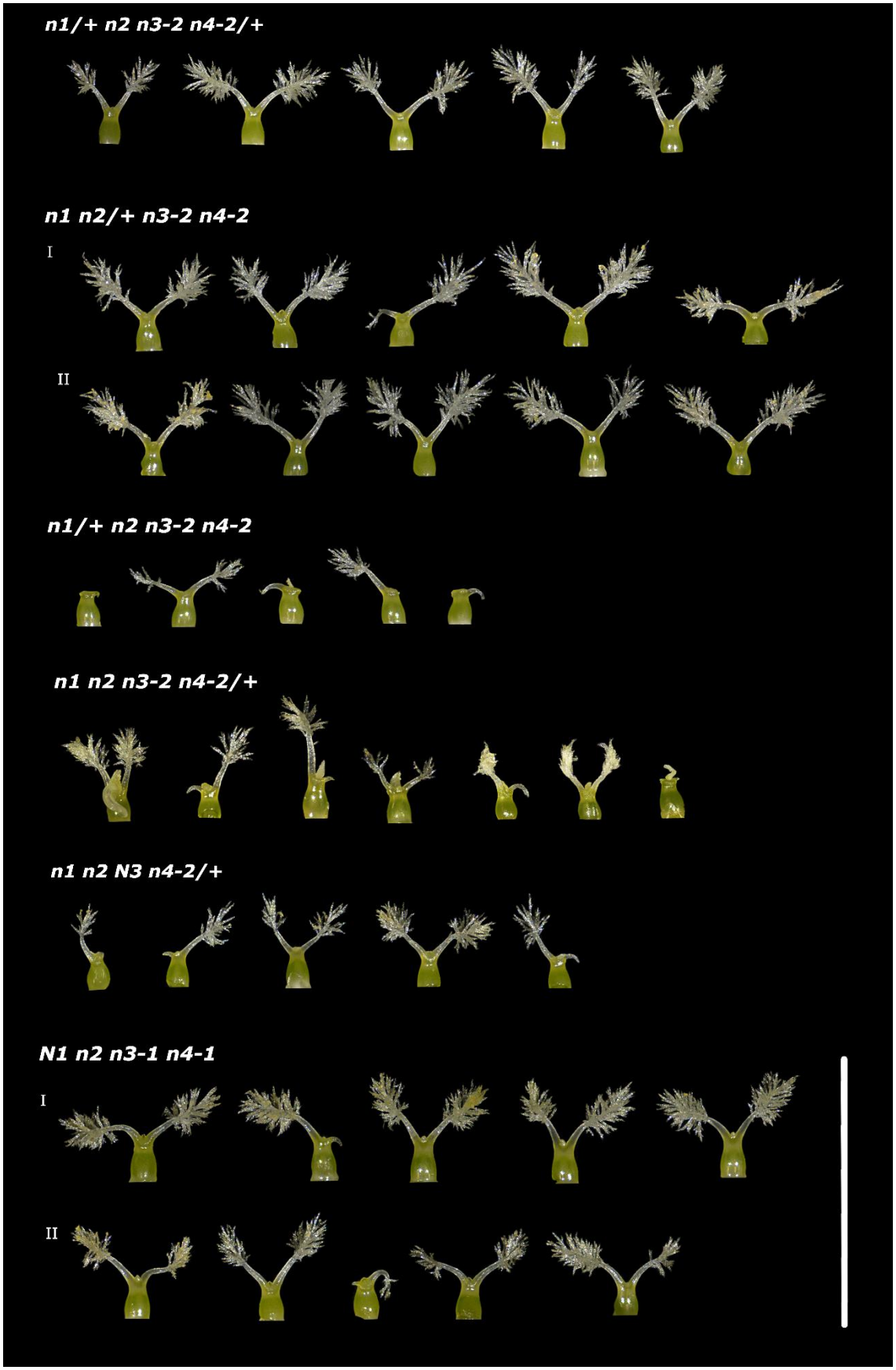
n1/+ n2 n3-2 n4-2/+
n1 n2/+ n3-2 n4-2
I
II
n1/+ n2 n3-2 n4-2
n1 n2 n3-2 n4-2/+
n1 n2 N3 n4-2/+
N1 n2 n3-1 n4-1
I
II

Figure 4.4. Images of the pistils from DJ (WT) plants and from the different mutants analyzed in the first generation of plants (*nga1/+ nga2/+ nga3-2/+ nga4-2/+, nga1 nga2/+ nga3-2 nga4-2/+, nga1/+ nga2 nga3-2 nga4-2/+, nga1 nga2/+ nga3-2 nga4-2, nga1/+ nga2 nga3-2 nga4-2, nga1 nga2 nga3-2 nga4-2/+* and *nga1 nga2 NGA3 nga4-2/+*) and from the independent group of triple mutant plants (*NGA1 nga2 nga3-1 nga4-1*) (*n = nga*; *N = NGA*). They show the effects of the *NGA* mutations in the rice pistil. The symbols I and II are indicating that the pistils belong to two different plants with the same genotype. The scale bar represents 5 cm.

To understand the effect of the rice *NGA* genes on style and stigma development, I took pictures of the pistils from the first and second generation of mutant plants (**Figures 4.4 and 4.5**). From the first generation, I took pictures of the pistils from the same mutants seen in the previous analysis except the quadruple homozygous mutant, because I did not have enough independent plants. I also took images from the *nga1 nga2 NGA3 nga4-2/+* mutant, from which I don't have fertility or fruit development data. From each genotype I photographed 5 pistils, except the DJ (WT), for which I took 10 images, and from the *nga1 nga2/+ nga3-2 nga4-2* and *NGA1 nga2 nga3-1 nga4-1*, from which I took 5 pictures from two independent plants with the same genotype (**Figure 4.4**). As we can see, as the amount of *NGA* mutations in homozygosis increases, the stigmas and the styles are more affected; even the quadruple mutant heterozygous (that is nearly as fertile as the DJ) have the stigmas a little bit reduced. Then, the plants with two mutant genes in homozygosis and the other two in heterozygosis (*nga1 nga2/+ nga3-2 nga4-2/+* and *nga1/+ nga2 nga3-2 nga4-2/+*) also possess reduced stigmas; there is a little bit of variability between pistils, but the stigmas tend to be smaller than the ones from the quadruple mutant heterozygous. When we reach the mutants with all the genes in homozygosis except for one that is in heterozygosis, we begin to see that some pistils lack one or both stigmas. The less affected ones are from the *nga1 nga2/+ nga3-2 nga4-2* genotype, that have both stigmas present in almost all the pistils, even if they are smaller. However, the *nga1/+ nga2 nga3-2 nga4-2* have a lot of pistils without stigmas and with reduced or without styles; and the few stigmas present are heavily reduced. One of them even has an overgrown tissue emerging from the space between the styles. Finally, almost all the pistils from the *nga1 nga2 nga3-2 nga4-2/+* plants have at least one stigma (even if it is reduced), but most of these pistils have the same overgrown tissue seen in the last genotype. This tissue is more prominent in these pistils than in the previous ones; in one of them it even folds and grows down.

Some of the *nga1 nga2 NGA3 nga4-2/+* pistils have only one stigma, and in all cases the present stigmas are reduced. This genotype is considerably affected considering that the *NGA3* gene is WT in homozygosis; this suggests that *NGA3*

gives the minor contribution to style and stigma development. The triple mutants from the independent group of plants (*NGA1 nga2 nga3-1 nga4-1*) show a lot of variability in the level of pistil defects; some are very similar to WT pistils while others lack almost both stigmas.

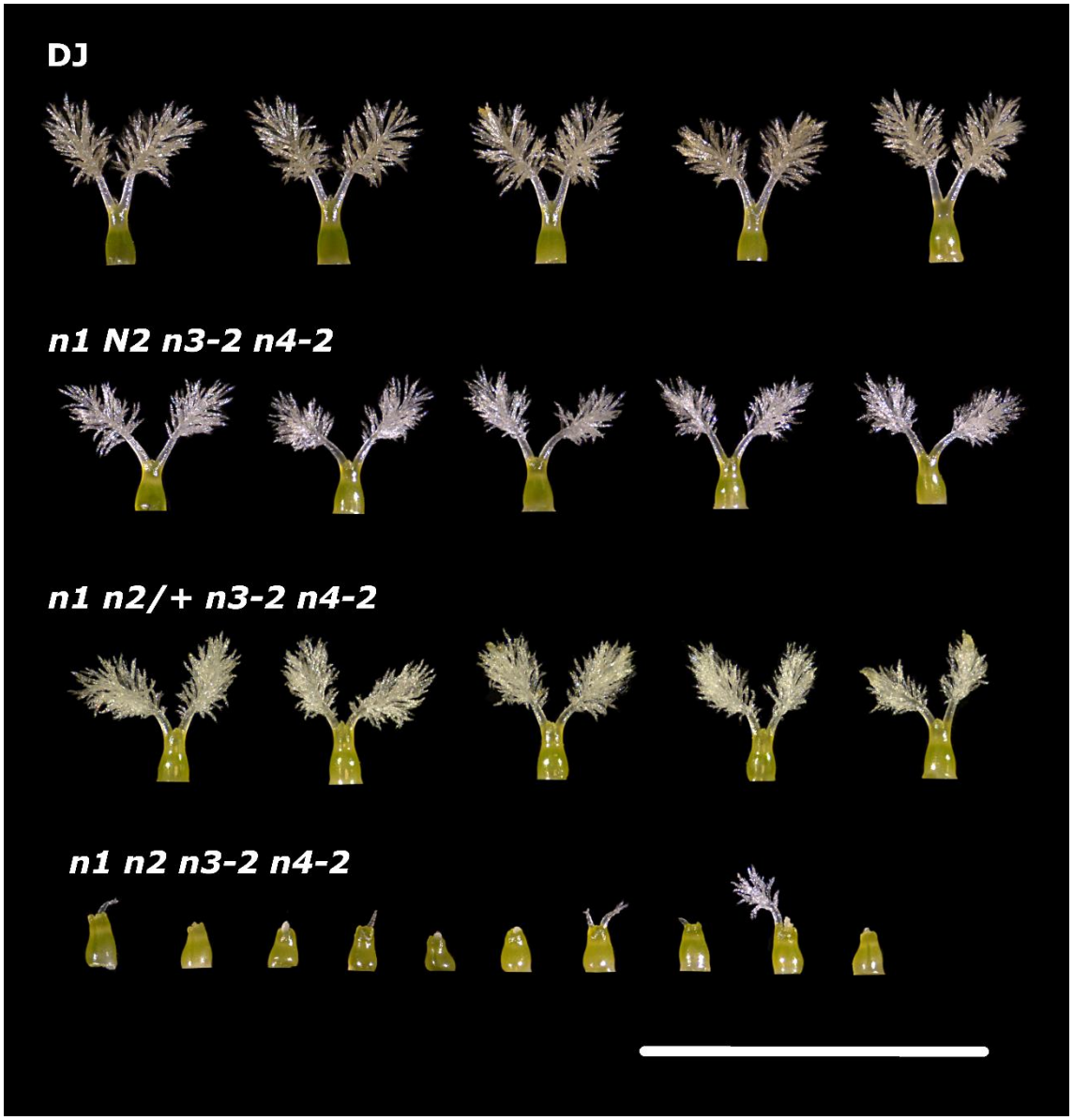

Figure 4.5. Images of the pistils from DJ (WT) plants and from the different mutants analyzed in the second generation of plants (*nga1 NGA2 nga3-2 nga4-2*, *nga1 nga2/+ nga3-2 nga4-2* and *nga1 nga2 nga3-2 nga4-2/+*) (*n* = *nga*; *N* = *NGA*). They show the effects of the *NGA* mutations in the rice pistils. The I and II are indicating that the pistils belong to two different plants with the same genotype. The scale line indicates 5cm.

From the second generation of plants, I took pictures from all the segregating genotypes (DJ, *nga1 NGA2 nga3-2 nga4-2*, *nga1 nga2/+ nga3-2 nga4-2* and *nga1 nga2 nga3-2 nga4-2*) (**Figure 4.5**). The DJ (WT) pistils from the second generation of plants are comparable with the ones from the first generation. The

nga1 NGA2 nga3-2 nga4-2 and *nga1 nga2/+ nga3-2 nga4-2* pistils are very similar and have the stigmas a bit reduced and more compact compared with the DJ ones. The *nga1 nga2/+ nga3-2 nga4-2* pistils seem to be less affected than the ones with the same genotype from the previous generation. Finally, the quadruple homozygous mutant (*nga1 nga2 nga3-2 nga4-2*) pistils almost never have any stigmas and rarely possess styles. Some of them also have a little bit of overgrown tissue emerging from the space between where the styles should be, like the ones seen in some mutant pistils from the previous generation.

4.1.4. Analysis of the mutant's developing fruit

From the second generation of plants, I also took pictures of the developing fruits found in DJ and in the quadruple homozygous mutant plants (the fruits were taken from the plants at the same time) (**Figure 4.6**). As we can see, not all the quadruple homozygous mutant flowers begin to develop fruits (**Figure 4.6B-a**); there are also some fruits that abort very early (**Figure 4.6B-b**); and the ones that grew more are still smaller than the DJ fruits at the same stage (**Figure 4.6A and B-c to f**). All the quadruple mutant fruits will abort sooner or later, as these plants do not develop mature fruits. It is also worth noting that most quadruple mutant fruits developed from ovaries completely devoid of style and stigmas (**Figure 4.6b, e, and f**), suggesting either that 1) the presence of style and stigmas in the pistil is not mandatory for successful pollination, pollen tube guidance and embryo sac fertilization, which seems extremely unlikely; 2) that indeed parthenocarpic phenomena do occur in *nga* mutants. Histological analysis of fruits is pending.

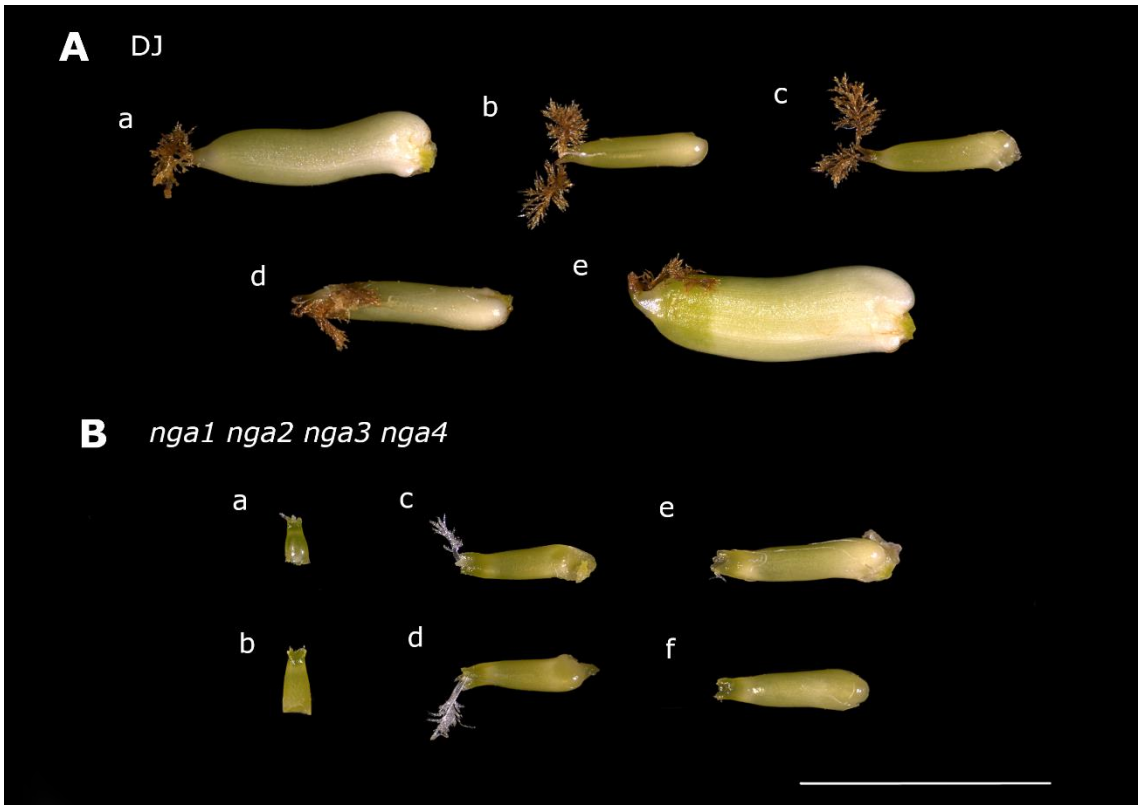

Figure 4.6. Pictures of the developing fruits from (A) DJ (WT) plants and (B) quadruple homozygous mutant (*nga1 nga2 nga3-2 nga4-2*) plants taken at the same time, from 2 to 7 days after anthesis and pollination. The scale line indicates 5cm.

4.1.5. Analysis of the mutant's flag leaf

Rice leaves have two distinctive parts: the sheath, a hollow cylinder that surrounds the shoot apex and young leaves to protect them from damage (all the leave sheaths overlapping each other from the shoot); and the blade (lamina), which is flat, with parallel venation, and found above the sheath. In the blade there are different types of vascular bundles: there is the mid-vein in the center, which is the bigger one and is holding the leaf blade; parallel to it there are large vascular bundles, that reach until the leaf margin; and between these, there are a series of small vascular bundles (**Figure 4.7D**) (Itoh *et al.*, 2005). In this thesis I analyzed the blade of the flag leaf from DJ and *nga* quadruple homozygous plants.

Leaf width and vascular bundle number were measured in 5 DJ and 5 quadruple homozygous mutant (*nga1 nga2 nga3-2 nga4-2*) flag leaves (the last leaf subtending the inflorescence) taken after plant flowering (**Figure 4.7**) (**Annex 9,10**). The results show that, while there is no statistically significant difference between the widths of the flag leaves from the two groups (p-value=0,23), the mutant leaves seem to have a tendency to be wider (**Figure 4.7A**). In the mutant leaves there is an increase in the number of vascular bundles compared to the

WT leaves. This happens with the large vascular bundles (p-value=0,005; **Figure 4.7B**) and with the small vascular bundles (p-value=0,014; **Figure 4.7C**). These results suggest that *NGA* genes also have an important role in vegetative development, determining plant height (**Figure 4.1**), leaf shape, and vascular bundle development (**Figure 4.7**).

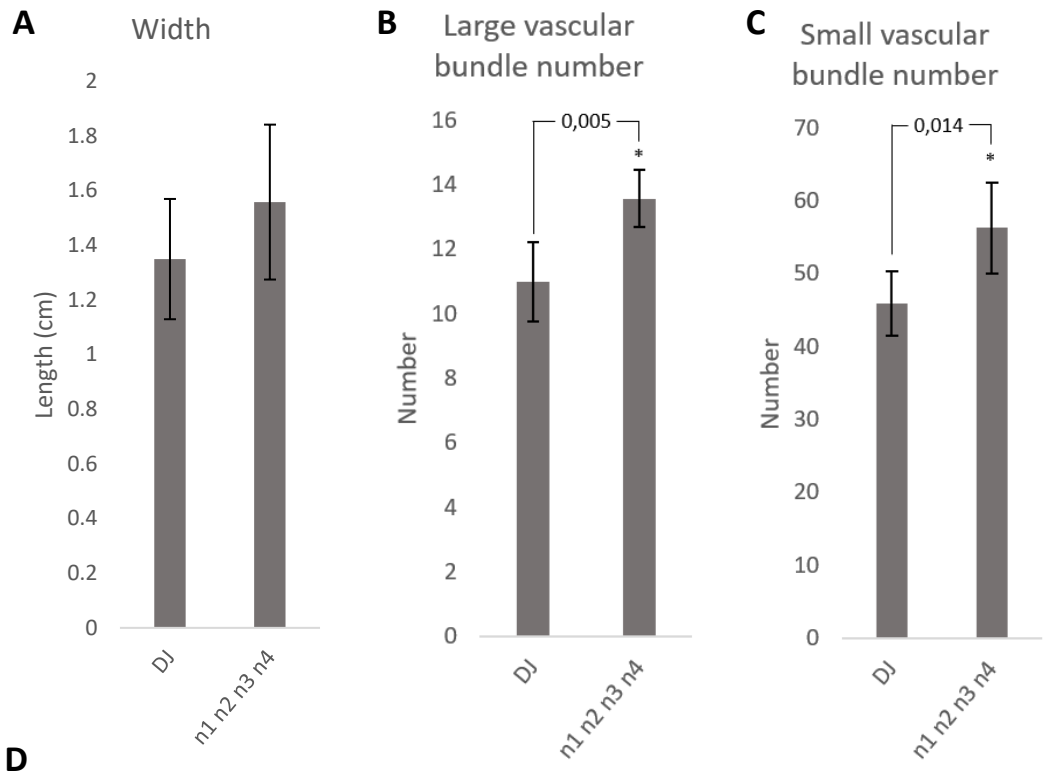

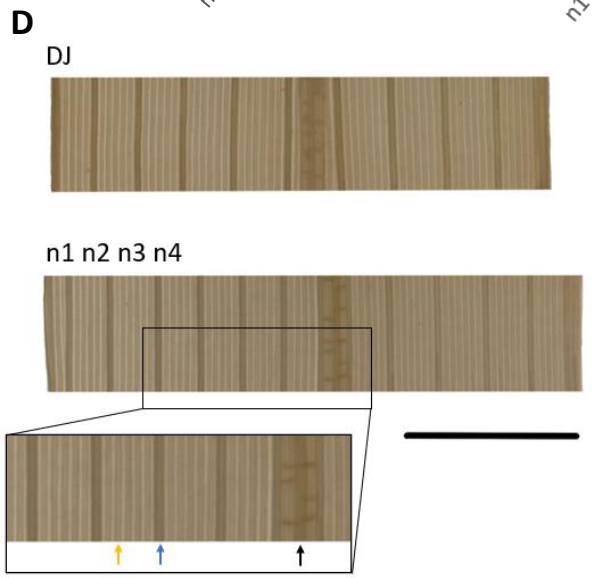

Figure 4.7. (A, B, C) Graphs showing the width (A), the number of large vascular bundles (B), and the number of small vascular bundles (C) found in the flag leaves form DJ (WT) and quadruple homozygous mutant (*nga1 nga2 nga3-2 nga4-2*) plants (n=5). The asterisk indicates statistically significant differences with the p-value indicated above the bars. (Statistic test: T-test; p-value < 0,05). (D) Images of the middle region of the flag leaf from a DJ and from a quadruple homozygous mutant (*nga1 nga2 nga3-2 nga4-2*) plant. The square shows an amplification of the leaf in which the mid-vein (black arrow), large vascular bundles (blue arrow), and small vascular bundles (orange arrow) can be appreciated. The scale bar indicates 5cm.

4.2. Pollen viability

Rice *NGA* expression have previously been detected in the anthers, especially in the microspore mother cells (see next paragraph and **Figure 4.9**). To determine if *NGA* genes are also important for pollen viability, we crossed DJ and *nga* quadruple homozygous mutant plants. We used the DJ as the female parent and the mutant as the pollen donor, so the pistil is WT and therefore develops correctly, and the pollen is *nga1 nga2 nga3-2 nga4-2* (DJ♀ X *nga1 nga2 nga3-2 nga4-2*♂). From each parental genotype we used two panicles and obtained 51 mature fruits from a total of 61 emasculated florets, so the cross had an 83,6% efficiency which is in line to what is typically obtained in the lab from WT pollen. To check if the cross had any unwanted pollen contamination, we germinated 12 of the fruits and genotyped *NGA2* by PCR sequencing (**Figure 4.9**). The results indicated that almost all the plants were descendants from the desired parents: only 2 of them had *NGA2* WT, while the other 10 had it in heterozygosis (*nga2/+*). This means that the cross was mostly successful, so the quadruple mutant pollen is able to generate descendants when applied to normal pistils and is unlikely to contribute to the dramatic sterility seen in *nga* mutants.

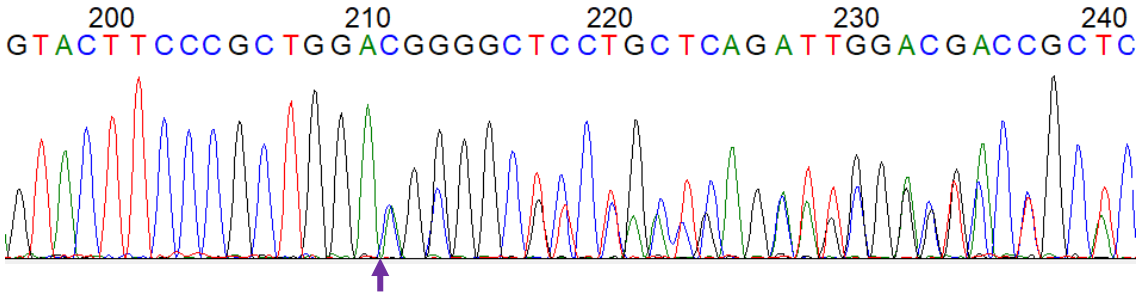

Figure 4.8. Chromatogram of the *NGA2* gene sequencing in one of the descendants of the DJ♀ X *nga1 nga2 nga3-2 nga4-2*♂ cross. The plant is *nga2/+,* so it has one *NGA2* WT allele and one carrying the deletion, which causes the chromatogram to split (purple arrow).

4.3. Histological analysis

During rice flower development, the three carpel primordia emerge laterally from the floral meristem after the formation of the six stamen primordia. Then, they fuse at the top enclose the meristem, that will gradually turn downwards and differentiate into the ovule (**Figure 4.9A, B, C**). From these tree carpel primordia, only the two lateral ones will produce style and stigma (**Figure 4.9C**) (Dreni *et al.*, 2013).

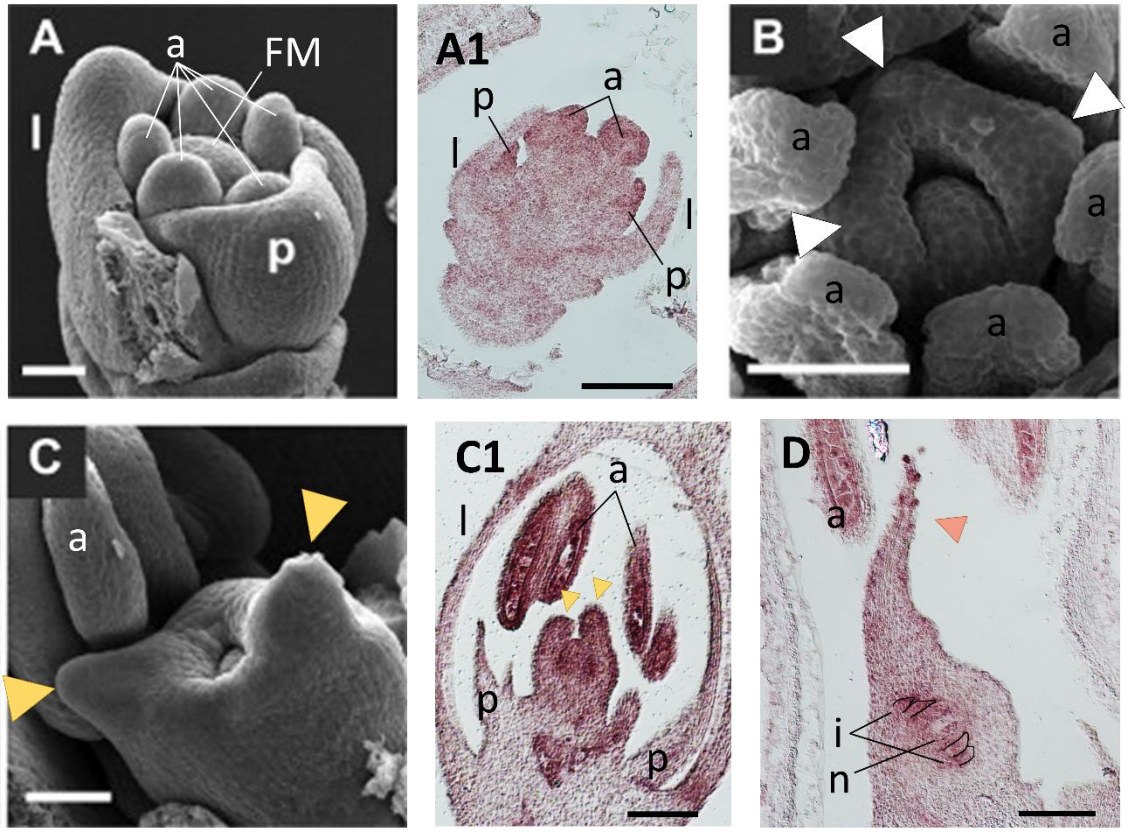

Figure 4.9. SEM images showing early stages of rice pistil development (A, B, C) and *in situ* hybridizations depicting *NGA1* expression pattern in these and a later stage (A1, C1, D). (A) Stage in which the stamen primordia are differentiating from the rest of the undifferentiated floral meristem. (B) Stage in which the three carpel primordia (white arrowheads) are differentiated and beginning to enclose the ovule primordium. (C) Stage in which the ovary wall almost completely envelopes the ovule primordium and the two lateral carpel primordia are differentiating the stigmas (yellow arrowheads). (D) Stage in which the ovary wall completely envelopes the ovule, the integuments are developing (marked with black lines for a better visualization), the style is differentiated, and the stigma branches are being initiated (orange arrowhead). a: anther; FM: floral meristem; i: integuments (divided in inner and outer integument); l: lemma; n: nucellus; p: palea. White bars represent 25 µm; black bars represent 100 µm. (Dreni *et al.*, 2013; Dreni *et al.*, unpublished).

Previous lab results showed the *NGA* expression pattern during floral meristem development (**Figure 4.9A1, C1, D**). They are expressed in the anthers since the beginning of anther primordia development (**Figure 4.9A1**), and this expression continues as they develop; when the microspore mother cells are formed, *NGA* expression is concentrated there and in the anther tapetum (**Figure 4.9D**). In the pistil, they are strongly expressed in the actively dividing cells of the distal part of the ovary and ovary wall before the carpel primordia fusion (**Figure 4.9C1**); and in later stages, *NGA* is also heavily expressed in the integuments (structure not developed in previous stages) (**Figure 4.9D**). Finally, at the beginning of stigma development, they are also strongly expressed in the stigmatic cells that are

initiating the stigmatic branches (**Figure 4.9D**) (Dreni *et al.*, unpublished). **Figure 4.9** shows the expression using an antisense probe specific for *NGA1*, but it has been seen that the other *NGA* genes show similar behavior.

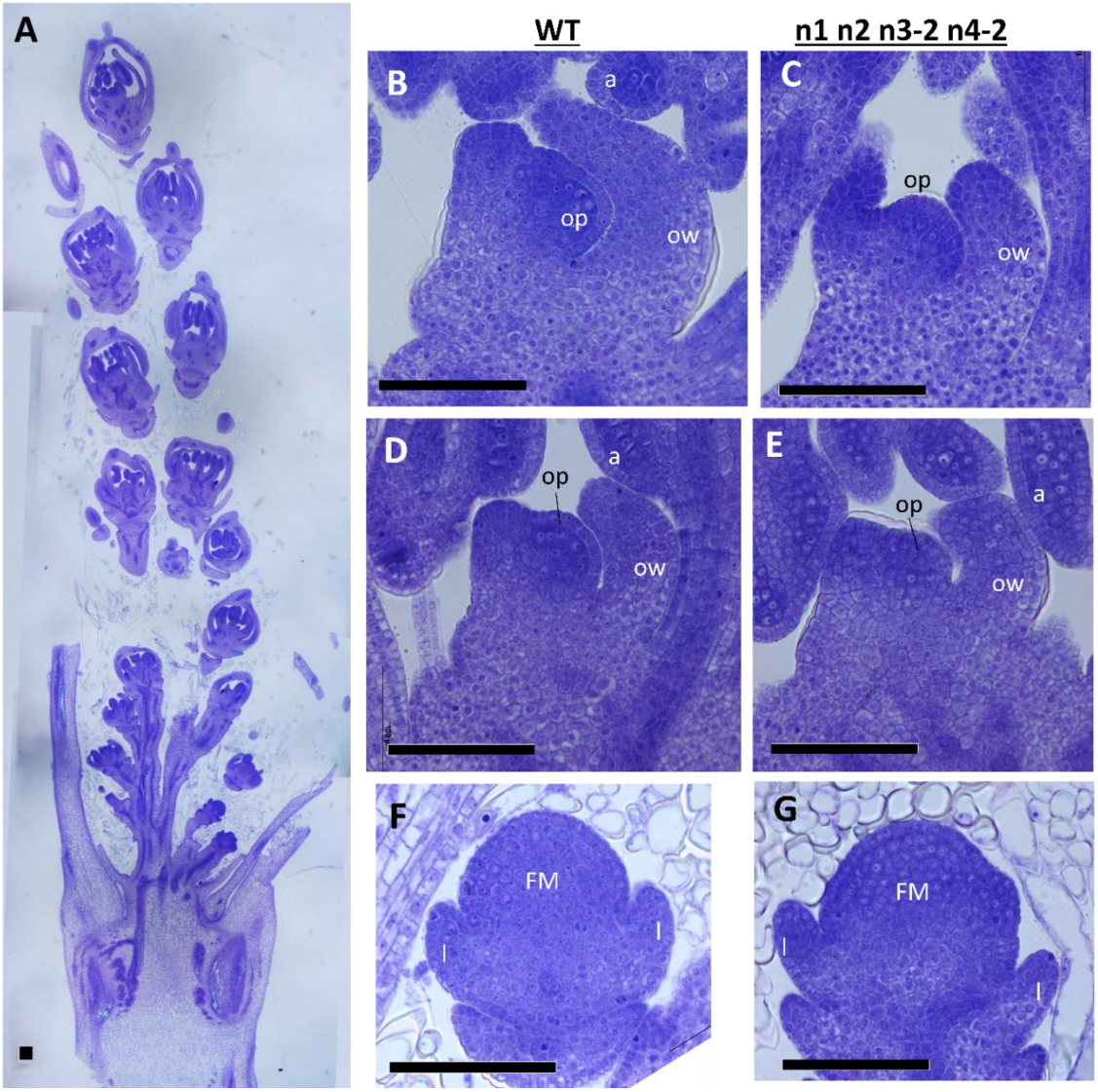

Figure 4.10. Sections from 7 mm long inflorescence primordia stained with Toluidine Blue. (A) Mid-section of a whole mutant inflorescence primordium, showing the less developed flowers at the base and the more advanced ones at the top. (B, C) Most advanced floral development stage found at the apical region in these inflorescence primordia, in which the WT carpel primordia are almost fused (B), which does not happen in the mutant (C). (D, E) WT (D) and mutant (E) floral development middle stages found in these inflorescence primordia, where the mutant defect in the carpel fusion just starts to be visible. (F, G) Earliest stages of floral development found in the base of WT (F) and mutant (G) inflorescence primordia, before the anthers and gynoecium differentiation from the floral meristem, where the mutant is still identical to WT. a: anther; FM: floral meristem; l: lemma; op: ovary primordium; ow: ovary wall. The bars represent 100 µm.

To understand better the effect of *NGA* genes in pistil development, we took pictures of different stages of developing pistils found in inflorescence primordia

(7 mm long – **Figure 4.10**; and 20 mm long – **Figure 4.11A, B**), and fully developed pistils (**Figure 4.11C, D**) from WT and quadruple mutant homozygous (*nga1 nga2 nga3-2 nga4-2*) plants. These pictures show that the lack of *NGA* is preventing the total enclosure of the ovule by the carpel primordia (**Figure 4.10, 11**). In early stages, before stamen and carpel primordia differentiation, there are not apparent differences between the WT and the mutant. Then, during pistil development the ovary wall seems to go slower when encompassing the ovary (**Figure 4.10B – E**). And, when the WT carpel primordia have already fused apically to initiate the stigmas and styles, and are completely enclosing the ovule (**Figure 4.11A**), the mutant ones are still not fused (they are not even touching at the top) (**Figure 4.11B**); and they will remain unfused, as this apical opening is also maintained in the developed pistils (**Figure 4.11C, D**). Rice *NGA* genes are also involved in determining embryo sac shape and position in the nucellus, and ovule and integument growth (**Figure 4.11C, D**). In the mutant pistils, the embryo sac is rounder and pointing more upwards than in the WT pistils. And the ovule is longer, even growing inside the apical aperture left by the unfused ovary; we can also see integument outgrowths coming out from this aperture. It is not clear if this excessive and uncontrolled expansion of the ovary and the integument is a direct consequence of the lack of *NGA*, or if it is due the opening left by the carpel primordia, although this outgrowth has also been observed with intermediate genotypes still producing style and stigma (*nga1/+ nga2 nga3-2 nga4-2* and *nga1 nga2 nga3-2 nga4-2/+* – **Figure 4.4**).

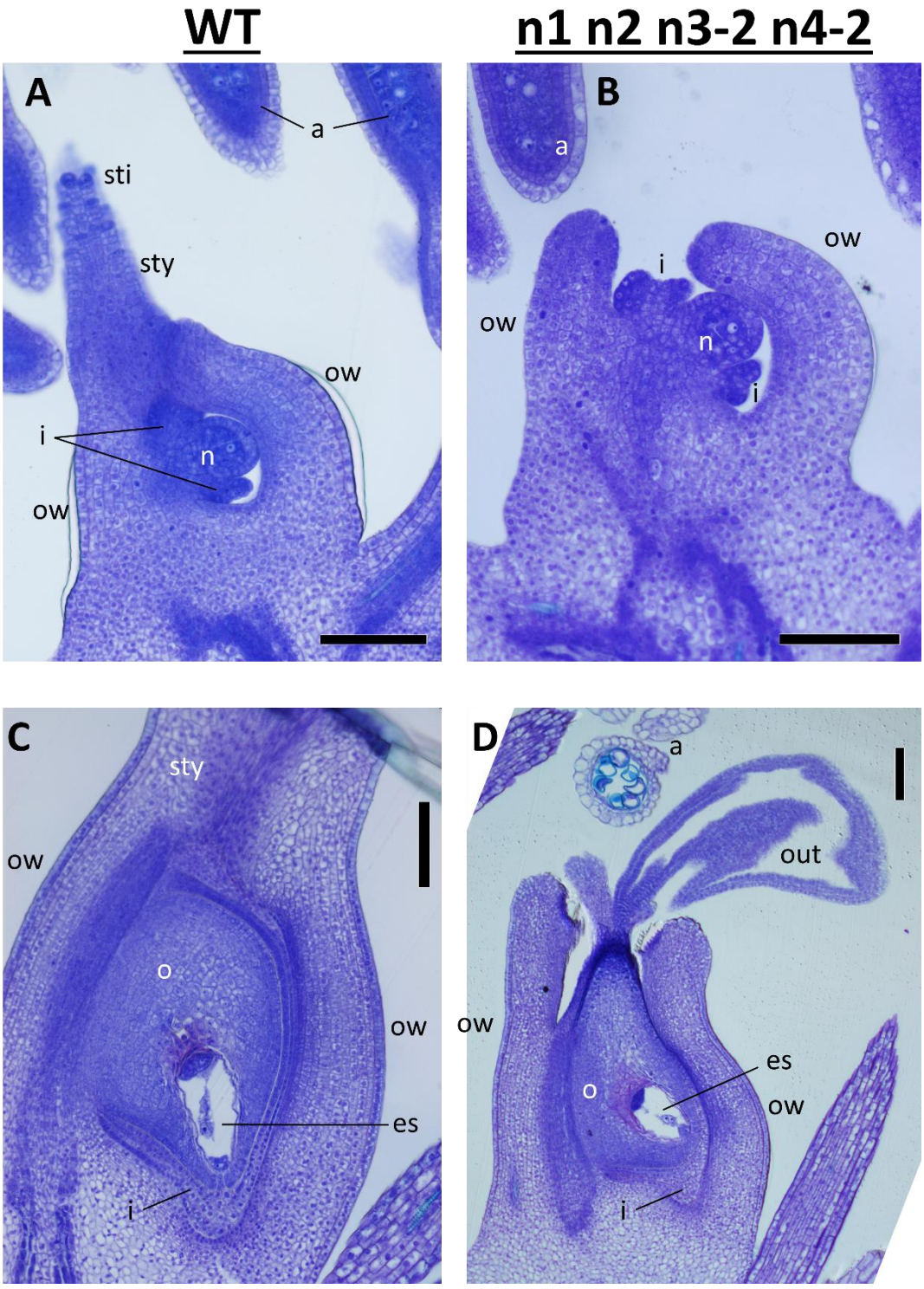

Figure 4.11. (A, B) Sections from 20 mm long inflorescence primordia stained with Toluidine Blue depicting a WT (A) and mutant (B) pistils in the stage of development, when usually the carpel primordia have fused and the stigma begins to develop. (C, D) Sections of WT (C) and mutant (D) mature pistils stained with Toluidine Blue with the embryo sac visible. a: anther; es: embryo sac; i: integuments (divided in inner and outer integument); n: nucellus; sty: style; sti: stigma; o: ovary; out: integument outgrowth; ow: ovary wall. The bars represent 100 µm.

4.4. RNA sequencing

The samples used for RNA-seq were three independent 7-9 mm long inflorescence primordia (**Figure 4.10A**) from each genotype: 3 from DJ plants and 3 from *nga* quadruple homozygous plants (*nga1 nga2 nga3-2 nga4-2*). This stage was chosen because the inflorescence primordia have developed enough that the effects of the lack of *NGA* are apparent, but style and stigma development have not begun yet in WT primordia, which could alter the RNA-seq results as there is an organ present in one of the genotypes that is completely absent in the other. The RNA was extracted from these primordia, purified, and sent to sequence to BGI Hong Kong genomics service.

From a total of 33252 protein-coding genes that are annotated in the rice genome, 460 were expressed differently in the two genotypes with statistical significance (p-value < 0,05) (206 upregulated and 254 downregulated in the mutant, respectively), and from them, 229 also had a fold change (FC) bigger than 2 (or smaller than -2) (126 upregulated and 103 downregulated in the mutant, respectively). To analyze these results, I used the MapMan software to see in which processes the differentially expressed genes were involved (whole list of 460 deregulated genes); and, because most rice genes are not functionally characterized yet, I also screened the sublist of 229 most deregulated genes for information about their annotation (in the MSU Rice Genome Annotation Project and the Rice Annotation Project (RAP) data base) and homology versus *Arabidopsis* genes (in The Arabidopsis Information Resource (TAIR) data base).

A

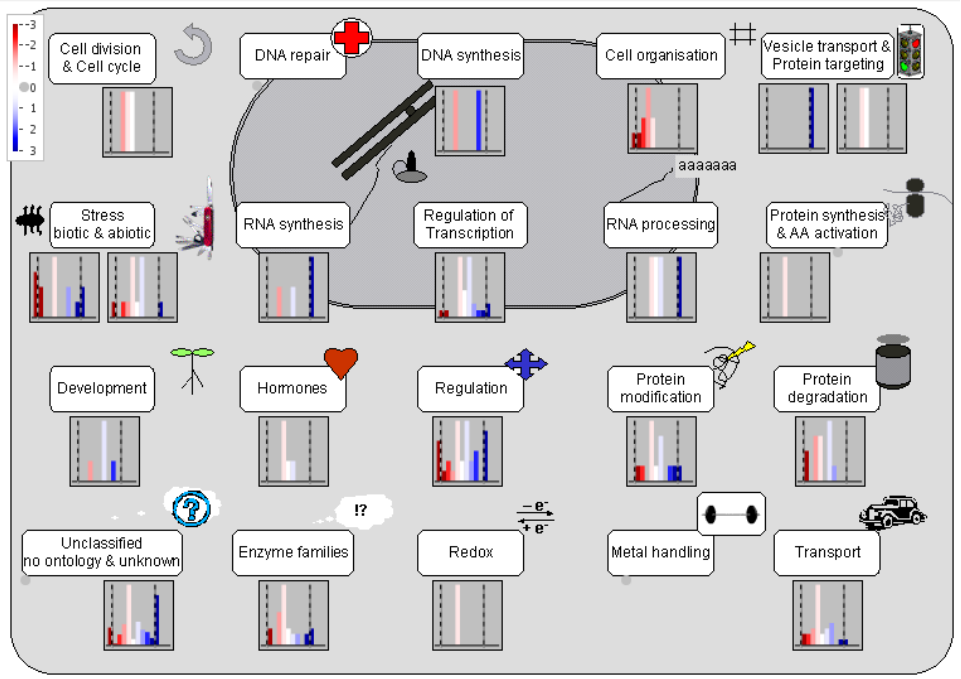

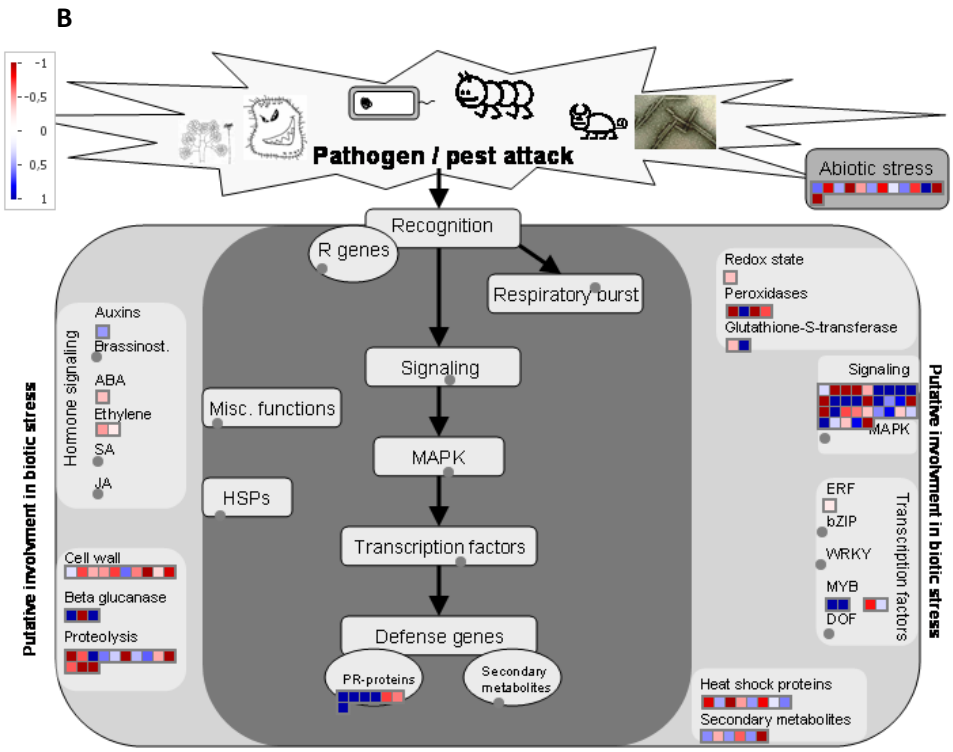

Figure 4.12. Outlines generated by the MapMan software depicting in which processes are participating the deregulated genes. Blue is indicating upregulation and red in indicating downregulation; the higher the color intensity, the greater the deregulation. (A) Image showing deregulated genes participating in the distinct cell functions. The x-axis of frequency histograms is indicating the level of deregulation (in the same way as the colors are doing), and the y-axis is representing the number of genes in each class. (B) Image showing deregulated genes implicated in different processes of the stress response.

Using MapMan I was able to get a broad idea of the processes in which the deregulated genes were involved (**Figure 4.12**). I saw that a lot of upregulated and downregulated genes were involved the biotic and abiotic stress response. When looking at this process in more detail (**Figure 4.12B**) I found that there were a lot of genes differentially expressed involved in signaling receptor kinases. I also found a change in expression in genes encoding pathogenesis-related proteins (mainly upregulated); it has been previously reported that other RAV family members are involved in pathogen response (Li *et al.*, 2011), so the *NGA* genes may also be implicated in this biological process. The genes encoding proteins important for cell wall regulation were also affected (principally downregulated), as well as the ones encoding for β-glucanases (with strong expression changes), and the ones dictating proteolysis (a process that seems downregulated). Finally, the peroxidase-encoding genes were mainly downregulated.

RNA synthesis, transcription regulation, and processing were also affected; the genes involved in these processes seemed to be mainly upregulated. Genes related to protein modification were deregulated (upregulated and downregulated alike); and, as seen before, genes involved in protein degradation were downregulated. Molecular transport was also affected, as genes encoding transporters were deregulated. Finally, I also saw that genes related to cell organization were downregulated.

When looking directly at the list of genes, the first noticeable thing was that most of the top upregulated genes are transposons and retrotransposons, a thing that does not happen in the downregulated genes. Another important upregulated gene is the *NITRITE REDUCTASE 2* (*NIR2*) (LOC_Os02g52730) (**Table 4.4**), which encodes an enzyme that catalyzes the reduction of nitrite (NO_2^-) into ammonium (NH_4^+) in the chloroplast; helping in nitrogen assimilation and NO_2^- elimination (it can be toxic if it accumulates in the cells). In **Table 4.4** are also indicated the most deregulated transporters and aquaporins (with FC > 2); as indicated in the table, these transporters are very diverse and some of them are upregulated while others are downregulated.

Table 4.4. Differential expression between WT and mutant inflorescence primordia of the NIR2 gene and the molecular transporters.

Gene ID	log2 (*nga* mutant / *NGA* WT)	Q - value	FC	Gene
LOC_Os02g52730	6.17493	0.00027	72.25	NITRITE REDUCTASE 2 (NIR2)
LOC_Os01g69010	5.21704	0.00089	37.19	MATE efflux protein (multidrug and toxin efflux family)
LOC_Os03g07480	2.80163	0.00000	6.97	Sucrose transporter
LOC_Os09g20490	-2.477089	4.76E-07	-5.57	Transporter similar to hydrogen symporter.
LOC_Os07g26660	-2.358069	0.01661011	-5.13	Aquaporin protein
LOC_Os12g31860	-1.839174	1.52E-19	-3.58	UREIDE PERMEASE 1
LOC_Os12g32760	-1.787192	1.16E-04	-3.45	Sugar/inositol transporter domain containing protein.
LOC_Os05g27304	-1.771710	1.31E-20	-3.41	Peptide transporter PTR2
LOC_Os01g66010	1.25222	0.00000	2.38	Amino acid transporter
LOC_Os11g03070	1.14944	0.04562	2.22	CATION/H+ EXCHANGER 10
LOC_Os01g50160	-1.072675	0.00303551	2.10	MDR-like ABC transporter
LOC_Os10g13830	-1.071767	0.00389878	2.10	PLEIOTROPIC DRUG RESISTANCE PROTEIN 13 (PDR13)
LOC_Os01g13130	-1.031823	0.0013991	2.05	Aquaporin protein

Among those deregulated genes that encode for transcription factors, I focused on three particularly interesting cases (**Table 4.5**). LOC_Os12g40070 is dramatically downregulated in the mutant primordia; it still does not have an

annotated function in rice, but its encoded protein possesses homology with a lot of REPRODUCTIVE MERISTEM (REM) proteins from *Arabidopsis*. The *REM* gene family belongs to the B3 DNA-binding domain superfamily; the exact role of all their members is still not described, but several members seem to be involved in floral meristem identity determination and promoting flower development. They have been found to be preferentially expressed during flower and ovule development, and some of them are targets of floral identity transcription factors, such as LFY, (APETALA1) AP1, (APETALA3) AP3, and AG (Mantegazza *et al.*, 2014). Another drastically downregulated gene is *TCP25* (LOC_Os09g34950). The *TCP* genes are divided into class I genes, involved in the activation of growth-associated genes, and class II genes, that act as transcriptional repressors of growth-associated genes (Kosugi and Ohashi 2002); *TCP25* belongs to the first class, which means it is promoting plant growth (Sharma *et al.*, 2010). Finally, LOC_Os09g26200 is upregulated; but even if it still has an FC > 2, its expression is much less affected than the other two transcription factors. Its encoded protein shows homology with KNUCKLES (KNU) from *Arabidopsis*, a small protein with a C2H2 zinc finger that acts as a transcriptional repressor and regulates cellular proliferation during floral development by inducing floral meristem termination (Payne *et al.*, 2004).

Table 4.5. Differential expression of the REM, TCP25, and KNU transcription factors between WT and mutant inflorescence primordia.

Gene ID	log2 (*nga* mutant / *NGA* WT)	Q - value	FC	Gene
LOC_Os12g40070	-6.8480462	4.46E-05	-115.20	Homology with REPRODUCTIVE MERISTEM (REM)
LOC_Os09g34950	-5.4434256	2.41E-04	-43.51	TCP25
LOC_Os09g26200	1.29373	0.00595	2.45	Homology with KNUCKLES (KNU)

Hormonal pathways seem also fairly affected in the mutant inflorescence primordia ; especially auxins, as there are upregulated genes related to their synthesis, transport, and response (**Tables 4.6-8**). Auxin (IAA) synthesis can be accomplished by different pathways (**Figure 4.13**), and genes encoding for enzymes that act in more than one of them have their expression altered in the mutant (**Tables 4.6**). First of all, the *ALDEHYDE OXIDASE 2* (*AAO2*) (LOC_Os03g58380) and a gene belonging to the YUCCA (YUC) family (LOC_Os01g53200) are upregulated. These two genes encode enzymes that are catalyzing the last reaction of auxin formation while using different substrates. And secondly, two *Cytochrome P450* are also deregulated. The *CYP71A1* (LOC_Os02g09260) is pretty upregulated, while LOC_Os04g08828, whose encoded protein presents homology with *Arabidopsis*'s *CYP79B2* and *B3*, is a

little downregulated. The proteins encoded by these two genes are participating in the *Brassicaceae* species-specific auxin biosynthesis pathway, but the presence of this or a similar route in rice or other monocots has not been studied yet; this means that these genes could also be acting in auxin biosynthesis.

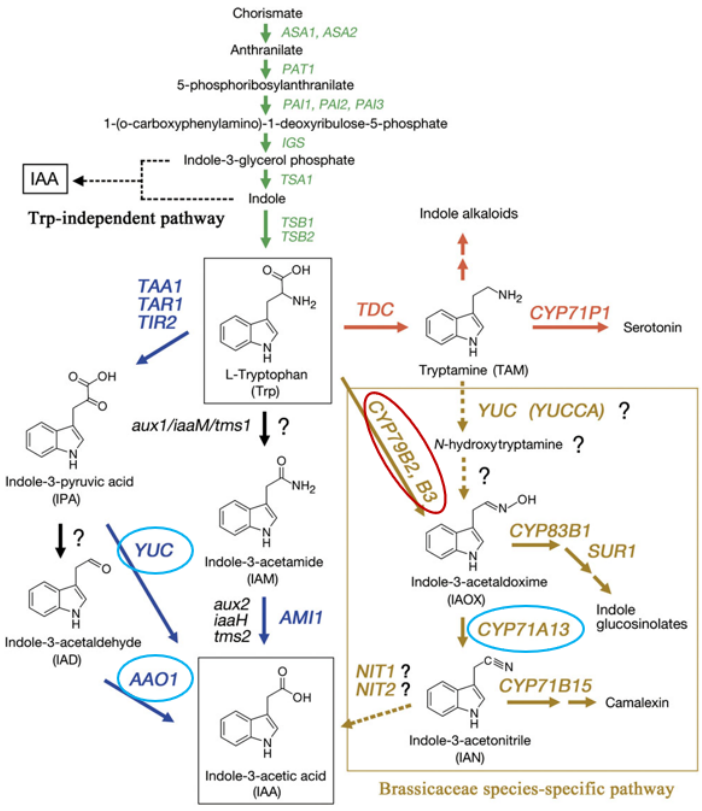

Figure 4.13. Described auxin biosynthesis pathways in plants. The green arrows are indicating the tryptophan synthetic pathway taking place in the chloroplast. The thin dashed black arrow is representing the tryptophan-independent auxin biosynthetic pathway. The blue arrows are denoting the steps for which the gene and enzymatic function are known in the tryptophan-dependent auxin biosynthetic pathway; while the black arrows are indicating the steps for which the gene(s) and enzymatic function(s) are unknown. The red arrows stand for the indole alkaloid and serotonin biosynthetic pathways. The yellow arrows are indicating the *Brassicaceae* species-specific pathway (however, its possible presence in rice has yet to be verified); and the dashed yellow arrows is denoting the steps for which the gene and enzymatic function(s) remain poorly understood. The letters in italics are showing the genes involved in each process, while lowercase letters in italics are indicating bacterial genes. The circles are indicating the deregulated genes in our analysis: the blue ones mean that the encircled genes are upregulated, and the red one is signaling that the gene is downregulated. (Adapted from Mano and Nemoto, 2012).

Table 4.6. Differential expression of genes related to auxin biosynthesis between WT and mutant inflorescence primordia.

Gene ID	log2 (*nga* mutant / *NGA* WT)	Q - value	FC	Gene
LOC_Os03g58380	5.58919	0.02251	48.14	ALDEHYDE OXIDASE 2 (AAO2)
LOC_Os02g09260	3.68844	0.01115	12.89	Cytochrome P450 71A1
LOC_Os01g53200	1.08473	0.00001	2.12	YUCCA
LOC_Os04g08828	-1.655723	6.56E-04	-3.15	Cytochrome P450 - Homology with CYP79B2, B3

Auxin transport seem also deregulated (**Table 4.7**). LOC_Os11g01140 and LOC_Os12g01140, two AGC kinases, are found upregulated in the mutant primordia. AGC kinases are involved in regulating auxin transport by interacting

with PIN exporters (and phosphorylating them) to mediate their polarity (Rademacher and Offringa, 2012; Glanc *et al.*, 2021). AGC kinases are activated by PDK1 (3-phosphoinositide-dependent protein kinase 1), another AGC kinase, and one of them is PID (PINOID), which is widely known for determining PIN polarity (Rademacher and Offringa, 2012; Xiao and Offringa, 2020). However, LOC_Os01g50160, a gene that encodes for a protein with homology with several auxin transporters (such as MDR4, PGP21, and MDR1), is downregulated in the mutant inflorescence primordia, but at lower magnitude than the AGC kinases upregulation.

Table 4.7. Differential expression of genes related to auxin transport between WT and mutant inflorescence primordia.

Gene ID	log2 (*nga* mutant / *NGA* WT)	Q - value	FC	Gene
LOC_Os11g01140	2.92060	0.00000	7.57	AGC_PVPK_like_kin82y.18 - AGC kinases include homologs to PKA, PKG and PKC
LOC_Os12g01140	1.95499	0.00000	3.88	AGC_PVPK_like_kin82y.2 - AGC kinases include homologs to PKA, PKG and PKC
LOC_Os01g50160	-1.072674	0.0030355	-2.10	MDR-like ABC transporter - Homology with auxin transporters

In agreement with the results explained previously, auxin response genes are also upregulated, consistently with higher auxin levels in the mutant (**Table 4.8**). Four genes activated by auxin were overexpressed in the mutant: the *AUXIN RESPONSE FACTOR 1* (*ARF1*) (LOC_Os01g13520), the Auxin-induced protein *5NG4*, and two auxin-responsive Aux/IAA gene family members, *OsIAA27* (LOC_Os11g11410) and *OsIAA17* (LOC_Os05g14180). Even so, these genes are not as upregulated as the ones related to auxin synthesis and transport (most of them do not exceed an FC of 2).

Table 4.8. Differential expression of genes related to auxin response between WT and mutant inflorescence primordia.

Gene ID	log2 (*nga* mutant / *NGA* WT)	Q - value	FC	Gene
LOC_Os01g13520	1.06460	0.00000	2.09	AUXIN RESPONSE FACTOR 1 (ARF1)
LOC_Os05g33900	0.69422	0.00150	1.62	Auxin-induced protein 5NG4
LOC_Os11g11410	0.48718	0.00675	1.40	OsIAA27 - Auxin-responsive Aux/IAA gene family member
LOC_Os05g14180	0.29205	0.00363	1.22	OsIAA17 - Auxin-responsive Aux/IAA gene family member

Other affected hormones are cytokinin and gibberellin, the latter to a lesser degree than the former (**Table 4.9**). *OsRR3* A-type response regulator (LOC_Os02g58350), a cytokinin signaling gene, is fairly upregulated (Buechel *et*

al., 2010). While a cytokinin dehydrogenase precursor (LOC_Os01g56810) is downregulated. Cytokinin dehydrogenases (CKX) are a gene group in charge of cytokinin inactivation by acting in their catabolism (Frebort *et al.*, 2011). In the case of gibberellins, two gibberellin receptors *GID1L2* are deregulated, one upregulated (LOC_Os08g37040) and the other downregulated (LOC_Os11g13670) at similar levels (Ueguchi-Tanaka *et al.*, 2007). And *GIBBERELLIN 2-BETA-DIOXYGENASE* (*GA2OX1*) is downregulated; this is a gene encoding for an enzyme responsible for the inactivation of several biologically active gibberellins by participating in their catabolism (Lo *et al.*, 2008).

Table 4.9. Differential expression of genes related to cytokinin and gibberellin between WT and mutant inflorescence primordia.

Gene ID	log2 (*nga* mutant / *NGA* WT)	Q - value	FC	Gene
LOC_Os02g58350	2.07452	0.00000	4.21	OsRR3 A-type response regulator, cytokinin signaling
LOC_Os01g56810	-0.89439	0.03193082	-1.86	Cytokinin dehydrogenase precursor
LOC_Os08g37040	0.50403	0.01095	1.42	Gibberellin receptor GID1L2
LOC_Os01g55240	-0.50353	0.03191176	-1.42	Gibberellin 2-beta-dioxygenase
LOC_Os11g13670	-0.44166	0.00945838	-1.36	Gibberellin receptor GID1L2

5. Discussion

In this master's thesis, I studied the function of *NGATHA* (*NGA*) genes in rice plants, determining their effect on plant fertility, and fruit and pistil development. NGA is a small subfamily of transcription factors that belong to the RAV family (Alvarez *et al.*, 2009; Trigueros *et al.*, 2009). They are expressed in numerous plant organs such as leaves, shoot meristems, flowers, seeds, and roots (Swaminathan *et al*. 2008; https://ricexpro.dna.affrc.go.jp/). They are mainly involved in style and stigma development in *Arabidopsis* (Alvarez *et al.*, 2009; Trigueros *et al.*, 2009; Ballester *et al.*, 2021) and other eudicot species (Fourquin and Ferrándiz, 2014) in a redundant and dose-dependent manner (Alvarez *et al.*, 2009; Trigueros *et al.*, 2009). However, there is a lack of research on their function in monocot species, such as rice. The results obtained in this thesis try to shed some light on this unexplored topic.

The *NGA* genes are also involved in *Arabidopsis* vegetative development by regulating lateral organs growth, such as leaf morphogenesis (Shao *et al.*, 2020; Salava *et al.*, 2022; Ballester *et al.*, 2015; Alvarez *et al.*, 2009; Trigueros *et al.*, 2009); it has been described that *nga* quadruple mutants develop wider and more serrated leaves than WT (Alvarez, *et al.*, 2009, Trigueros *et al.*, 2009; Ballester

et al., 2015). Our results also maintain this notion in rice, as the quadruple homozygous mutants (*nga1 nga2 nga3-2 nga4-2*) are shorter and more compact than the WT plants (**Figure 4.1**); and their flag leaves showed an increase in the number of vascular bundles and a tendency to be wider when compared to WT leaves (**Figure 4.7**). Even so, most *NGA* studies are related to flower development, so there is still much research in this field to be done.

Our results confirmed that the *NGA* genes's role as style and stigma development regulators is also conserved in rice. In the pictures of the pistils taken from the several mutants analyzed (**Figures 4.4 and 4.5**), we can see reduced stigmas in almost all of them when compared to the WT ones. Moreover, style and stigma development is entirely abolished in the more severe phenotypes. These results also show that they are acting redundantly and in a dose-dependent manner in rice, in the same way as previously described in *Arabidopsis*; nevertheless, some of them are more important for pistil development than others. They are clearly acting in a dose dependent-manner, because as the number of mutated *NGA* genes in homozygosis increases, the style and stigma defects are more prominent until reaching the quadruple mutant homozygote (*nga1 nga2 nga3-2 nga4-2*), where most pistils do not differentiate any stigma and style (**Figure 4.5**). Their redundant action can be especially appreciated when comparing the pistils from plants with all *NGA* genes mutated in homozygosis except one that is in heterozygosis (*nga1 nga2/+ nga3-2 nga4-2, nga1/+ nga2 nga3-2 nga4-2*, and *nga1 nga2 nga3-2 nga4-2*/+) with those from the quadruple mutant homozygote (*nga1 nga2 nga3-2 nga4-2*); as we can see, the mutants with a gene in heterozygosis have their pistils less affected than the quadruple mutant homozygote (**Figures 4.4 and 4.5**), even if they only have a WT allele left in just one of the four *NGA* genes.

The lack of *NGA* also affects rice plant fertility and fruit development capacity (**Figures 4.2 and 4.3**). When analysing these parameters, we can see again how these genes are acting redundantly and in a dose-dependent manner. It is easy to see that, as the number of mutations increases, the plant fertility decreases; and that the mutant plants with only one gene in heterozygosis have similar, extremely low levels of fertility (even if in some of them it is higher because of the different degree of gene relevance, in particular *NGA2*). However, while the increase in the number of mutated genes causes the reduction of the number of mature fruits developed, it does not influence the number of not pollinated flowers or early aborted fruits found; instead, it is the number of late aborted fruits that increases (**Figure 4.3**). This, together with the fact that many genotypes with considerable fertility reduction do not have their pistil morphology heavily altered,

indicates that the style and stigma morphology defects are not the only factors impairing plant fertility and fruit development capacity. Moreover, lack of pollination is not the main factor that causes the mutant's loss of fertility because in all of the mutant genotypes, including the quadruple homozygote, anthers shed pollen normally, and we have proven that their pollen if functional when applied to WT pistils. These results led us to think that the rice *NGA* genes are involved in other factors affecting floral fertility and fruit development capacity apart from morphological development of the style and stigma. We theorized that *NGA* genes may also be involved in other processes, such as ovule development, which was recently confirmed by histological analysis.

Even so, *NGA* genes are expressed in the anther tapetum and male germ line (**Figure 4.9**). So, to check if pollen viability was also affected by the lack of *NGA*, we crossed DJ♀ and *nga1 nga2 nga3-2 nga4-2*♂ plants and obtained viable descendants with an 83,6% efficiency, which means that the pollen is still functional and suggests that the *NGA* genes are not affecting its viability. However, complementary experiments are needed, such as *in vitro* and *in vivo* assays of pollen germination and pollen tube growth, to confirm this for sure, as a lack of *NGA* genes could slightly affect pollen viability. Nonetheless, this cross test had an exceptionally high efficiency, similar to wild type pollen donors, supporting the idea that the mutant pollen was fully functional.

We observed that each gene, when mutated, affected pistil development and plant fertility at a different level (**Figures 4.2 and 4.4**); a similar thing has already been described in *Arabidopsis*, where *nga3-3* and *nga1-1* showed stronger phenotypes than the rest of *nga* mutants studied (Alvarez *et al.*, 2009; Trigueros *et al.*, 2009). In rice, when comparing the genotypes with three mutant genes in homozygosis and one that is in heterozygosis, we saw that *nga1 nga2*/+ *nga3-2 nga4-2* had more fertility than the others across independent generations (even if it was not statistically significant in the post hoc test) and its pistils were the less affected ones, suggesting that *NGA2* is the most important rice *NGA* gene for style and stigma development and plant fertility. Next, *nga1*/+ *nga2 nga3-2 nga4-2* developed some viable fruits, unlike *nga1 nga2 nga3-2 nga4-2*/+, that was infertile. However, *nga1 nga2 nga3-2 nga4-2*/+ pistils seemed to display a better style and stigma development. Nonetheless, they also developed more overgrown tissue in the space between the styles, which is probably associated to plant sterility, since we have shown by histology that this ectopic tissue derives from the degeneration of ovule integuments. This suggests that *NGA1* is more critical for ovule development and associated female fertility, whereas *NGA4* is more important for style and stigma development. Finally, I did not focus much

on the individual contribution of*NGA3*, because previous studies done in the host lab already suggested that it contributes less than the other three to style and stigma specification. However, I took pictures of the *nga1 nga2 NGA3 nga4-2/+* mutant pistils, which had very similar styles and stigmas as the *nga1 nga2 nga3-2 nga4-2/+* ones, suggesting that *NGA3* has a minimal role in the style and stigma development. Still, they did not possess any overgrown tissue from inside the ovary, which indicated that *NGA3* is probably sustaining ovule development. Nonetheless, we have to consider that our *nga3* and *nga4* mutations affect the promoter regions and should not be considered null mutants. But this would not affect much the proposed order of gene importance because *nga1 nga2 NGA3 nga4-2/+* and *nga1 nga2 nga3-2 nga4-2/+* already have some of the most extreme phenotypes in the style and stigma development, only surpassed by the *nga1/+ nga2 nga3-2 nga4-2* and quadruple mutant homozygote *nga1 nga2 nga3-2 nga4-2*.

We also performed a histological analysis of the rice pistil and ovule early development in WT and *nga* quadruple homozygous plants, using 7 mm and 20 mm inflorescence primordia. Our results show that, right before inducing the apical growth of style and stigma, *NGA* genes are also necessary for the carpel (ovary wall) primordia to correctly enclose the ovule apically, as that does not happen in the *nga* quadruple mutants (**Figures 4.10, 11**). In the mature flowers, either as a direct result of the lack of *NGA* or because on the lack of total ovule enclosure, the ovule grows too much, specifically its integuments are so overgrown that they exit the top of the pistil, which explains the origin of the overgrown tissue observed in the pistil pictures taken using the macroscope. A similar integument overgrowth is observed also in other genotypes, suggesting that ovule defects are the leading cause of female sterility in those genotypes that still develop plenty of stylar and stigmatic tissues (**Figure 4.4**). In these mature flowers, we also saw defects in the mutant embryo sac shape and position (**Figure 4.11**). It remains to be determined if the aborted fruits derive by fertilization events which cannot develop till maturity, for example because of milder integument defects, or by parthenocarpic phenotypes, which seems more likely at least for the quadruple homozygous mutant; wild type and mutant fruits have been already fixed and embedded, and histological analysis will be completed soon.

In *Arabidopsis*, *NGA* genes seem to be promoting auxin biosynthesis to direct pistil development (Alvarez *et al.*, 2009; Ballester *et al.*, 2021); as it has been previously reported in RNA-seq results, where genes involved in auxin biosynthesis had a reduced expression in the quadruple *nga* mutant (Martínez-

Fernández *et al.*, 2014). However, our RNA-seq results suggest that rice *NGA* genes are repressing them instead: when comparing gene expression in developing inflorescence primordia from quadruple homozygous mutant (*nga1 nga2 nga3-2 nga4-2*) and WT plants, we found that genes related to auxin biosynthesis, transport, and response were upregulated in the mutant. This indicates that the lack of *NGA* allows a higher expression of these genes that otherwise would be repressed. We were surprised by this discovery, and more studies are needed to discern the role of *NGA* in this process, starting by performing *in situ* hybridizations in WT and mutant inflorescence primordia at different developmental stages to see the expression pattern of these genes and how and where it changes in the *nga* quadruple mutant. We also found genes related to cytokinin and gibberellin deregulated, but they were fewer and less deregulated than the ones involved on auxin pathway; our results suggest that the *NGA* genes could promote these two hormones.

We also focused on three transcription factors that were deregulated. First, we found an extremely downregulated gene that belong to the REM family. This gene family is involved in floral meristem identity determination and flower development promotion (Mantegazza *et al.*, 2014). Strongly downregulated was also *TCP25*, which is involved in activating growth-associated genes (Kosugi and Ohashi, 2002; Sharma *et al.*, 2010). Finally, a gene we hypothesize could be homolog to Arabidopsis *KNU*, which induces floral meristem termination during floral development (Payne *et al.*, 2004), was upregulated. These results suggest that as a consequence of *NGA* action, flower development and growth were promoted via the activation of *REM* and *TCP25*, respectively; and meristem termination was inhibited via the *KNU* homolog repression. This means that *NGA* genes would encourage floral development by regulating these three transcription factors (either directly or indirectly). In *Arabidopsis*, there is evidence that *TCP* and *NGA* form a regulatory module that controls leaf expansion (Ballester *et al.*, 2015); our results showed expression in panicle primordium, but there is the possibility that *TCP* activation could also be conserved in the leaves. It is also worth noting that our RNA-seq results were showing expression changes between mutant and WT entire inflorescence primordia, which means that a gene could be upregulated in a very specific region or cell type and downregulated in another, or significantly deregulated in a particular area, but the result from the whole sample would show it as not very affected due to ‘dilution’ effect. The next step would be to do *in situ* hybridizations of these deregulated genes to see their expression pattern in WT and mutant samples, particularly in the pistil and ovule primordia at their earliest stages.

To sum up, we verified that *NGA* genes promote rice style and stigma development in a redundant and dose-dependent way, just like in *Arabidopsis*. However, unlike in this model plant, rice *NGA* genes may suppress auxin biosynthesis, transport, and response. We also found that they regulate plant fertility, fruit development capacity, and vegetative growth; they did not seem important for pollen viability.

6. Conclusions

This master's thesis results allow us to formulate a series of conclusions:

- Rice *NGA* genes act redundantly and in a dose-dependent manner in regulating style and stigma development, like in *Arabidopsis*. From an evolution-development (evo-devo) perspective, *NGA* function in style and stigma specification is therefore essential and conserved across core and basal eudicots and monocots. So, it is very likely that they have been essential for the evolution of style and stigma in angiosperm plants.
- Rice *NGA* genes are important for plant fertility and fruit development, as well as plant growth and leaf development.
- Our results suggest that not all rice *NGA* have the same level of importance in style and stigma development and plant fertility. *NGA2* seem to be the most important one, followed by *NGA4* in style and stigma development and *NGA1* in female fertility. And finally, *NGA3* seems to be the less relevant one.
- Style and stigma morphological defects present in the rice *nga* mutants are not the only factors impairing floral fertility, suggesting the existence of additional *NGA* gene functions. They do not seem to be involved in pollen development and fertility. However, we have discovered a new essential function of *NGA* genes in ovule and especially integument development, which has not been reported in eudicot model plants so far.
- Rice *NGA* genes seem to inhibit auxin biosynthesis and transport, leading to a decrease in auxin response, which is the opposite of what happens in *Arabidopsis*. And *NGA* gene action might be partially carried out by promoting *REM* and *TCP25* transcription factors and repressing a *KNU* homolog.

Annex

Annex 1. Agarose gels that that indicate the genotype of the first generation of plants (8 – 4B14), and from the independent group of plants (7 – F2 8-5). DJ WT: not mutant control; x14: quadruple mutant heterozygous control; H_2O: negative control.

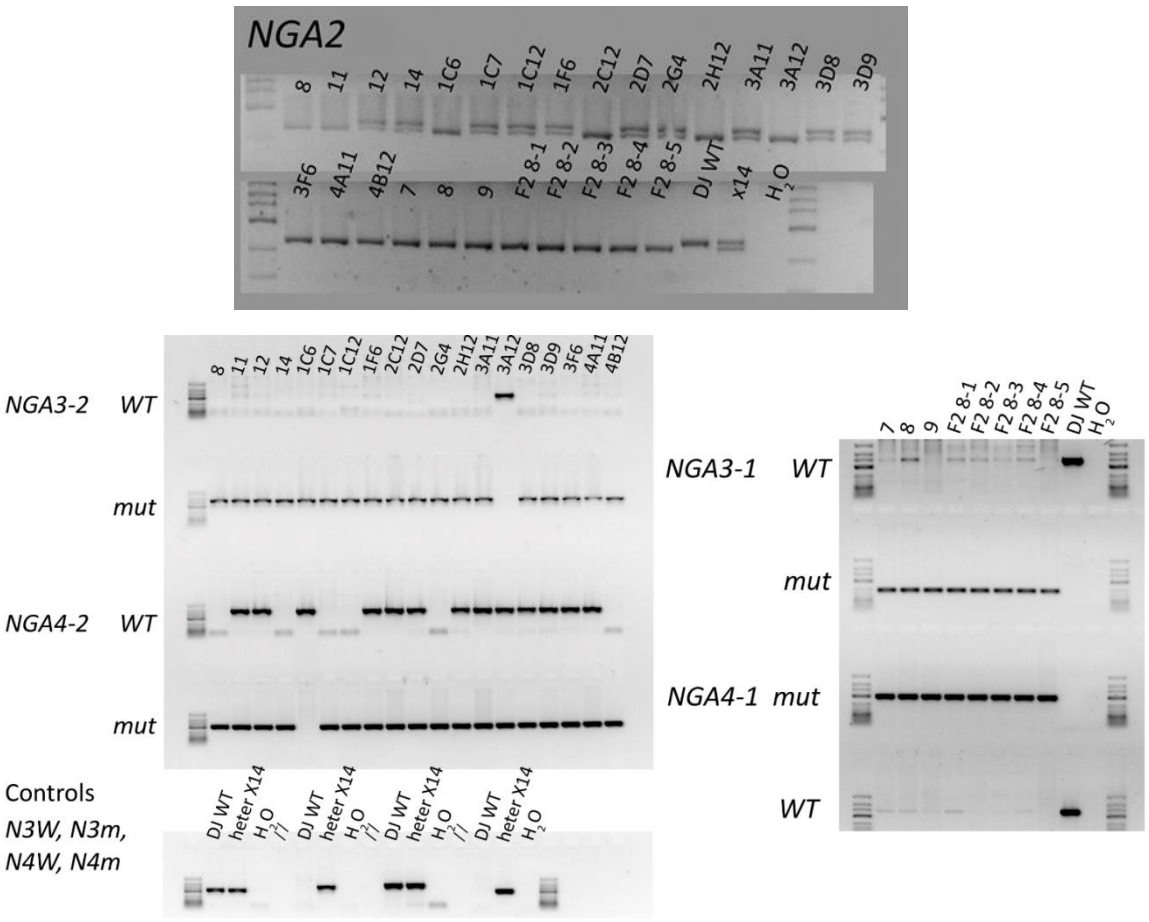

Annex 2. Agarose gels that that indicate the genotype of the second generation of plants. x14: quadruple mutant heterozygous.

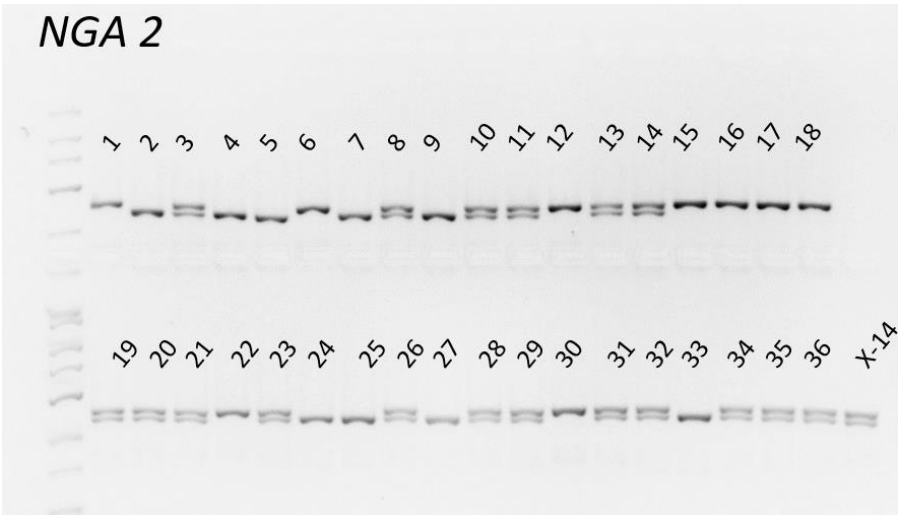

Annex 3. Fertility levels of the selected genotypes from the first generation of plants and the independent group of plants. St.dev.: Standard deviation; *n: nga*.

	Fertility	*St.dev*
DJ	95.77	4.17
n1/+ n2/+ n3-2/+ n4-2/+	91.94	2.31
n1 n2/+ n3-2 n4-2/+	45.25	5.89
n1/+ n2 n3-2 n4-2/+	30.20	7.75
n1 n2/+ n3-2 n4-2	9.92	5.44
n1/+ n2 n3-2 n4-2	0.71	1.01
n1 n2 n3-2 n4-2/+	0.00	0.00
n1 n2 n3-2 n4-2	0.00	0.00
N1 n2 n3-1 n4-1	1.57	1.41

Annex 4. ANOVA and Post Hoc test performed using JASP software determining statistically significant differences between the fertility levels of the genotypes from the first generation and the independent group of plants.

ANOVA - Fertility

Cases	Sum of Squares	df	Mean Square	F	p
Sample	34809.831	8	4351.229	232.536	< .001
Residuals	299.394	16	18.712		

Note. Type III Sum of Squares

Post Hoc Comparisons - Sample

		Mean Difference	SE	t	p_{tukey}
DJ	(N1 n2 n3-1 n4-1)	94.206	3.532	26.672	< .001
	(n1 n2 n3-2 n4-2)	95.773	3.532	27.116	< .001
	(n1 n2 n3-2 n4-2/+)	95.773	3.949	24.253	< .001
	(n1 n2/+ n3-2 n4-2)	85.850	3.532	24.307	< .001
	(n1 n2/+ n3-2 n4-2/+)	50.525	3.532	14.305	< .001
	(n1/+ n2 n3-2 n4-2)	95.059	3.949	24.072	< .001
	(n1/+ n2 n3-2 n4-2/+)	65.575	3.532	18.566	< .001
	(n1/+ n2/+ n3-2/+ n4-2/+)	3.828	3.532	1.084	0.969
(N1 n2 n3-1 n4-1)	(n1 n2 n3-2 n4-2)	1.567	3.532	0.444	1.000
	(n1 n2 n3-2 n4-2/+)	1.567	3.949	0.397	1.000
	(n1 n2/+ n3-2 n4-2)	-8.356	3.532	-2.366	0.362
	(n1 n2/+ n3-2 n4-2/+)	-43.682	3.532	-12.368	< .001
	(n1/+ n2 n3-2 n4-2)	0.853	3.949	0.216	1.000
	(n1/+ n2 n3-2 n4-2/+)	-28.631	3.532	-8.106	< .001
	(n1/+ n2/+ n3-2/+ n4-2/+)	-90.378	3.532	-25.589	< .001
(n1 n2 n3-2 n4-2)	(n1 n2 n3-2 n4-2/+)	2.132×10^{-14}	3.949	5.398×10^{-15}	1.000
	(n1 n2/+ n3-2 n4-2)	-9.923	3.532	-2.810	0.186
	(n1 n2/+ n3-2 n4-2/+)	-45.248	3.532	-12.811	< .001
	(n1/+ n2 n3-2 n4-2)	-0.714	3.949	-0.181	1.000
	(n1/+ n2 n3-2 n4-2/+)	-30.198	3.532	-8.550	< .001
	(n1/+ n2/+ n3-2/+ n4-2/+)	-91.945	3.532	-26.032	< .001
(n1 n2 n3-2 n4-2/+)	(n1 n2/+ n3-2 n4-2)	-9.923	3.949	-2.513	0.295
	(n1 n2/+ n3-2 n4-2/+)	-45.248	3.949	-11.459	< .001
	(n1/+ n2 n3-2 n4-2)	-0.714	4.326	-0.165	1.000
	(n1/+ n2 n3-2 n4-2/+)	-30.198	3.949	-7.647	< .001
	(n1/+ n2/+ n3-2/+ n4-2/+)	-91.945	3.949	-23.284	< .001
(n1 n2/+ n3-2 n4-2)	(n1 n2/+ n3-2 n4-2/+)	-35.325	3.532	-10.002	< .001
	(n1/+ n2 n3-2 n4-2)	9.209	3.949	2.332	0.379
	(n1/+ n2 n3-2 n4-2/+)	-20.275	3.532	-5.740	< .001
	(n1/+ n2/+ n3-2/+ n4-2/+)	-82.021	3.532	-23.223	< .001
(n1 n2/+ n3-2 n4-2/+)	(n1/+ n2 n3-2 n4-2)	44.534	3.949	11.278	< .001
	(n1/+ n2 n3-2 n4-2/+)	15.051	3.532	4.261	0.013
	(n1/+ n2/+ n3-2/+ n4-2/+)	-46.696	3.532	-13.221	< .001
(n1/+ n2 n3-2 n4-2)	(n1/+ n2 n3-2 n4-2/+)	-29.483	3.949	-7.466	< .001
	(n1/+ n2/+ n3-2/+ n4-2/+)	-91.230	3.949	-23.103	< .001
(n1/+ n2 n3-2 n4-2/+)	(n1/+ n2/+ n3-2/+ n4-2/+)	-61.747	3.532	-17.482	< .001

Note. P-value adjusted for comparing a family of 9

Annex 5. Fertility levels of the selected genotypes from the second generation of plants. St.dev.: Standard deviation; *n: nga*.

	Fertility	*St.dev*
DJ	94.04	2.11
n1 N2 n3 n4	43.86	13.66
n1 n2/+ n3 n4	17.82	6.59
n1 n2 n3 n4	0.00	0.00

Annex 6. ANOVA and Post Hoc test performed using JASP software determining statistically significant differences between the fertility levels of the genotypes from the second generation of plants.

ANOVA - Fertility

Cases	Sum of Squares	df	Mean Square	F	p
Genotype	15067.659	3	5022.553	85.746	< .001
Residuals	468.600	8	58.575		

Note. Type III Sum of Squares

Post Hoc Comparisons - Genotype

		Mean Difference	SE	t	p_{tukey}
DJ	n1 N2 n3 n4	50.179	6.249	8.030	< .001
	n1 n2 n3 n4	94.039	6.249	15.049	< .001
	(n1 n2/+ n3 n4)	76.220	6.249	12.197	< .001
n1 N2 n3 n4	n1 n2 n3 n4	43.861	6.249	7.019	< .001
	(n1 n2/+ n3 n4)	26.041	6.249	4.167	0.013
n1 n2 n3 n4	(n1 n2/+ n3 n4)	-17.819	6.249	-2.852	0.082

Note. P-value adjusted for comparing a family of 4

Annex 7. Percentage of the fruits produced by the first generation of plants and the independent group of plants divided into mature fruits, late abortions, early abortions and not pollinated flowers. *n: nga*.

	Mature	*Late abortion*	*Early abortion*	*Not pollinated*
DJ	95.77	0.00	0.00	4.23
n1/+ n2/+ n3-2/+ n4-2/+	91.94	2.42	0.41	5.23
n1 n2/+ n3-2 n4-2/+	45.25	17.70	5.13	31.91
n1/+ n2 n3-2 n4-2/+	30.20	36.82	17.95	15.03
n1 n2/+ n3-2 n4-2	9.92	55.50	5.71	28.87
N1 n2 n3-1 n4-1	1.57	33.86	1.13	63.44
n1/+ n2 n3-2 n4-2	0.71	73.79	13.82	11.68
n1 n2 n3-2 n4-2/+	0.00	76.00	3.13	20.87
n1 n2 n3-2 n4-2	0.00	19.56	4.88	75.56

Annex 8. Percentage of the fruits produced by the second generation of plants divided into mature fruits, late abortions, early abortions and not pollinated flowers. *n: nga*.

	Mature	*Late abortion*	*Early abortion*	*Not pollinated*
DJ	94.29	1.14	0.57	4.00
n1 N2 n3 n4	42.55	28.19	6.91	22.34
n1 n2/+ n3 n4	17.65	45.10	9.15	28.10
n1 n2 n3 n4	0.00	82.67	0.00	17.33

Annex 9. Leaf width, and number of large and small vascular bundles from 5 WT flag leaves and 5 quadruple homozygous mutant flag leaves. St.dev.: Standard deviation; *n: nga*.

	Leaf width	*St.dev*
DJ	1.35	0.22
n1 n2 n3 n4	1.56	0.28

	Large vascular bundles	*St.dev*
DJ	11.00	1.22
n1 n2 n3 n4	13.60	0.89

	Small vascular bundles	*St.dev*
DJ	46.00	4.36
n1 n2 n3 n4	56.40	6.27

Annex 10. Student's t-test performed using JASP software determining statistically significant differences between leaf width, and number of large and small vascular bundles.

Independent Samples T-Test

	t	df	p
Width	-1.300	8	0.230

Note. Student's t-test.

Independent Samples T-Test

	t	df	p
Large vascular bundles	-3.833	8	0.005

Note. Student's t-test.

Independent Samples T-Test

	t	df	p
Small vascular bundles	-3.233	7	0.014

Note. Student's t-test.

Annex 11. Sustainable Development Goals (SDGs) related to this thesis.

BOUPV
Butlletí Oficial de la Universitat Politècnica de València

Núm. 118/2022 27/07/2022 16

ANEXO I. RELACIÓN DEL TRABAJO CON LOS OBJETIVOS DE DESARROLLO SOSTENIBLE DE LA AGENDA 2030

Anexo al Trabajo de Fin de Grado y Trabajo de Fin de Máster: Relación del trabajo con los Objetivos de Desarrollo Sostenible de la agenda 2030

Grado de relación del trabajo con los Objetivos de Desarrollo Sostenible (ODS).

Objetivos de Desarrollo Sostenibles	Alto	Medio	Bajo	No Procede
ODS 1. **Fin de la pobreza.**			X	
ODS 2. **Hambre cero.**	X			
ODS 3. **Salud y bienestar.**		X		
ODS 4. **Educación de calidad.**				X
ODS 5. **Igualdad de género.**				X
ODS 6. **Agua limpia y saneamiento.**				X
ODS 7. **Energía asequible y no contaminante.**				X
ODS 8. **Trabajo decente y crecimiento económico.**			X	
ODS 9. **Industria, innovación e infraestructuras.**			X	
ODS 10. **Reducción de las desigualdades.**				X
ODS 11. **Ciudades y comunidades sostenibles.**				X
ODS 12. **Producción y consumo responsables.**				X
ODS 13. **Acción por el clima.**				X
ODS 14. **Vida submarina.**				X
ODS 15. **Vida de ecosistemas terrestres.**				X
ODS 16. **Paz, justicia e instituciones sólidas.**				X
ODS 17. **Alianzas para lograr objetivos.**				X

Descripción de la alineación del TFG/TFM con los ODS con un grado de relación más alto.

***Utilice tantas páginas como sea necesario.

Editor: Secretaria General / UPV · D.L.: V-5092-2006 · ISSN: 1887-2298 · www.upv.es/secgen

Bibliography

Alvarez, J. P., Goldshmidt, A., Efroni, I., Bowman, J. L., & Eshed, Y. (2009). The NGATHA distal organ development genes are essential for style specification in Arabidopsis . The Plant Cell, 21(5), 1373–1393. https://doi.org/10.1105/tpc.109.065482

Alvarez, J. P., Pekker, I., Goldshmidt, A., Blum, E., Amsellem, Z., & Eshed, Y. (2006). Endogenous and Synthetic MicroRNAs Stimulate Simultaneous, Efficient, and Localized Regulation of Multiple Targets in Diverse Species. The Plant Cell, 18(5), 1134–1151. https://doi.org/10.1105/tpc.105.040725

Alvarez, J., & Smyth, D. R. (1999). CRABS CLAW and SPATULA, two Arabidopsis genes that control carpel development in parallel with AGAMOUS. Development, 126(11), 2377–2386. https://doi.org/10.1242/dev.126.11.2377

ANGENENT, G., & COLOMBO, L. (1996). Molecular control of ovule development. Trends in Plant Science, 1(7), 228–232. https://doi.org/10.1016/s1360-1385(96)86900-0

Arora, R., Agarwal, P., Ray, S., Singh, A. K., Singh, V. P., Tyagi, A. K., & Kapoor, S. (2007). MADS-box gene family in rice: Genome-wide identification, organization and expression profiling during reproductive development and stress. BMC Genomics, 8(1). https://doi.org/10.1186/1471-2164-8-242

Ballester, P., Martínez-Godoy, M. A., Ezquerro, M., Navarrete-Gómez, M., Trigueros, M., Rodríguez-Concepción, M., & Ferrándiz, C. (2021). A transcriptional complex of NGATHA and bHLH transcription factors directs stigma development in Arabidopsis. The Plant Cell, 33(12), 3645–3657. https://doi.org/10.1093/plcell/koab236

Ballester, P., Navarrete-Gómez, M., Carbonero, P., Oñate-Sánchez, L., & Ferrándiz, C. (2015). Leaf expansion in Arabidopsis is controlled by a TCP-NGA regulatory module likely conserved in distantly related species. Physiologia Plantarum, 155(1), 21–32. https://doi.org/10.1111/ppl.12327

Becker, A. (2020). A molecular update on the origin of the carpel. Current Opinion in Plant Biology, 53, 15–22. https://doi.org/10.1016/j.pbi.2019.08.009

Bennett, S. R. M., Alvarez, J., Bossinger, G., & Smyth, D. R. (1995). Morphogenesis in pinoid mutants of Arabidopsis thaliana. The Plant Journal, 8(4), 505–520. https://doi.org/10.1046/j.1365-313x.1995.8040505.x

Bommert, P., Satoh-Nagasawa, N., Jackson, D., & Hirano, H.-Y. (2005). Genetics and evolution of inflorescence and flower development in grasses. Plant and Cell Physiology, 46(1), 69–78. https://doi.org/10.1093/pcp/pci504

Bowman, J. L., & Smyth, D. R. (1999). CRABS CLAW, a gene that regulates carpel and nectary development in Arabidopsis, encodes a novel protein with zinc finger and helix-loop-helix domains. Development, 126(11), 2387–2396. https://doi.org/10.1242/dev.126.11.2387

Bowman, J. L., Sakai, H., Jack, T., Weigel, D., Mayer, U., & Meyerowitz, E. M. (1992). SUPERMAN, a regulator of floral homeotic genes in Arabidopsis. Development, 114(3), 599–615. https://doi.org/10.1242/dev.114.3.599

Brand, U., Fletcher, J. C., Hobe, M., Meyerowitz, E. M., & Simon Rüdiger. (2000). Dependence of Stem Cell Fate in Arabidopsis on a Feedback Loop Regulated by CLV3 Activity. Science, 289(5479), 617–619. https://doi.org/10.1126/science.289.5479.617

Buechel, S., Leibfried, A., To, J. P. C., Zhao, Z., Andersen, S. U., Kieber, J. J., & Lohmann, J. U. (2010). Role of A-type ARABIDOPSIS RESPONSE REGULATORS in meristem maintenance and regeneration. European Journal of Cell Biology, 89(2-3), 279–284. https://doi.org/10.1016/j.ejcb.2009.11.016

Causier, B., Schwarz-Sommer, Z., & Davies, B. (2010). Floral organ identity: 20 years of ABCs. Seminars in Cell & Developmental Biology, 21(1), 73–79. https://doi.org/10.1016/j.semcdb.2009.10.005

Chae, E., Tan, Q. K.-G., Hill, T. A., & Irish, V. F. (2008). An Arabidopsis F-box protein acts as a transcriptional co-factor to regulate floral development. Development, 135(7), 1235–1245. https://doi.org/10.1242/dev.015842

Chen, M., SanMiguel, P., de Oliveira, A. C., Woo, S.-S., Zhang, H., Wing, R. A., & Bennetzen, J. L. (1997). Microcolinearity in sh2-homologous regions of the maize, rice, and sorghum genomes. Proceedings of the National Academy of Sciences, 94(7), 3431–3435. https://doi.org/10.1073/pnas.94.7.3431

Cheng, Y., Dai, X., & Zhao, Y. (2006). Auxin biosynthesis by the YUCCA flavin monooxygenases controls the formation of floral organs and vascular tissues in Arabidopsis. Genes & Development, 20(13), 1790–1799. https://doi.org/10.1101/gad.1415106

Clark, S. E., Running, M. P., & Meyerowitz, E. M. (1993). CLAVATA1, a regulator of meristem and flower development in Arabidopsis. Development, 119(2), 397–418. https://doi.org/10.1242/dev.119.2.397

Colombo, L., Franken, J., Koetje, E., van Went, J., Dons, H. J., Angenent, G. C., & van Tunen, A. J. (1995). The Petunia MADS box gene FBP11 determines ovule identity. The Plant Cell, 7(11), 1859–1868. https://doi.org/10.1105/tpc.7.11.1859

Cucinotta, M., Colombo, L., & Roig-Villanova, I. (2014). Ovule development, a new model for lateral organ formation. Frontiers in Plant Science, 5. https://doi.org/10.3389/fpls.2014.00117

Cui, R., Han, J., Zhao, S., Su, K., Wu, F., Du, X., Xu, Q., Chong, K., Theißen, G., & Meng, Z. (2010). Functional conservation and diversification of class E floral homeotic genes in rice (Oryza sativa). The Plant Journal, 61(5), 767–781. https://doi.org/10.1111/j.1365-313x.2009.04101.x

Dreni, L., & Kater, M. M. (2013). MADS reloaded: evolution of the AGAMOUS subfamily genes. New Phytologist, 201(3), 717–732. https://doi.org/10.1111/nph.12555

Dreni, L., Jacchia, S., Fornara, F., Fornari, M., Ouwerkerk, P. B., An, G., Colombo, L., & Kater, M. M. (2007). The D-lineage MADS-box gene OSMADS13 controls ovule identity in Rice. The Plant Journal, 52(4), 690–699. https://doi.org/10.1111/j.1365-313x.2007.03272.x

Dreni, L., Osnato, M., & Kater, M. M. (2013). The Ins and Outs of the Rice AGAMOUS Subfamily. Molecular Plant, 6(3), 650–664. https://doi.org/10.1093/mp/sst019

Dreni, L., Pilatone, A., Yun, D., Erreni, S., Pajoro, A., Caporali, E., Zhang, D., & Kater, M. M. (2011). Functional analysis of all AGAMOUS subfamily members in Rice reveals their roles in reproductive organ identity determination and Meristem determinacy. The Plant Cell, 23(8), 2850–2863. https://doi.org/10.1105/tpc.111.087007

Favaro, R., Pinyopich, A., Battaglia, R., Kooiker, M., Borghi, L., Ditta, G., Yanofsky, M. F., Kater, M. M., & Colombo, L. (2003). MADS-box protein complexes control carpel and ovule development in Arabidopsis. The Plant Cell, 15(11), 2603–2611. https://doi.org/10.1105/tpc.015123

Ferrándiz, C., Fourquin, C., Prunet, N., Scutt, C. P., Sundberg, E., Trehin, C., & Vialette-Guiraud, A. C. M. (2010). Carpel development. Advances in Botanical Research, 1–73. https://doi.org/10.1016/b978-0-12-380868-4.00001-6

Fourquin, C., & Ferrándiz, C. (2014). The essential role of NGATHA genes in style and stigma specification is widely conserved across eudicots. New Phytologist, 202(3), 1001–1013. https://doi.org/10.1111/nph.12703

Frebort, I., Kowalska, M., Hluska, T., Frebortova, J., & Galuszka, P. (2011). Evolution of cytokinin biosynthesis and degradation. Journal of Experimental Botany, 62(8), 2431–2452. https://doi.org/10.1093/jxb/err004

Glanc, M., Van Gelderen, K., Hoermayer, L., Tan, S., Naramoto, S., Zhang, X., Domjan, D., Včelařová, L., Hauschild, R., Johnson, A., de Koning, E., van Dop, M., Rademacher, E., Janson, S., Wei, X., Molnár, G., Fendrych, M., De Rybel, B., Offringa, R., & Friml, J. (2021). AGC kinases and MAB4/MEL proteins maintain PIN polarity by limiting lateral diffusion in plant cells. Current Biology, 31(9). https://doi.org/10.1016/j.cub.2021.02.028

Gomariz-Fernández, A., Sánchez-Gerschon, V., Fourquin, C., & Ferrándiz, C. (2017). The Role of SHI/STY/SRS Genes in Organ Growth and Carpel Development Is Conserved in the Distant Eudicot Species Arabidopsis thaliana and Nicotiana benthamiana. Frontiers in Plant Science, 8. https://doi.org/10.3389/fpls.2017.00814

Gómez-Mena Concepción, de Folter, S., Costa, M. M., Angenent, G. C., & Sablowski, R. (2005). Transcriptional program controlled by the floral homeotic gene AGAMOUS during early organogenesis. Development, 132(3), 429–438. https://doi.org/10.1242/dev.01600

Hardke, J. T., Moldenhauer, K., & Counce, P. (2013). Chapter2: Rice Growth and Development. In Arkansas Rice Production Handbook (pp. 9–20). essay, Cooperative Extension Service, University of Arkansas.

He, Y., Yan, L., Ge, C., Yao, X.-F., Han, X., Wang, R., Xiong, L., Jiang, L., Liu, C.-M., & Zhao, Y. (2019). PINOID Is Required for Formation of the Stigma and Style in Rice. Plant Physiology, 180(2), 926–936. https://doi.org/10.1104/pp.18.01389

Honma, T., & Goto, K. (2001). Complexes of MADS-box proteins are sufficient to convert leaves into floral organs. Nature, 409(6819), 525–529. https://doi.org/10.1038/35054083

Hu, Y., Liang, W., Yin, C., Yang, X., Ping, B., Li, A., Jia, R., Chen, M., Luo, Z., Cai, Q., Zhao, X., Zhang, D., & Yuan, Z. (2015). Interactions of OSMADS1 with floral homeotic genes in rice flower development. Molecular Plant, 8(9), 1366–1384. https://doi.org/10.1016/j.molp.2015.04.009

Ikeda, K., Nagasawa, N., & Nagato, Y. (2005). ABERRANT PANICLE ORGANIZATION 1 temporally regulates meristem identity in rice. Developmental Biology, 282(2), 349–360. https://doi.org/10.1016/j.ydbio.2005.03.016

Ikeda, M., Mitsuda, N., & Ohme-Takagi, M. (2009). Arabidopsis WUSCHEL Is a Bifunctional Transcription Factor That Acts as a Repressor in Stem Cell Regulation and as an Activator in Floral Patterning. The Plant Cell, 21(11), 3493–3505. https://doi.org/10.1105/tpc.109.069997

Ikeda-Kawakatsu, K., Maekawa, M., Izawa, T., Itoh, J.-I., & Nagato, Y. (2011). ABERRANT PANICLE ORGANIZATION 2/RFL, the rice ortholog of Arabidopsis LEAFY, suppresses the transition from inflorescence meristem to floral meristem through interaction with APO1. The Plant Journal, 69(1), 168–180. https://doi.org/10.1111/j.1365-313x.2011.04781.x

Itoh, J.-I., Nonomura, K.-I., Ikeda, K., Yamaki, S., Inukai, Y., Yamagishi, H., Kitano, H., & Nagato, Y. (2005). Rice plant development: From zygote to Spikelet. Plant and Cell Physiology, 46(1), 23–47. https://doi.org/10.1093/pcp/pci501

Izawa, T. (2007). Adaptation of flowering-time by natural and artificial selection in Arabidopsis and Rice. Journal of Experimental Botany, 58(12), 3091–3097. https://doi.org/10.1093/jxb/erm159

Jackson, S. A. (2016). Rice: The first crop genome. Rice, 9(1). https://doi.org/10.1186/s12284-016-0087-4

Jain, R., Jenkins, J., Shu, S., Chern, M., Martin, J. A., Copetti, D., Duong, P. Q., Pham, N. T., Kudrna, D. A., Talag, J., Schackwitz, W. S., Lipzen, A. M., Dilworth, D., Bauer, D., Grimwood, J., Nelson, C. R., Xing, F., Xie, W., Barry, K. W., … Ronald, P. C. (2019). Genome sequence of the model rice variety KitaakeX. BMC Genomics, 20(1). https://doi.org/10.1186/s12864-019-6262-4

Kagaya, Y., Ohmiya, K., & Hattori, T. (1999). RAV1, a novel DNA-binding protein, binds to bipartite recognition sequence through two distinct DNA-binding domains uniquely found in higher plants. Nucleic Acids Research, 27(2), 470–478. https://doi.org/10.1093/nar/27.2.470

Karami, M., Fatahi, N., Lohrasebi, T., & Razavi, K. (2021). RAV transcription factor regulatory function in response to salt stress in two Iranian wheat landraces. Journal of Plant Research, 135(1), 121–136. https://doi.org/10.1007/s10265-021-01356-7

Kellogg, E. A. (2001). Evolutionary history of the grasses. Plant Physiology, 125(3), 1198–1205. https://doi.org/10.1104/pp.125.3.1198

Kellogg, E. A. (2015). Flowering plants. Monocots Poaceae. Springer International Publishing.

Koornneef, M., & Meinke, D. (2010). The development of Arabidopsis as a model plant. The Plant Journal, 61(6), 909–921. https://doi.org/10.1111/j.1365-313x.2009.04086.x

Kosugi, S., & Ohashi, Y. (2002). DNA binding and dimerization specificity and potential targets for the TCP protein family. The Plant Journal, 30(3), 337–348. https://doi.org/10.1046/j.1365-313x.2002.01294.x

Lee, I., Wolfe, D. S., Nilsson, O., & Weigel, D. (1997). A LEAFY co-regulator encoded by UNUSUAL FLORAL ORGANS. Current Biology, 7(2), 95–104. https://doi.org/10.1016/s0960-9822(06)00053-4

Lee, J.-Y., Baum, S. F., Alvarez, J., Patel, A., Chitwood, D. H., & Bowman, J. L. (2005). Activation of CRABS CLAW in the Nectaries and Carpels of Arabidopsis. The Plant Cell, 17(1), 25–36. https://doi.org/10.1105/tpc.104.026666

Lee, Z. H., Tatsumi, Y., Ichihashi, Y., Suzuki, T., Shibata, A., Shirasu, K., Yamaguchi, N., & Ito, T. (2019). CRABS CLAW and SUPERMAN Coordinate Hormone-, Stress-, and Metabolic-Related Gene Expression During Arabidopsis Stamen Development. Frontiers in Ecology and Evolution, 7. https://doi.org/10.3389/fevo.2019.00437

Li, C.-W., Su, R.-C., Cheng, C.-P., Sanjaya, You, S.-J., Hsieh, T.-H., Chao, T.-C., & Chan, M.-T. (2011). Tomato RAV Transcription Factor Is a Pivotal Modulator Involved in the AP2/EREBP-Mediated Defense Pathway . Plant Physiology, 156(1), 213–227. https://doi.org/10.1104/pp.111.174268

Li, H., Liang, W., Hu, Y., Zhu, L., Yin, C., Xu, J., Dreni, L., Kater, M. M., & Zhang, D. (2011). Rice MADS6 Interacts with the Floral Homeotic Genes SUPERWOMAN1, MADS3, MADS58, MADS13, and DROOPING LEAF in Specifying Floral Organ Identities and Meristem Fate. The Plant Cell, 23(7), 2536–2552. https://doi.org/10.1105/tpc.111.087262

Li, H., Liang, W., Yin, C., Zhu, L., & Zhang, D. (2011). Genetic Interaction of OsMADS3, DROOPING LEAF, and OsMADS13 in Specifying Rice Floral Organ Identities and Meristem Determinacy . Plant Physiology, 156(1), 263–274. https://doi.org/10.1104/pp.111.172080

Litt, A. (2007). An Evaluation of A-Function: Evidence from the APETALA1 and APETALA2 Gene Lineages. International Journal of Plant Sciences, 168(1), 73–91. https://doi.org/10.1086/509662

Lo, S.-F., Yang, S.-Y., Chen, K.-T., Hsing, Y.-I., Zeevaart, J. A. D., Chen, L.-J., & Yu, S.-M. (2008). A novel class of gibberellin 2-oxidases control semidwarfism, tillering, and root development in Rice. The Plant Cell, 20(10), 2603–2618. https://doi.org/10.1105/tpc.108.060913

Lohmann, J. U., & Weigel, D. (2002). Building beauty: the genetic control of floral patterning. Developmental Cell, 2(2), 135–142. https://doi.org/10.1016/s1534-5807(02)00122-3

Lombardo, F., & Yoshida, H. (2015). Interpreting lemma and Palea Homologies: A point of view from Rice Floral Mutants. Frontiers in Plant Science, 6. https://doi.org/10.3389/fpls.2015.00061

Malcomber, S. T., & Kellogg, E. A. (2005). SEPALLATA gene diversification: brave new whorls. Trends in Plant Science, 10(9), 427–435. https://doi.org/10.1016/j.tplants.2005.07.008

Mano, Y., & Nemoto, K. (2012). The pathway of auxin biosynthesis in plants. Journal of Experimental Botany, 63(8), 2853–2872. https://doi.org/10.1093/jxb/ers091

Mantegazza, O., Gregis, V., Mendes, M. A., Morandini, P., Alves-Ferreira, M., Patreze, C. M., Nardeli, S. M., Kater, M. M., & Colombo, L. (2014). Analysis of the arabidopsis REM gene family predicts functions during Flower Development. Annals of Botany, 114(7), 1507–1515. https://doi.org/10.1093/aob/mcu124

Martínez-Fernández, I., Sanchí-s, S., Marini, N., Balanzá, V., Ballester, P., Navarrete-Gómez, M., Oliveira, A. C., Colombo, L., & Ferrándiz, C. (2014). The effect of NGATHA altered activity on auxin signaling pathways within the Arabidopsis gynoecium. Frontiers in Plant Science, 5. https://doi.org/10.3389/fpls.2014.00210

Matías-Hernández, L., Aguilar-Jaramillo, A. E., Marín-González, E., Suárez-López, P., & Pelaz, S. (2014). Rav Genes: Regulation of floral induction and beyond. Annals of Botany, 114(7), 1459–1470. https://doi.org/10.1093/aob/mcu069

McSteen, P., Malcomber, S., Skirpan, A., Lunde, C., Wu, X., Kellogg, E., & Hake, S. (2007). Barren Inflorescence2 Encodes a Co-Ortholog of the PINOID Serine/Threonine Kinase and Is Required for Organogenesis during Inflorescence and Vegetative Development in Maize. Plant Physiology, 144(2), 1000–1011. https://doi.org/10.1104/pp.107.098558

Nagasawa, N., Miyoshi, M., Sano, Y., Satoh, H., Hirano, H., Sakai, H., & Nagato, Y. (2003). SUPERWOMAN1 and DROOPING LEAFgenes control floral organ identity in rice. Development, 130(4), 705–718. https://doi.org/10.1242/dev.00294

Ó'Maoiléidigh, D. S., Wuest, S. E., Rae, L., Raganelli, A., Ryan, P. T., Kwaśniewska, K., Das, P., Lohan, A. J., Loftus, B., Graciet, E., & Wellmer, F. (2013). Control of Reproductive Floral Organ Identity Specification inArabidopsisby the C Function Regulator AGAMOUS . The Plant Cell, 25(7), 2482–2503. https://doi.org/10.1105/tpc.113.113209

Okushima, Y., Mitina, I., Quach, H. L., & Theologis, A. (2005). AUXIN RESPONSE FACTOR 2 (ARF2): a pleiotropic developmental regulator. The Plant Journal, 43(1), 29–46. https://doi.org/10.1111/j.1365-313x.2005.02426.x

Parcy, F., Nilsson, O., Busch, M. A., Lee, I., & Weigel, D. (1998). A genetic framework for floral patterning. Nature, 395(6702), 561–566. https://doi.org/10.1038/26903

Pařenicová Lucie, de Folter, S., Kieffer, M., Horner, D. S., Favalli, C., Busscher, J., Cook, H. E., Ingram, R. M., Kater, M. M., Davies, B., Angenent, G. C., & Colombo, L. (2003). Molecular and phylogenetic analyses of the complete MADS-box transcription factor family in Arabidopsis. The Plant Cell, 15(7), 1538–1551. https://doi.org/10.1105/tpc.011544

Pautler, M., Tanaka, W., Hirano, H.-Y., & Jackson, D. (2013). Grass Meristems I: Shoot apical meristem maintenance, axillary meristem determinacy and the floral transition. Plant and Cell Physiology, 54(3), 302–312. https://doi.org/10.1093/pcp/pct025

Payne, T., Johnson, S. D., & Koltunow, A. M. (2004). KNUCKLES (KNU) encodes a C2H2 zinc-finger protein that regulates development of basal pattern elements of the Arabidopsis gynoecium. Development, 131(15), 3737–3749. https://doi.org/10.1242/dev.01216

Pelaz, S., Ditta, G. S., Baumann, E., Wisman, E., & Yanofsky, M. F. (2000). B and C floral organ identity functions require SEPALLATA MADS-box genes. Nature, 405(6783), 200–203. https://doi.org/10.1038/35012103

Pelaz, S., Tapia-López, R., Alvarez-Buylla, E. R., & Yanofsky, M. F. (2001). Conversion of leaves into petals in Arabidopsis. Current Biology, 11(3), 182–184. https://doi.org/10.1016/s0960-9822(01)00024-0

Pfannebecker, K. C., Lange, M., Rupp, O., & Becker, A. (2017). Seed plant specific gene lineages involved in carpel development. Molecular Biology and Evolution. https://doi.org/10.1093/molbev/msw297

Pinyopich, A., Ditta, G. S., Savidge, B., Liljegren, S. J., Baumann, E., Wisman, E., & Yanofsky, M. F. (2003). Assessing the redundancy of MADS-box genes during carpel and ovule development. Nature, 424(6944), 85–88. https://doi.org/10.1038/nature01741

Prasad, K., Parameswaran, S., & Vijayraghavan, U. (2005). OsMADS1, a rice MADS-box factor, controls differentiation of specific cell types in the lemma and palea and is an early-acting regulator of inner floral organs. The Plant Journal, 43(6), 915–928. https://doi.org/10.1111/j.1365-313x.2005.02504.x

Prunet, N., Yang, W., Das, P., Meyerowitz, E. M., & Jack, T. P. (2017). SUPERMAN prevents class B gene expression and promotes stem cell termination in the fourth whorl of Arabidopsis thaliana flowers. Proceedings of the National Academy of Sciences, 114(27), 7166–7171. https://doi.org/10.1073/pnas.1705977114

Rademacher, E. H., & Offringa, R. (2012). Evolutionary adaptations of plant AGC kinases: From light signaling to Cell Polarity Regulation. Frontiers in Plant Science, 3. https://doi.org/10.3389/fpls.2012.00250

Reinhardt, D., Pesce, E.-R., Stieger, P., Mandel, T., Baltensperger, K., Bennett, M., Traas, J., Friml, J., & Kuhlemeier, C. (2003). Regulation of phyllotaxis by Polar Auxin Transport. Nature, 426(6964), 255–260. https://doi.org/10.1038/nature02081

Rensink, W. A., & Buell, C. R. (2004). Arabidopsis to rice. Applying knowledge from a weed to enhance our understanding of a crop species. Plant Physiology, 135(2), 622–629. https://doi.org/10.1104/pp.104.040170

Riechmann, J. L., Krizek, B. A., & Meyerowitz, E. M. (1996). Dimerization specificity of Arabidopsis MADS domain homeotic proteins APETALA1, APETALA3, PISTILLATA, and AGAMOUS. Proceedings of the National Academy of Sciences, 93(10), 4793–4798. https://doi.org/10.1073/pnas.93.10.4793

Romanel, E. A., Schrago, C. G., Couñago, R. M., Russo, C. A., & Alves-Ferreira, M. (2009). Evolution of the B3 DNA binding superfamily: New insights into REM family gene diversification. PLoS ONE, 4(6). https://doi.org/10.1371/journal.pone.0005791

Sakai, H., Krizek, B. A., Jacobsen, S. E., & Meyerowitz, E. M. (2000). Regulation of SUP expression identifies multiple regulators involved in Arabidopsis floral meristem development. The Plant Cell, 12(9), 1607–1618. https://doi.org/10.1105/tpc.12.9.1607

Salava, H., Thula, S., Sánchez, A. S., Nodzyński, T., & Maghuly, F. (2022). Genome Wide Identification and Annotation of NGATHA Transcription Factor Family in Crop Plants. International Journal of Molecular Sciences, 23(13), 7063. https://doi.org/10.3390/ijms23137063

Schoof, H., Lenhard, M., Haecker, A., Mayer, K. F. X., Jürgens, G., & Laux, T. (2000). The Stem Cell Population of Arabidopsis Shoot Meristems Is Maintained by a Regulatory Loop between the CLAVATA and WUSCHEL Genes. Cell, 100(6), 635–644. https://doi.org/10.1016/s0092-8674(00)80700-x

Schrager-Lavelle, A., Klein, H., Fisher, A., & Bartlett, M. (2017). Grass flowers: An untapped resource for Floral Evo-Devo. Journal of Systematics and Evolution, 55(6), 525–541. https://doi.org/10.1111/jse.12251

Schultz, E. A., Pickett, F. B., & Haughn, G. W. (1991). The FLO10 gene product regulates the expression domain of homeotic genes AP3 and pi in arabidopsis flowers. The Plant Cell, 3(11), 1221. https://doi.org/10.2307/3869229

Sessions, A., Nemhauser, J. L., McColl, A., Roe, J. L., Feldmann, K. A., & Zambryski, P. C. (1997). ETTIN patterns the Arabidopsis floral meristem and reproductive organs. Development, 124(22), 4481–4491. https://doi.org/10.1242/dev.124.22.4481

Shang, E., Ito, T., & Sun, B. (2019). Control of floral stem cell activity in Arabidopsis. Plant Signaling & Behavior, 14(11), 1659706. https://doi.org/10.1080/15592324.2019.1659706

Shao, J., Meng, J., Wang, F., Shou, B., Chen, Y., Xue, H., Zhao, J., Qi, Y., An, L., Yu, F., & Liu, X. (2020). NGATHA-LIKEs Control Leaf Margin Development by Repressing CUP-SHAPED COTYLEDON2 Transcription. Plant Physiology, 184(1), 345–358. https://doi.org/10.1104/pp.19.01598

Sharma, R., Kapoor, M., Tyagi, A. k. & Kapoor, S. (2010). Comparative transcript profiling of TCP family genes provide insight into gene functions and diversification in rice and Arabidopsis. J Plant Mol Biol Biotechnol. 1 (1): 24-38

Shen, C., Li, G., Dreni, L., & Zhang, D. (2021). Molecular control of carpel development in the grass family. Frontiers in Plant Science, 12. https://doi.org/10.3389/fpls.2021.635500

Sohlberg, J. J., Myrenås, M., Kuusk, S., Lagercrantz, U., Kowalczyk, M., Sandberg, G., & Sundberg, E. (2006). STY1 regulates auxin homeostasis and affects apical-basal patterning of the Arabidopsis gynoecium. The Plant Journal, 47(1), 112–123. https://doi.org/10.1111/j.1365-313x.2006.02775.x

Song, S., Tian, D., Zhang, Z., Hu, S., & Yu, J. (2018). Rice genomics: Over the past two decades and into the future. Genomics, Proteomics & Bioinformatics, 16(6), 397–404. https://doi.org/10.1016/j.gpb.2019.01.001

Sugiyama, S.-H., Yasui, Y., Ohmori, S., Tanaka, W., & Hirano, H.-Y. (2019). Rice Flower Development Revisited: Regulation of Carpel Specification and Flower Meristem determinacy. Plant and Cell Physiology, 60(6), 1284–1295. https://doi.org/10.1093/pcp/pcz020

Sundberg, E., & Ferrndiz, C. (n.d.). Gynoecium patterning in Arabidopsis: A basic plan behind a complex structure. Fruit Development and Seed Dispersal, 35–69. https://doi.org/10.1002/9781444314557.ch2

SWAMINATHAN, K., PETERSON, K., & JACK, T. (2008). The plant B3 superfamily. Trends in Plant Science, 13(12), 647–655. https://doi.org/10.1016/j.tplants.2008.09.006

Theißen, G. (2001). Development of floral organ identity: stories from the MADS house. Current Opinion in Plant Biology, 4(1), 75–85. https://doi.org/10.1016/s1369-5266(00)00139-4

Theißen, G., Melzer, R., & Rümpler, F. (2016). MADS-domain transcription factors and the floral quartet model of Flower Development: Linking Plant Development and Evolution. Development, 143(18), 3259–3271. https://doi.org/10.1242/dev.134080

Trigueros, M., Navarrete-Gómez Marisa, Sato, S., Christensen, S. K., Pelaz, S., Weigel, D., Yanofsky, M. F., & Ferrándiz Cristina. (2009). The NGATHA Genes Direct Style Development in the Arabidopsis Gynoecium . The Plant Cell, 21(5), 1394–1409. https://doi.org/10.1105/tpc.109.065508

Ueguchi-Tanaka, M., Nakajima, M., Motoyuki, A., & Matsuoka, M. (2007). Gibberellin receptor and its role in gibberellin signaling in plants. Annual Review of Plant Biology, 58(1), 183–198. https://doi.org/10.1146/annurev.arplant.58.032806.103830

Weigel, D., Alvarez, J., Smyth, D. R., Yanofsky, M. F., & Meyerowitz, E. M. (1992). LEAFY controls floral meristem identity in Arabidopsis. Cell, 69(5), 843–859. https://doi.org/10.1016/0092-8674(92)90295-n

What is the difference between carpels and pistils? (n.d.). Retrieved January 8, 2023, from https://mammothmemory.net/biology/plants/sexual-reproduction-in-plants/what-is-the-difference-between-carpels-and-pistils.html

Willmann, M. R. (2000). CLV1 and CLV3: negative regulators of SAM stem cell accumulation. Trends in Plant Science, 5(10), 416. https://doi.org/10.1016/s1360-1385(00)01763-5

WOODWARD, A. W. (2005). Auxin: Regulation, action, and interaction. Annals of Botany, 95(5), 707–735. https://doi.org/10.1093/aob/mci083

Wopereis, M. C. S., Defoer T., Idinoba P., Diack S. & Dugué M. J. (2008). PLAR-IRM Curriculum: Technical Manual

Wu, D., Liang, W., Zhu, W., Chen, M., Ferrándiz, C., Burton, R. A., Dreni, L., & Zhang, D. (2017). Loss of LOFSEP transcription factor function converts spikelet to leaf-like structures in Rice. Plant Physiology, 176(2), 1646–1664. https://doi.org/10.1104/pp.17.00704

Xiao, Y., & Offringa, R. (2020). PDK1 regulates auxin transport and Arabidopsis vascular development through AGC1 kinase PAX. Nature Plants, 6(5), 544–555. https://doi.org/10.1038/s41477-020-0650-2

Xu, M., Tang, D., Cheng, X., Zhang, J., Tang, Y., Tao, Q., Shi, W., You, A., Gu, M., Cheng, Z., & Yu, H. (2019). OsPINOID Regulates Stigma and Ovule Initiation through Maintenance of the Floral Meristem by Auxin Signaling. Plant Physiology, 180(2), 952–965. https://doi.org/10.1104/pp.18.01385

Xu, W., Tao, J., Chen, M., Dreni, L., Luo, Z., Hu, Y., Liang, W., & Zhang, D. (2017). Interactions between FLORAL ORGAN NUMBER4 and floral homeotic genes in regulating rice flower development. Journal of Experimental Botany, 68(3), 483–498. https://doi.org/10.1093/jxb/erw459

Xu, W., Zhu, W., Yang, L., Liang, W., Li, H., Yang, L., Chen, M., Luo, Z., Huang, G., Duan, L., Dreni, L., & Zhang, D. (2021). SMALL REPRODUCTIVE ORGANS, a SUPERMAN-like transcription factor, regulates stamen and pistil growth in rice. New Phytologist, 233(4), 1701–1718. https://doi.org/10.1111/nph.17849

Yamaguchi, N., Huang, J., Xu, Y., Tanoi, K., & Ito, T. (2017). Fine-tuning of auxin homeostasis governs the transition from floral stem cell maintenance to Gynoecium Formation. Nature Communications, 8(1). https://doi.org/10.1038/s41467-017-01252-6

Yamaguchi, T., & Hirano, H.-Y. (2006). Function and diversification of MADS-box genes in Rice. The Scientific World JOURNAL, 6, 1923–1932. https://doi.org/10.1100/tsw.2006.320

Yamaguchi, T., Lee, D. Y., Miyao, A., Hirochika, H., An, G., & Hirano, H.-Y. (2005). Functional Diversification of the Two C-Class MADS Box Genes OSMADS3 and OSMADS58 in Oryza sativa. The Plant Cell, 18(1), 15–28. https://doi.org/10.1105/tpc.105.037200

Yamaguchi, T., Nagasawa, N., Kawasaki, S., Matsuoka, M., Nagato, Y., & Hirano, H.-Y. (2004). The YABBY Gene DROOPING LEAF Regulates Carpel Specification and Midrib Development in Oryza sativa. The Plant Cell, 16(2), 500–509. https://doi.org/10.1105/tpc.018044

Yamaki, S., Nagato, Y., Kurata, N., & Nonomura, K.-I. (2011). Ovule is a lateral organ finally differentiated from the terminating floral meristem in Rice. Developmental Biology, 351(1), 208–216. https://doi.org/10.1016/j.ydbio.2010.12.006

Yasui, Y., Tanaka, W., Sakamoto, T., Kurata, T., & Hirano, H.-Y. (2017). Genetic Enhancer Analysis Reveals that FLORAL ORGAN NUMBER2 and OsMADS3 Co-operatively Regulate Maintenance and Determinacy of the Flower Meristem in Rice. Plant and Cell Physiology, 58(5), 893–903. https://doi.org/10.1093/pcp/pcx038

Zahn, L. M., Kong, H., Leebens-Mack, J. H., Kim, S., Soltis, P. S., Landherr, L. L., Soltis, D. E., dePamphilis, C. W., & Ma, H. (2005). The evolution of the sepallata subfamily of MADS-box genes: A preangiosperm origin with multiple duplications throughout angiosperm history. Genetics, 169(4), 2209–2223. https://doi.org/10.1534/genetics.104.037770

Zhang, J., Nallamilli, B. R., Mujahid, H., & Peng, Z. (2010). OsMADS6 plays an essential role in endosperm nutrient accumulation and is subject to epigenetic regulation in rice (Oryza sativa). The Plant Journal, 64(4), 604–617. https://doi.org/10.1111/j.1365-313x.2010.04354.x